

REPUBLIC OF CAMEROON

REPUBLIQUE DU CAMEROUN

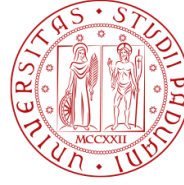


DEPARTMENT OF CIVIL ENGINEERING

DEPARTEMENT DE GENIE CIVIL

MINISTRY OF HIGHER EDUCATION

MINISTERE DE L'ENSEIGNEMENT SUPERIEUR



UNIVERSITÀ  
DEGLI STUDI  
DI PADOVA

DEPARTMENT OF CIVIL, ARCHITECTURAL

AND ENVIRONMENTAL ENGINEERING

**REDUNDANCY AND RESILIENCE OF ARCH BRIDGES.  
CASE STUDY OF THE POLCEVERA RAILWAY ARCH  
BRIDGE IN GENOA, ITALY.**

*A thesis submitted in partial fulfilment of the requirements for the degree of  
Master of Engineering (MEng) in Civil Engineering*

Curriculum: **Structural Engineering**

Presented by:

**KENNETH TIOTSOP Franck**

Student number: **16TP21156**

Supervised by:

**Prof. Eng. Carmelo MAJORANA**

Co-supervised by:

**Dr. Eng. Guillaume Hervé POH'SIE**

**Dr. Eng. Emanuele MAJORANA**

Academic year: 2020/2021

REPUBLIC OF CAMEROON

REPUBLIQUE DU CAMEROUN



DEPARTMENT OF CIVIL ENGINEERING

DEPARTEMENT DE GENIE CIVIL

MINISTRY OF HIGHER EDUCATION

MINISTERE DE L'ENSEIGNEMENT SUPERIEUR



UNIVERSITÀ  
DEGLI STUDI  
DI PADOVA

DEPARTMENT OF CIVIL, ARCHITECTURAL

AND ENVIRONMENTAL ENGINEERING

**REDUNDANCY AND RESILIENCE OF ARCH BRIDGES.  
CASE STUDY OF THE POLCEVERA RAILWAY ARCH  
BRIDGE IN GENOA, ITALY.**

*A thesis submitted in partial fulfilment of the requirements for the degree of  
Master of Engineering (MEng) in Civil Engineering*

Curriculum: **Structural Engineering**

Presented by:

**KENNETH TIOTSOP Franck**

Student number: **16TP21156**

Supervised by:

**Prof. Eng. Carmelo MAJORANA**

Co-supervised by:

**Dr. Eng. Guillaume Hervé POH'SIE**

**Dr. Eng. Emanuele MAJORANA**

Academic year: 2020/2021

## **DEDICATION**

---

*It is with genuine gratefulness and warmest regard that I dedicate this  
endeavour work to my late beloved grandfather*

*Inspector Keuha René.*

*You passed away just before the fulfilment of this work, which is the result of  
your unfailing encouragements, invaluable support, and unceasing follow-up.*

## ACKNOWLEDGMENTS

---

---

This thesis is the result of the combined efforts and contributions of several individuals, the names of whom may not all be mentioned. Their contributions are greatly appreciated and gratefully acknowledged. Nonetheless, it is with great honour that I express my gratitude to:

- The **President** of the jury for accepting to chair this jury;
- The **Examiner** of the jury for accepting to bring his criticisms and observations to ameliorate this work;
- The Director of the National Advanced School of Public Works (NASPW), **Prof. NKENG George ELAMBO** and **Prof. Eng. Carmelo MAJORANA** of the University of Padua, Italy who are the principal supervisors of this Master's in Engineering (MEng) curricula at NASPW in partnership with the University of Padua;
- The Vice-Director of the NASPW, **Dr. Eng. BWEMBA Charles** for his perpetual help and advices during our sojourn in this school;
- The Head of the Department of Civil Engineering, **Prof. Michel MBESSA**, for his tutoring, valuable advices and availability;
- My supervisors **Prof. Eng. Carmelo MAJORANA**, **Dr. Eng. Emanuele MAJORANA** and **Dr. Eng. Guillaume Hervé POH'SIE** for all the patience, guidance, criticisms, advices and availability throughout the making of this thesis work;
- My elder **Dr. Eng. Cyrille Denis TETOUGUENI** for all his help and availability;
- All the **teaching staff** of NASPW and **University of Padua** for their quality teaching and motivational skills;
- The **administrative staff** of the NASPW for their sense of professionalism;
- All my classmates and especially **my friends** of the **7<sup>th</sup> batch** of Master's in Engineering (MEng) for the spirit of togetherness;
- My beloved mother, **Mrs. KENNE Rachel** who offered me unwavering love, invaluable educational facilities, appropriate guidance, counselling and tremendous support;
- My siblings **Russelle, Jocelyne, Paulette** and **Christagi** for their true love and affection;
- The whole **FOPA, KEUHA, TCHIANZE, ZEBAZE** and **TIOTSOP** families for the moral, social and financial support;
- My **friends** for all the great moral support and special time spent together.

## **LIST OF ABBREVIATIONS**

---

<b>AD</b>	Anno Domini
<b>ASD</b>	Allowable Stress Design
<b>ASCE</b>	American Society of Civil Engineers
<b>AASHTO</b>	American Association of State Highway and Transportation Officials
<b>BC</b>	Before Christ
<b>CAD</b>	Computer Aided Design
<b>CP</b>	Collapse Prevention
<b>CE</b>	Common Era
<b>CFST</b>	Concrete Filled Steel Tube
<b>EC</b>	Eurocode
<b>EN</b>	European Norm
<b>IO</b>	Immediate Occupancy
<b>FCMs</b>	Fracture Critical Members
<b>PG</b>	Plate Girder
<b>FS</b>	Factor of Safety
<b>LFD</b>	Load Factor Method
<b>LF</b>	Load Factor
<b>LS</b>	Life Safety
<b>LSD</b>	Limit State Design

<b>LRFD</b>	Load and Resistance Factor Design
<b>NCHRP</b>	National Cooperative Highway Research Program
<b>LM</b>	Load Model
<b>SEI</b>	Structural Engineering Institute
<b>SLS</b>	Serviceability Limit State
<b>TNT</b>	Trinitrotoluene
<b>ULS</b>	Ultimate Limit State
<b>WSD</b>	Working Stress Design

## LIST OF SYMBOLS

$A_d$	Accidental load
$Q_{k,i}$	Accompanying variable loads
$\rho$	Air density
$P_o$	Ambient pressure
$N_{b,Rd}$	Axial buckling resistance
$v_b$	Basic wind velocity
$W$	Charge mass
$\psi_{0,i}$	Combination coefficients for the live loads
$y_G$	Coordinate y of gravity centre
$b$	Decay coefficient of the waveform
$N_{Ed}$	Design axial force value
$V_{pl,Rd}$	Design plastic shear resistance
$V_{Ed}$	Design shear value
$c_{dir}$	Directional factor
$R$	Distance of the surface from the centre of a spherical explosion in $m$ .
$A_{slab}$	Effective area of slab
$W_{eff,min}$	Effective section modulus
$E_{cm}$	Elastic modulus
$W_{el,min}$	Elastic section modulus
$c_f$	Force coefficient
$H_{exp}^d$	Heat of detonation of the actual explosive
$H_{TNT}^d$	Heat of detonation of the TNT

$Q_{k,1}$	Leading variable load
$v_m(z)$	Mean wind velocity at height $z$
$J$	Moment of inertia of the section
$y$	Neutral axis position
$c_o(z)$	Orography coefficient
$\gamma_{G,j}$	Partial factors of permanent loads
$\gamma_{Q,i}$	Partial factors of variable loads
$\gamma_{G,j}$	Partial safety factors applied to permanent loads
$\gamma_{Q,i}$	Partial safety factors applied to variable loads
$P_{s0}$	Peak overpressure
$q_p(z_e)$	Peak velocity pressure at reference height $z_e$
$G_{k,j}$	Permanent loads
$W_{pl}$	Plastic section modulus
$t_0$	Positive phase duration
$\chi$	Reduction factor
$t_0$	Reference zero time
$RH$	Relative humidity
$A_v$	Resisting shear area
$c_r(z)$	Roughness coefficient
$z_o$	Roughness length
$\varepsilon_{su}$	Rupture or ultimate strain of the material
$Z$	Scaled distance
$V_{b,Rd}$	Shear buckling resistance
$A_c$	Slab section area

$\bar{\lambda}$	Slenderness
$c_{season}$	Season factor
$\varepsilon_{sh}$	Strain at the onset of strain hardening
$\sigma_{low,steel}$	Stress at steel lower section
$\sigma_{up,steel}$	Stress at steel upper section
$\sigma_s$	Stress in steel
$c_s \cdot c_d$	Structural factor
$T_k$	Temperature load
$T_{beam}$	Temperature load per beam
$k_r$	Terrain factor
$\varepsilon$	Thermal coefficient
$t$	Time elapsed, from the instant of blast arrival
$W_e$	TNT equivalent weight
$d_{tot}$	Total depth of the structural element $z_e$
$k_l$	Turbulence factor
$I_v(z)$	Turbulence intensity
$\alpha_{Qik}$	Values of adjustment factors
$W_{exp}$	Weight of the actual explosive
$F_W$	Wind force
$\varepsilon_y$	Yielding strain of the material
$f_u$	Ultimate strength
$f_y$	Yielding strength

## **ABSTRACT**

---

This thesis work was aimed at analysing the redundancy of the hangers of an arch bridge and the resilient behaviour of the bridge when subjected to accidental extreme loading. To achieve this objective, a state of art was done in order to have an insight on arch bridges, their main features, followed by their redundancy and resilience when subjected to extreme events such as blast loading. The case study used for the various analyses was an 80 metres long span of a steel tied-arch railway bridge crossing the Polcevera river in the city of Genoa, Italy. This work started by creating numerical models of the case study using the MIDAS/Civil 2022 software, applying adequately computed loads and all the necessary load combinations in order to perform a linear static analysis. The various solicitations were determined and the structure statically verified according to Eurocode norms. Afterwards, the redundancy analysis of the bridge was conducted by considering 10 hanger failure cases in the symmetric and asymmetric configuration. In each case considered, a particular number of hangers was removed on each side of the arch bridge then the stress redistribution and global behaviour of the bridge assessed. A resilience analysis was also performed through a non-linear dynamic time-history analysis of the bridge subjected to a blast load of 500 kg of TNT applied 1 metre above the deck at two different locations of the bridge ( $x = 10$  m and  $x = 40$  m). According to the results obtained, the first hangers at the edges of the bridge are the most stressed and so are the first fracture critical members whose failure induce a stress increase of more than 60% in the next hangers. Moreover, it was observed that for hanger failures close to the edge of the bridge, the stress redistribution is local and thus little or no impact is felt for hangers far away. Conversely, for hanger failures between the edge and the midspan of the bridge, the stress distribution is global observing stress increments of just about 20%. However, the stress redistribution greatly depends on the number of hangers that are ruptured. A progressive collapse mechanism is found to be related to the redundancy of the hangers given that the rupture of some of these induce successive member rupture. On the other hand, the resilience analysis showed that the bridge is more vulnerable to blast load located at the beginning of the bridge longitudinal section ( $x = 10$  m). The damage of the bridge element, which is a key factor for the resilience, is dependent on the distance from the detonation point.

**Keywords:** Redundancy, resilience, blast, hangers, progressive collapse, stress distribution.

---

## **RESUME**

---

L'objectif principal de ce travail était d'analyser la redondance des suspentes d'un pont en arc et la résilience de ce dernier lorsqu'il est soumis à des charges accidentelles extrêmes telles que les explosions. À cet effet, une revue de la littérature a été réalisée dans l'optique de l'appropriation des concepts liés aux ponts en arc. Le cas d'étude utilisé pour les différentes analyses est une travée de 80 mètres de long d'un pont ferroviaire en arc suspendu traversant le fleuve Polcevera dans la ville de Gênes, en Italie. Ce travail a débuté par la modélisation numérique du cas d'étude à l'aide du logiciel MIDAS/Civil 2022, en appliquant des charges et les combinaisons de charges nécessaires afin d'effectuer une analyse statique linéaire. Les différentes sollicitations ont été déterminées et la structure vérifiée statiquement selon les normes de l'Eurocode. Par la suite, l'analyse de la redondance du pont a été menée en considérant 10 cas de rupture des suspentes dans des configurations symétriques et asymétriques. Pour chaque cas, un nombre particulier de suspentes a été retiré de chaque côté du pont en arc puis la redistribution des contraintes et le comportement global du pont ont été évalués. L'analyse de la résilience a également été réalisée à travers une analyse dynamique non-linéaire du pont soumis à une charge explosive de 500 kg de TNT appliquée à 1 mètre au-dessus du tablier à deux emplacements ( $x = 10$  m et  $x = 40$  m). D'après les résultats obtenus, les suspentes aux extrémités du pont sont les plus sollicitées et de ce fait, elles sont des éléments critiques dont la rupture a induit une augmentation des contraintes de plus de 60 % dans les suspentes adjacentes. De plus, il a été observé que suite à la rupture des suspentes proches des extrémités, la redistribution des contraintes est locale et n'a donc presque pas d'impact sur les suspentes éloignées. Cependant, pour les ruptures de suspentes vers la mi-travée, la répartition des contraintes est globale avec des incréments de contrainte d'environ 20 %. Toutefois, la redistribution des contraintes dépend fortement du nombre de suspentes rompues. Un mécanisme d'effondrement progressif s'avère lié à la redondance des suspentes puisque la rupture de certaines d'entre elles induit des ruptures successives des autres. D'autre part, l'analyse de résilience a montré que le pont est plus vulnérable à la charge explosive située au début de la section longitudinale du pont ( $x = 10$  m). L'endommagement du pont est un facteur déterminant de sa résilience, dont l'ampleur dépend de la distance du point de détonation.

**Mots-clés** : Redondance, résilience, explosion, suspentes, effondrement progressif, redistribution des contraintes.

---

---

## LIST OF FIGURES

---

Figure 1.1. Kasarmi Bridge, Argolide (Google Map) .....	3
Figure 1.2. Volterra arch, Tuscany (Pipinato, 2016).....	3
Figure 1.3. Sant’Angelo Bridge, Rome (Owen, 2017).....	4
Figure 1.4. The Roman Alcántara Bridge, Spain (Wikimedia Commons) .....	5
Figure 1.5. Pont du Gard aqueduct, France (Beyer, 2012).....	5
Figure 1.6. Old London Bridge (Encyclopaedia Britannica) .....	6
Figure 1.7. The Rialto Bridge, Venice (Bernabei et al., 2019) .....	7
Figure 1.8. Iron bridge at Coalbrookdale, England. (Beyer, 2012).....	8
Figure 1.9. Craigellachie Bridge, Scotland (tripadvisor.com). .....	8
Figure 1.10. The Plougastel Bridge (Beyer, 2012) .....	9
Figure 1.11. The Martín Gil Viaduct, Spain (Pipinato, 2021) .....	9
Figure 1.12. The Bayonne Bridge, New York (Pipinato, 2021) .....	9
Figure 1.13. Krk Island Bridges (Beyer, 2012).....	10
Figure 1.14. Chaotianmen Yangtze River Bridge (Wikipedia).....	11
Figure 1.15. Arch bridge nomenclature (Owen, 2017) .....	11
Figure 1.16. Forces in an arch (Beyer, 2012).....	12
Figure 1.17. Abutment of the Blackfriars Railway bridge (midasbridge.com).....	13
Figure 1.18. Spandrels of a deck arch bridge (midasbridge.com).....	14
Figure 1.19. Hangers of a bridge (midasbridge.com) .....	14
Figure 1.20. Deck arch bridges sub-types .....	16
Figure 1.21. Various through arch bridges types (midasbridge.com).....	17
Figure 1.22. Half-through arch bridges types (Chen & Duan, 2014).....	17
Figure 1.23. Fixed and hinged arch bridges (Fu & Wang, 2014) .....	18
Figure 1.24. The Stone Dock Bridge in China (Owen, 2017).....	19
Figure 1.25. The Spectacle Bridge in Nagasaki (Owen, 2017).....	19
Figure 1.26. The Kintai Bridge, Japan (wakuwaku.today) .....	20
Figure 1.27. Tied Arch Structural Arrangement (Finke, 2016) .....	20
Figure 1.28. Tied Arch Structural Action (Finke, 2016).....	21
Figure 1.29. Flowchart for identifying FCMs of complex steel bridges (Caltrans, 2004).....	33
Figure 1.30. Representation of typical behavior of bridge systems (Ghosn et al., 2014) .....	34

---

---

Figure 1.31. Redundancy and progressive analysis procedure (Khuyen, 2016) .....	39
Figure 1.32. Different levels of structural safety (Fang & Fan, 2011).....	40
Figure 1.33. Estimation of resilience measures through absorptive, adaptive, and restorative capacity of a system (Alipour, 2017) .....	45
Figure 1.34. Proposed framework for resilience quantification (UTCP, 2014).....	46
Figure 1.35. Blast pressure distribution over time (Karlos et al., 2016) .....	51
Figure 1.36. Influence of distance on the blast positive pressure phase (Karlos et al., 2016) .	53
Figure 1.37. Types of external explosions and blast loadings (Karlos & Solomos, 2013).....	56
Figure 2.1. Load Model 71 and characteristic values for vertical loads (EN 1991-2, 2003) ...	59
Figure 2.2. Correlation between minimum/maximum shade air temperature and minimum/maximum uniform bridge temperature component (EN 1991-1-5, 2003) .....	63
Figure 2.3. Time dependent concrete creep and shrinkage (MIDAS/Civil software).....	67
Figure 2.4. Illustration of some key blast parameters (Mbakop, 2020) .....	69
Figure 2.5. Parameters of positive phase of shock spherical wave of TNT charges from surface bursts (Karlos & Solomos, 2013) .....	70
Figure 2.6. MIDAS/Civil 2022 menus .....	76
Figure 2.7. Buckling curves (EN 1993-1-1, 2005).....	81
Figure 2.8. Park model for non-linear behaviour of elements .....	89
Figure 3.1. Geographical location of Genoa on the map of Italy (roughguides.com) .....	92
Figure 3.2. Location of the project (Faccini et al., 2021).....	93
Figure 3.3. Mean monthly rainfall and temperatures in Genoa (climate-data.org).....	94
Figure 3.4. Population trend in the city of Genoa (Paliaga et al., 2019).....	96
Figure 3.5. View of the Polcevera railway arch bridge.....	97
Figure 3.6. Longitudinal view plan of one arch of the Polcevera railway arch bridge .....	98
Figure 3.7. Cross sectional view in the midspan of the bridge .....	99
Figure 3.8. Load Model 71 rail traffic vehicle load definition in MIDAS/Civil.....	103
Figure 3.9. Wind map zones of Italy (Sonda, 2019) .....	104
Figure 3.10. Graph of creep coefficient of concrete with time .....	106
Figure 3.11. Graph of the evolution of shrinkage strain with time .....	107
Figure 3.12. Numerical model for the arch bridge in MIDAS/Civil software.....	110
Figure 3.13. Diagram for maximum positive bending moment (kNm) in the main girder....	115
Figure 3.14. Diagram for maximum negative bending moment (kNm) in the main girder...	115
Figure 3.15. Maximum axial compression (kN) in the arch rib.....	115

---

Figure 3.16. Envelope of bending moment for the arch ribs and main girders.....	116
Figure 3.17. Envelope shear force for the arch ribs and main girders .....	116
Figure 3.18. Envelope of axial force for the arch ribs and main girders.....	116
Figure 3.19. Envelope of bending moment for cross beams .....	117
Figure 3.20. Envelope of shear force for cross beams .....	117
Figure 3.21. Envelope of axial force for cross beams .....	117
Figure 3.22. Tensile stresses in the hangers .....	117
Figure 3.23. Deflection of the arch bridge .....	121
Figure 3.24. Stress distribution in hangers following symmetric failure mechanism.....	125
Figure 3.25. Variation of the maximum stress in the arch for the different cases .....	126
Figure 3.26. Variation of the maximum stress in the main girder for the different cases.....	127
Figure 3.27. Variation of global bridge deflection.....	127
Figure 3.28. Hanger stress distribution for assymetric configuration .....	129
Figure 3.29. Blast loading positions along the bridge.....	131
Figure 3.30. Blast loading parameters computation.....	131
Figure 3.31. Stress distribution in the slab for blast case 1.....	133
Figure 3.32. Stress distribution in the hangers for blast case 1.....	134
Figure 3.33. Stress distribution in the arch and girder for blast case 1.....	134
Figure 3.34. Stress distribution in the slab for blast case 2.....	135
Figure 3.35. Stress distribution in the hangers for blast case 2.....	136
Figure 3.36. Stress distribution in the arch and girder for blast case 1.....	136
Figure 3.37. Evolution of stresses in Hanger 1 and 2 after blast loading case 1.....	137
Figure 3.38. Evolution of node elongation 1 and 2 after blast loading case 1.....	138
Figure 3.39. Evolution of stresses in Hanger 8 and 7 after blast loading case 2.....	139
Figure 3.40. Evolution of node elongation 8 and 7 after blast loading case 2.....	139
Figure 3.41. Variation of the displacement of the slab with time at different postions from the blast load. ....	140

## LIST OF TABLES

Table 1.1. Consideration of redundancy enhancement in different phases (Fang & Fan, 2011)	42
Table 1.2. Expected likelihood of different hazards across U.S. States identified by state bridge and hydraulic engineers (Alipour, 2017)	49
Table 2.1. Table of terrain categories and terrain parameters (EN 1991-1-4, 2005)	62
Table 2.2. Recommended values of linear temperature difference component for different types of bridge decks for road, foot and railway bridges (EN 1991-1-5, 2003)	65
Table 2.3. Recommended values of $k_{sur}$ to account for different surfacing thickness (EN 1991-1-5, 2003)	65
Table 2.4. Formulae of various shrinkage strain components	68
Table 2.5. Recommended values of partial safety factors for ULS combination (EN 1990, 2002)	72
Table 2.6. Recommended values of $\psi$ factors for railway bridges (EN 1990 Annex A2, 2005)	73
Table 2.7. Maximum width-to-thickness ratios for internal compression parts (EN 1993-1-1, 2005)	77
Table 2.8. Maximum width-to-thickness ratios for outstand flanges (EN 1993-1-1, 2005)	78
Table 2.9. Maximum width-to-thickness ratios for angle compression part (EN 1993-1-1, 2005)	78
Table 2.10. Selection of buckling curve for a cross section (EN 1993-1-1, 2005)	81
Table 2.11. Critical-Load Parameter and Critical Horizontal Reaction Parameter for Uniform Elastic Arches in Pure Compression (Trahair, 1989)	83
Table 3.1. Mechanical characteristics of main structural steel used	100
Table 3.2. Mechanical characteristics of steel used for hangers	100
Table 3.3. Mechanical characteristics of concrete	101
Table 3.4. Mechanical characteristics of concrete slab steel reinforcement	101
Table 3.5. Self-weight of structural elements	102
Table 3.6. Self-weight of non-structural elements	102
Table 3.7. Basic wind reference velocity for wind zones in Italy (Sonda, 2019)	104
Table 3.8. Computed wind coefficients and parameters	105

Table 3.9. Wind force computation.....	105
Table 3.10. Temperature load parameters .....	106
Table 3.11. Computation of the shrinkage force .....	107
Table 3.12. Load description symbols .....	108
Table 3.13. ULS load combinations.....	108
Table 3.14. SLS load combinations .....	109
Table 3.15. Main girder section properties.....	111
Table 3.16. Main girder section classification .....	111
Table 3.17. Cross beam section properties.....	112
Table 3.18. Cross beam section classification.....	112
Table 3.19. Arch rib section properties .....	113
Table 3.20. Arch rib section classification .....	113
Table 3.21. Hanger section properties.....	114
Table 3.22. Bracing element properties .....	114
Table 3.23. Tensile stress in each hanger of the arch bridge.....	118
Table 3.24. Main girder section verifications.....	118
Table 3.25. Arch rib section verifications .....	118
Table 3.26. Arch rib buckling verification .....	119
Table 3.27. Cross beam section verifications.....	119
Table 3.28. Hanger and slab bracing element stress verification.....	120
Table 3.29. Serviceability state stress limitation verification .....	120
Table 3.30. Hanger failure configurations .....	122
Table 3.31. Frequency and periods of the first 10 modes .....	132
Table 3.32. Modal participation ratios for the first 10 modes.....	132

## TABLE OF CONTENT

DEDICATION .....	i
ACKNOWLEDGMENTS.....	ii
LIST OF ABBREVIATIONS .....	iii
LIST OF SYMBOLS .....	v
ABSTRACT .....	viii
RESUME.....	ix
LIST OF FIGURES.....	x
LIST OF TABLES .....	xiii
TABLE OF CONTENT .....	xv
GENERAL INTRODUCTION .....	1
CHAPTER 1: LITERATURE REVIEW .....	2
Introduction .....	2
1.1. Arch bridges .....	2
1.1.1. Historical background .....	2
1.1.1.1. Pre-roman era.....	3
1.1.1.2. Roman era .....	4
1.1.1.3. The Middle Ages.....	6
1.1.1.4. The renaissance .....	6
1.1.1.5. The period of modernity .....	7
1.1.2. Main parts of an arch bridge.....	11
1.1.2.1. Arch.....	11
1.1.2.2. Abutments and supports.....	13
1.1.2.3. Hangers and spandrels .....	14
1.1.3. Classification of arch bridges .....	15
1.1.3.1. According to deck location .....	15
1.1.3.2. According to structural systems.....	17
1.1.3.3. According to construction materials .....	19
1.1.4. Structural behaviour of arch bridges .....	20
1.1.5. Generalities on arch bridge design .....	21
1.1.5.1. Bridge design methods.....	22
1.1.5.2. Design of arch ribs and ties.....	23
1.1.5.3. Design of other elements .....	26

---

1.1.6.	Erection of arch bridges .....	27
1.1.6.1.	Cantilever erection .....	27
1.1.6.2.	Scaffolding method .....	28
1.1.6.3.	Swing method .....	28
1.1.6.4.	Construction methods for tied arch bridges .....	28
1.2.	Redundancy .....	29
1.2.1.	Definitions .....	29
1.2.2.	Redundancy classifications .....	30
1.2.2.1.	Load path redundancy .....	30
1.2.2.2.	Structural redundancy .....	31
1.2.2.3.	Internal redundancy .....	31
1.2.3.	Basis of bridge redundancy .....	32
1.2.4.	Measures of bridge redundancy .....	33
1.2.4.1.	Typical behaviour of bridge systems .....	34
1.2.4.2.	Measure of the level of bridge redundancy .....	35
1.2.5.	Redundancy and progressive collapse .....	38
1.2.5.1.	Generalities .....	38
1.2.5.2.	Redundancy and progressive collapse analysis .....	38
1.2.6.	Redundancy and structural safety .....	40
1.2.7.	Enhancing redundancy .....	41
1.2.7.1.	Design of new bridges .....	41
1.2.7.2.	Rating and retrofit of existing bridges .....	42
1.3.	Resilience .....	43
1.3.1.	Definitions .....	43
1.3.2.	Illustration of resilience in a system .....	44
1.3.3.	Framework for estimating resilience .....	46
1.3.4.	Extreme events .....	47
1.3.4.1.	Definition .....	47
1.3.4.2.	Holistic consideration of extreme events .....	48
1.3.5.	Blast event characterisation .....	50
1.3.5.1.	Ideal blast wave characteristics .....	50
1.3.5.2.	Blast parameters .....	52
1.3.5.3.	Blast pressure determination .....	54
1.3.5.4.	Explosion and blast-loading types .....	55

---

---

Conclusion.....	56
CHAPTER 2: METHODOLOGY .....	57
Introduction .....	57
2.1. General site recognition .....	57
2.2. Data collection.....	57
2.2.1. Geometrical data .....	58
2.2.2. Material properties .....	58
2.3. Design codes and actions on the structure .....	58
2.3.1. Design codes .....	58
2.3.2. Actions on the structure.....	59
2.3.2.1. Permanent loads .....	59
2.3.2.2. Live loads.....	59
2.3.2.3. Blast load .....	69
2.3.3. Load combinations .....	71
2.3.3.1. Static load cases .....	71
2.3.3.2. Dynamic load cases.....	73
2.4. Structural analysis and design .....	74
2.4.1. Numerical modelling.....	74
2.4.1.1. MIDAS/Civil 2022 description.....	74
2.4.1.2. Bridge modelling procedure .....	75
2.4.2. Steel sections classification .....	76
2.4.3. Steel members design at Ultimate Limit States .....	79
2.4.3.1. Design of members subjected to axial force .....	79
2.4.3.2. Design of beam elements .....	83
2.4.4. Serviceability Limit States (SLS) verifications.....	86
2.5. Redundancy analysis .....	87
2.6. Resilience analysis .....	87
2.6.1. Explosive weights and positions of explosion .....	88
2.6.2. Blast loading.....	88
2.6.3. Eigen value analysis .....	88
2.6.4. Non-linear time-history analysis .....	89
2.6.4.1. Non-linear behaviour of elements.....	89
2.6.4.2. Dynamic equilibrium consideration.....	90
Conclusion.....	90

---

---

CHAPTER 3: RESULTS AND DISCUSSIONS.....	91
Introduction .....	91
3.1. General site presentation .....	91
3.1.1. Physical parameters.....	91
3.1.1.1. Geographical location .....	91
3.1.1.2. Climate .....	93
3.1.1.3. Relief and hydrology.....	94
3.1.1.4. Geology.....	95
3.1.2. Human and socio-economic parameters .....	95
3.1.2.1. Population .....	95
3.1.2.2. Economy .....	96
3.1.2.3. Transport .....	96
3.2. Presentation of the project.....	97
3.2.1. Geometrical and structural characteristics .....	97
3.2.2. Materials characteristics .....	99
3.3. Load determination and combinations .....	101
3.3.1. Load determination .....	101
3.3.1.1. Permanent actions .....	102
3.3.1.2. Live loads.....	103
3.3.2. Load combinations .....	107
3.4. Design and verifications.....	110
3.4.1. Numerical modelling.....	110
3.4.2. Steel section presentation and classification .....	110
3.4.2.1. Main girder.....	111
3.4.2.2. Cross beam.....	112
3.4.2.3. Arch rib .....	113
3.4.2.4. Hangers .....	113
3.4.2.5. Bracing elements.....	114
3.4.3. Section verifications.....	114
3.4.3.1. Diagrams of internal actions .....	115
3.4.3.2. Verifications of sections .....	118
3.4.4. Serviceability limit state verifications.....	120
3.4.4.1. Stress limitation .....	120
3.4.4.2. Deflection control .....	121

---

---

3.5. Redundancy analysis results.....	121
3.5.1. Hanger failure cases .....	121
3.5.2. Symmetric configuration.....	122
3.5.2.1. Stresses distribution for hangers following hanger failure .....	122
3.5.2.2. Maximum stress in the arch rib and main girder .....	126
3.5.2.3. Variation of the global bridge deflection .....	127
3.5.3. Asymmetric configuration.....	128
3.5.3.1. Maximum hanger stress .....	128
3.5.3.2. Maximum stress in elements and deflection .....	130
3.6. Resilience analysis results .....	130
3.6.1. Blast loading positions .....	130
3.6.2. Blast load computation.....	131
3.6.3. Eigen value analysis result .....	132
3.6.4. Effect of blast on the bridge .....	133
3.6.4.1. Blast case 1 .....	133
3.6.4.2. Blast case 2 .....	135
3.6.5. Time history results .....	137
3.6.5.1. Blast case 1 .....	137
3.6.5.2. Blast case 2 .....	138
3.6.5.3. Effect of the blast loading on slab displacement .....	140
3.6.6. Comments on the robustness of arch bridge .....	141
Conclusion .....	141
GENERAL CONCLUSION .....	142
BIBLIOGRAPHY .....	144
WEBOGRAPHY.....	148
ANNEXES .....	I
ANNEX A: Table and figures used in methodology.....	I
ANNEX B: Structural detailing of the arch bridge .....	III

## **GENERAL INTRODUCTION**

---

Arch bridges are one of the oldest and most prominent type of bridge in the world. Like every civil construction, they could be exposed to extreme accidental actions. During the last few decades, accidental explosions and premeditated attacks on bridges have prompted governments and design professionals to pay more attention to the vulnerability and survivability of bridge structures relative to blast events. The importance of designing more robust public transportation infrastructure, especially bridges has become more significant. However, the current engineering design codes have few specific provisions or guidelines for the design of sufficiently resilient bridges.

As technologies, abilities, and techniques improve, new bridges may not fit into the “normal” criteria that form the basis of current design codes. In addition, in light of the increasing frequency of intense and unforeseen loading events such as blasts, it will be necessary for bridge structures to be better equipped in order to properly adapt. With this in mind, structural engineers and other professionals are continuously researching and developing cost-effective methodologies for the design of more robust bridge to protect lives and prevent total or partial structural collapse. New design strategies that address redundancy and resilience may be the next step to design the bridges of the future. Arch bridges construction has greatly increased in the world and because of their strong presence, they are more exposed to blast attacks. For better performance, the design of these structures has then to be improved. Thus, the main purpose of this thesis work is to analyse the redundancy of the hangers of a tied-arch bridge and the resilient behaviour of the bridge when subjected to blast loading.

In order to achieve this objective, this thesis is divided in three main chapters hereafter outlined. The first chapter focuses on the state of art on arch bridges, their main features, types and generalities of their design. Also, a general overview of the concepts of redundancy and resilience in relation to bridges is presented. The second chapter which is the methodology describes the procedures to be followed in modelling and performing a linear static analysis followed by non-linear dynamic time history analysis in MIDAS/Civil. In the third chapter, the results of the design and verifications of the bridge followed by those of redundancy analysis are shown. Furthermore, the presentation of the results obtained from the time history resilience analysis of the bridge subject to blast loading is done.

# **CHAPTER 1: LITERATURE REVIEW**

---

## **Introduction**

Arch bridges are bridges in which the main structural elements are arches. The basic principle of arch bridge is its curved design, which does not push load forces straight down, but instead they are conveyed along the curve of the arch to the supports at each end. Their behaviour is quite different from that of other bridges. For a better understanding of their structural behaviour, it is necessary to have a general overview of arch bridges and related concepts. Firstly, this chapter will present a brief history of arch bridges, their main general characterisation, design and erection methods. Following that, the basic concept of redundancy, its definitions and basis in arch bridge design will be discussed. Lastly, a general overview will be made on resilience of bridges in relation to accidental and extreme events.

### **1.1. Arch bridges**

An arch is a curved structure that support the loads parallel to its axis of symmetry, and a bridge with an arch as its load carrying system is called an arch bridge. An arch bridge is usually defined as a vertically curved and axially compressed structural member spanning an opening and providing a support for the moving loads above the opening. An arch bridge generally has abutments at each end, and works by transferring the self-weight and other external loads in vertical directions partially into a horizontal thrust restrained by the abutments (or piers) at both sides. In addition to compressive forces in axial direction, the arch usually also needs to resist the bending moments and shear forces. The structural properties of arches vary depending on the shape of the arches and the number of hinges. In general, arches become stronger as the number of hinges decreases; however, it greatly impacts settlement. Arch bridges can either be built as one-span with two abutments, or can be made from a series of continuous arches. Arch bridges have been widely used around the world because of their unique aesthetics, and are used for long-span bridges after suspension and cable-stayed bridges.

#### **1.1.1. Historical background**

From a general point of view, bridges represent a real challenge in the built environment. They provide the most appropriate connection of what nature has divided: a river, a valley, or something that is impossible to be reached. The first bridge was a natural gift to humanity and

was probably a tree that fell across a small river or the observation of rock bridges. This suggested to the first prehistoric builders that it is possible to overpass obstacles. And from these simple structures, a relevant part of the entire structural engineering worldwide has been produced over the centuries. The application of arches to bridge structures came much later than girder and suspension types, but an arch is the first and greatest of Man's inventions in the field of structures because it transfers loads relating to its shape.

#### **1.1.1.1. Pre-roman era**

The first bridge was a simply supported beam made of wood. This was probably developed in the Palaeolithic age. Around 4000 B.C., Sumerians built arch entrance and small arch bridges with sun-baked bricks (Pipinato, 2021). In the Mesolithic period, an increasing amount of bridge structures were built. For example, consider the Sweet Track, 1800 m long, which was recently discovered at Somerset Levels in Great Britain and harked to the early stage of the Neolithic period (3806 B.C.), according to dendrochronological analysis. In Egypt, such small examples have been found as the stone bridge at Gizah (2620 B.C.). Meanwhile, in Greece, the Kasarmi Bridge, at Argolide (1400 B.C.), was one of the first type of Miceneus bridges (Figure 1.1). It is a common historical belief that Etruschi taught the Romans how to build arch bridges, even if they left no relevant bridges behind to document this. In fact, the Romans learned about this from defence and hydraulic buildings such as the Volterra arch (4<sup>th</sup> century B.C.) presented on Figure 1.2.



**Figure 1.1.** Kasarmi Bridge, Argolide (Google Map)



**Figure 1.2.** Volterra arch, Tuscany (Pipinato, 2016)

### **1.1.1.2. Roman era**

Although wooden bridges were common at first, stone bridges (especially arch bridges) increasingly dominated until the Middle Ages; as Palladio said: “Stone bridges were built for their longer life, and to glorify their builder” (Palladio, 1570). One of the most incredible periods of bridge construction was started during the Roman Empire, in which stone arch bridge building techniques were developed. Although true arches were already known by the Etruscans and ancient Greeks, the Romans were as with the vault and the dome the first to fully realize the potential of arches for bridge construction. Two fundamental elements greatly influenced the development of this technique bridge building techniques. Firstly, geopolitical, as the military and political objective to grow faster as an empire required a large amount of infrastructure. The Romans began organized bridge building to help their military campaigns. Engineers and skilled workmen formed guilds that were dispatched throughout the empire, and these guilds spread and exchanged building ideas and principles. Secondly, technological, lying on the discovery and growing popularity of the pozzolana, as this fact made a strong turning in these construction types.

Roman bridges are famous for using the circular arch form, which allowed for spans much longer than stone beams and for bridges of more permanence than wood. Where several arches were necessary for longer bridges, the building of strong piers was critical. This was a problem when the piers could not be built on rock, as in a wide river with a soft bed. To solve this dilemma, the Romans developed the cofferdam, a temporary enclosure made from wooden piles driven into the riverbed to make a sheath, which was often sealed with clay. Concrete was then poured into the water within the ring of piles. Although most surviving Roman bridges were built on rock, the Sant’Angelo Bridge (Figure 1.3) in Rome stands on cofferdam foundations built in the Tiber River more than 1,800 years ago.



**Figure 1.3.** Sant’Angelo Bridge, Rome (Owen, 2017)

The Romans built many wooden bridges, but none has survived, and their reputation rests on their masonry bridges. One beautiful example is the bridge over the Tagus River at Alcántara, Spain (built 103-106 AD) shown on Figure 1.4. The arches, each spanning 29 metres, feature huge arch stones (voussoirs) weighing up to eight tons each. Typical of the best stone bridges, the voussoirs at Alcántara were so accurately shaped that no mortar was needed in the joints. This bridge has remained standing for nearly 2,000 years.



**Figure 1.4.** The Roman Alcántara Bridge, Spain (Wikimedia Commons)

Another surviving monument is the Pont du Gard aqueduct near Nîmes in southern France (Figure 1.5), completed in 14 CE. This structure, almost 270 metres long, has three tiers of semi-circular arches, with the top tier rising more than 45 metres above the river. The bottom piers form diamond-shaped points, called cutwaters, which offer less resistance to the flow of water.



**Figure 1.5.** Pont du Gard aqueduct, France (Beyer, 2012)

### **1.1.1.3. The Middle Ages**

After the fall of the Roman Empire, progress in European bridge building slowed considerably until the Renaissance. Fine bridges sporadically appeared, however. Medieval bridges are particularly noted for the ogival, or pointed arch. With the pointed arch the tendency to sag at the crown is less dangerous, and there is less horizontal thrust at the abutments. Medieval bridges served many purposes. Chapels and shops were commonly built on them, and many were fortified with towers and ramparts. Some featured a drawbridge, a medieval innovation. In the Middle Ages, a particular type of bridge started to be built: the inhabited bridge. The most famous bridge of that age was Old London Bridge (Figure 1.6) begun in the late 12<sup>th</sup> century under the direction of a priest, Peter of Colechurch, and completed in 1209, four years after his death. London Bridge was designed to have 19 pointed arches, each with a 7.2-metre span and resting on piers 6 metres wide. There were obstructions encountered in building the cofferdams, however, so that the arch spans eventually varied from 4.5 to 10.2 metres. The uneven quality of construction resulted in a frequent need for repair, but the bridge held a large jumble of houses and shops and survived more than 600 years before being replaced.



**Figure 1.6.** Old London Bridge (Encyclopaedia Britannica)

### **1.1.1.4. The renaissance**

A refined use of stone arch bridges came up during the Renaissance. The large variety and quantity of bridges that were constructed in this period make it impossible to keep a complete list of what was built. However, some masterpieces can be cited, which represent innovations of the time. The first of these was the inhabited Ponte Rialto in Venice (Figure 1.7),

an ornate stone arch made of two segments with a span of 27 metres and a rise of 6 metres. The present bridge was designed by Antonio da Ponte, the winner of a design competition, who overcame the problem of soft and wet soil, by drilling thousands of timber piles straight down under each of the two abutments, upon which the masonry was placed in such a way that the bed joints of the stones were perpendicular to the line of thrust of the arch (Figure 1.7). Other notable structures of this period include the Pont de la Concorde in Paris, designed by J. R. Perronet at the end of the 18th century; London's Waterloo Bridge, by J. Rennie started in 1811; and finally, the New London Bridge (1831).



**Figure 1.7.** The Rialto Bridge, Venice (Bernabei et al., 2019)

#### **1.1.1.5. The period of modernity**

The Industrial Revolution, which began in the late 18<sup>th</sup> century, completely changed the use of material not only in traditional buildings, but also in bridges. Wood and masonry constructions were replaced by iron. In 1779, the first famous cast Iron Bridge (Figure 1.8) was constructed at Coalbrookdale, England, across the Severn River with a semi-circular arch spanning 43 m, heralding the beginning of a new era of arch bridge construction. The great reputation of this bridge, earned for its shape and robustness (for instance, it was the only one that successfully resisted against a disastrous flood in 1795), spurred the master engineer Thomas Telford to design a great number of arched metal bridges, including the surviving Craigellachie Bridge (1814) over the River Spey in Scotland, a 45 m flat arch made of two curved arches connected by X-bracing and featuring two masonry towers at each side (Figure 1.9).



**Figure 1.8.** Iron bridge at Coalbrookdale, England. (Beyer, 2012)



**Figure 1.9.** Craigellachie Bridge, Scotland (tripadvisor.com).

The nineteenth century was a century of advanced iron/steel bridges including arch bridges, suspension bridges, truss bridges, large cantilever bridges and viaducts, built for railway traffic. Eiffel designed two notable railway wrought iron two hinged sickle shaped arch bridges, the Maria Pia Bridge in Porto, Portugal with a span of 160 m and the 165 m span Garabit Viaduct across the Truyeres River at St. Flour, France. The Eads steel bridge at St. Louis is another notable arch bridge of this period, which comprises three 158.5 m spans. This bridge is notable not only for being the first steel bridge but also the first bridge in the world using the cantilever construction method.

In addition to steel, concrete is the other most important construction material for civil engineering works today. The emergence of concrete bridges was at the end of the nineteenth century. The weak-in tension but strong-in-compression nature of concrete makes it perfectly suitable for arch bridges. In 1875, the first reinforced concrete (RC) arch bridge – Marquis of Tilière de Chazelet was designed by Monier.

With the booming development of railway and canal systems in the first half of the twentieth century, more and more bridges were built, especially in Europe. Most of the short and medium bridges were masonry arch bridges. Very few long-span arch bridges were built using masonry because they were not competitive with the new materials, iron, steel and concrete. In the twentieth century, more and more concrete arch bridges were built. In 1904, Hennebique built the Risorgimento Bridge in Rome with a span over 100 m. Freyssinet designed a series of arch bridges in the first half of the twentieth century. A typical example is the Albert Louppe Bridge at Plougastel in France (Figure 1.10) used for both highway and

railway traffic. He also contributed to the arch bridge construction method by employing hydraulic jacks in the crown to lift the completed arch from its false work. The arches designed in this period by Maillart should also be noted for their novelty and beauty. Later on, the Martin Gil Viaduct (Figure 1.11) with a span of 210 m in Spain was completed in 1942; and the Sandö Bridge with a span of 264 m in Sweden was completed in 1943.

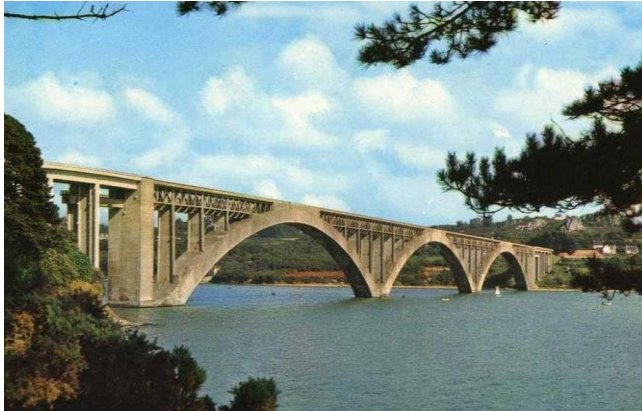


**Figure 1.10.** The Plougastel Bridge (Beyer, 2012)

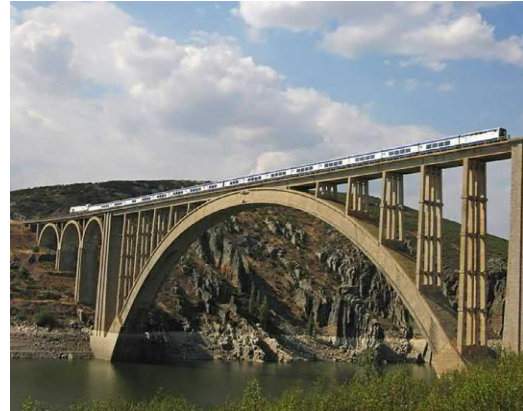


**Figure 1.11.** The Martín Gil Viaduct, Spain (Pipinato, 2021)

With the development of concrete arch bridges, the application of steel arch bridges was also advanced. At the beginning of 1930s, a further breakthrough in steel arch bridges was accomplished with the Bayonne Bridge with a main span of 503.6 m in New York (Figure 1.12) and the Sydney Harbour Bridge in Australia with a main span of 503 m.



**Figure 1.12.** The Bayonne Bridge, New York (Pipinato, 2021)

In the last half of the twentieth century, the record spans of both the steel and concrete arch bridges were successively eclipsed. The New River Gorge Bridge in Fayetteville, West Virginia, completed in 1977, extended the world record of steel arch bridge span to 518.3 m. The primary structure of the bridge is a two-hinged truss arch, with a rise-to-span ratio of 1:4.6.

A few representative concrete arch bridges built in the second half of the twentieth century are the Arrabida Bridge over the Douro River in Porto, Portugal with a main span of 270 m completed in 1963; the Gladesville Bridge in Australia with a clear span of 305 m, completed in 1964; and the Amizade Bridge connecting Brazil and Paraguay with a span of 290 m, completed in 1965. In 1979, the span record for concrete arch bridges was broken by Krk Bridges in Croatia (see Figure 1.13) with a main span of 390 m. It was built using the cantilever truss method. The cross-section of the arch consists of assembled precast elements with in-situ concreted joints.



**Figure 1.13.** Krk Island Bridges (Beyer, 2012)

With the continuing economic development since 1980s, numerous bridges have been built, including a large number of arch bridges accompanying the development of material, construction methods as well as design theory. The Wanxian Yangtze River Bridge is a concrete arch bridge with the longest span of 420 m in the world. An innovative construction method was used: a stiff three-dimensional arch steel truss frame, consisting of longitudinal steel tubes filled with concrete as the upper and lower chords, was erected over this span. The steel tubes served as the embedded scaffolding of the arch and held the cast-in-place concrete.

In 2003, the Lupu Bridge in Shanghai, China, crossing the Huangpu River, was opened to traffic. The main span of the bridge is 550 m, the longest span of an arch bridge in the world at that time. However, this record was broken again 6 years later by the Chaotianmen Yangtze River Bridge (Figure 1.14) with a main span of 552 m in Chongqing, China (Xiang et al. 2010).

This bridge is a half-through tied arch bridge with double decks carrying six lanes of highway traffic on the upper level, and two reserved highway lanes and a two railway tracks on the lower level.



Figure 1.14. Chaotianmen Yangtze River Bridge (Wikipedia)

### 1.1.2. Main parts of an arch bridge

Arch bridges are extremely elegant and very effective structures and they are also architectural landmarks. There are various parts that make up arch bridges, but the main ones that will be presented in this section are the following: the arch, abutments and supports, hangers and spandrels. The combination of multiple simple systems allows for a structure where the role of each of its components is well defined.

#### 1.1.2.1. Arch

A distinctive terminology originating from the classic masonry arch and relevant terms is shown in Figure 1.15.

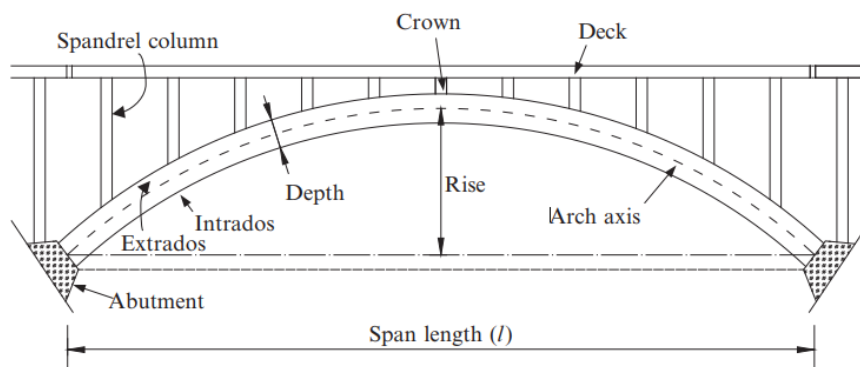
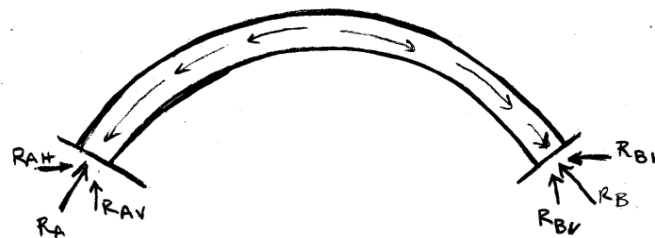


Figure 1.15. Arch bridge nomenclature (Owen, 2017)

An arch is sometimes defined as a curved structural member spanning an opening and serving as a support for the loads above the opening. This definition omits a description of what type of structural element; a bending and/or an axial force element makes up the arch. More specifically, an arch can be referred to as a curved structural form where the forces from dead load are transferred as compression, and tensile forces are eliminated. Depending on the shape of the arch this is more or less true, the “perfect” arch will only carry compression as shown on Figure 1.16, but there is only one perfect arch for any given set of loads so heavy moving loads can often put parts of an arch into tension. Because the arch relies on compression to carry load it is well suited to both masonry and concrete, materials that are strong in compression but weak in tension.



**Figure 1.16.** Forces in an arch (Beyer, 2012)

The arch rib is the main structural member of the arch and is responsible of carrying the different loads generated in the structure. The arch ribs are commonly built using reinforced concrete or steel, but new innovative materials have been used for the arch ribs, including concrete-filled steel tubular, high-performance concrete, steel concrete composites, etc. The arch rib can be built as a truss, a box girder, a plate girder, or as a hollow section, depending on its usage. For long span bridges, the arch rib is composed of truss sections in order to counter the traffic loadings caused by the various vehicles crossing the bridge. The arch rib doesn't only represent the main load-bearing element of an arch bridge, but also represent the most aesthetic component of the bridge.

The arch is particularly suited for bridge construction, especially where steep valley walls provide natural confinement for abutments. The arch is necessary for masonry bridges, because it develops mainly compressive stresses and, as a result, was the preferred form for thousands of years. The arch is still used today, constructed of steel and concrete though not often of true load-bearing masonry, because of its superior aesthetics and use of materials.

### **1.1.2.2. Abutments and supports**

An abutment is the substructure at the ends of a bridge span or dam supporting its superstructure. Single-span arch bridges have abutments at each end which provide vertical and lateral support for the span, as well as acting as retaining walls to resist lateral movement of the earthen fill of the bridge approach. On the other hand, multi-span arch bridges require piers to support ends of spans unsupported by abutments.

An abutment may also refer to the structure supporting one side of an arch, or masonry used to resist the lateral forces of a vault. The impost or abacus of a column in classical architecture may also serve as an abutment to an arch. The word derives from the verb "abut", meaning to "touch by means of a mutual border".

The abutments/supports are one of the most important components of arch bridges because most of the loads carried by the arch rib are transmitted into the abutments. Therefore, the abutments must be heavy and large enough (as on Figure 1.17) to carry the horizontal thrust from the arch. Reinforced concrete and steel are common materials used for the abutments, but new materials like cellular reinforced concrete and mass concrete are used in order to reduce costs. For example, in cellular reinforced concrete abutments, the cellular portion of the abutment is filled with soil in order to adjust the necessary weight of the abutment.

Summarily, the abutments have the following main functions:

- Transfer loads from a superstructure to its foundation elements;
- Resist or transfer self-weight, lateral loads (such as the earth pressure) and wind loads;
- Support one end of an approach slab.



**Figure 1.17.** Abutment of the Blackfriars Railway bridge (midasbridge.com)

### **1.1.2.3. Hangers and spandrels**

Depending on the type of arch bridge, the deck can be supported by spandrels on top of the arch rib or suspended by vertical hangers. For deck arch bridges, solid spandrel walls can be placed on top of the arch rib to support the bridge deck. The fill on the walls are mostly made out of masonry or concrete. However, modern bridges use a different approach by adding vertical spandrels (columns shown on Figure 1.18) made out of steel or concrete that directly support the deck of the bridge.



**Figure 1.18.** Spandrels of a deck arch bridge (midasbridge.com)

For through arch bridges, the deck of the bridge is suspended by hangers (the cables shown on Figure 1.19), which are loaded in tension. The hangers can be designed as I-sections, circular hollow sections, or cables depending on the conditions to which the arch bridge is situated. Furthermore, recent studies on hanger arrangement optimization have shown that sparse hanger systems provide advantages such as better mechanical performance.

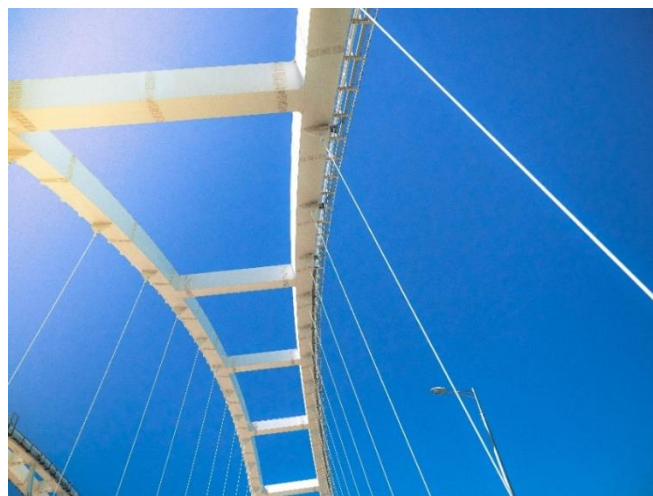


**Figure 1.19.** Hangers of a bridge (midasbridge.com)

### **1.1.3. Types of arch bridges**

Like other kinds of bridges, arch bridges can be grouped in a number of ways. They may be grouped according to different parameters, such as the shape of the arch rib, namely circular-arc or a parabola-shape. However, in this section, the classification focuses on the type of arch bridges according to the deck locations, structural systems and construction materials.

#### **1.1.3.1. According to deck location**

One of the most common ways in which arch bridges can be classified is according to the position of the arch relative to the deck. Doing so, we distinguish three main types of arch bridges namely deck arch, through arch, and half-through arch bridges.

##### **a. Deck arch bridge**

A deck arch bridge represents an arch bridge in which the deck is completely above the crown of the arch. This is the usual type of true arch bridge. It is the most common type of arch and is ideal for crossing a valley with sound rock walls. The space between the deck and the arch, called spandrel (as seen in section 1.1.2.3). When the spandrel is filled with soil or other solid materials, the traffic loading is transmitted through this material onto the extrados of the arch. This type of arch is called filled spandrel arch or solid spandrel arch Figure 1.20a. If there are openings in this space, then the arch is called an open spandrel arch Figure 1.20b in which the loads from the deck are transferred to the arch by struts, or spandrel columns. In an open spandrel arch bridge, the deck may be simple or continuously supported on the spandrel columns, or rigidly connected to tall spandrel columns. If diagonals are added, the arch rib, deck, verticals and diagonals form a truss structure, called a braced spandrel arch or truss arch as shown in Figure 1.20c (Chen & Duan, 2014). In the case when the horizontal girder at deck level meets the arch rib at the crown and is supported by straight inclined legs, this structure is called a rigid-frame arch, as shown in Figure 1.19d. It is convenient to use this type as an overpass with a shallow rise-to-span ratio, satisfying the clearance requirement for traffic underneath.

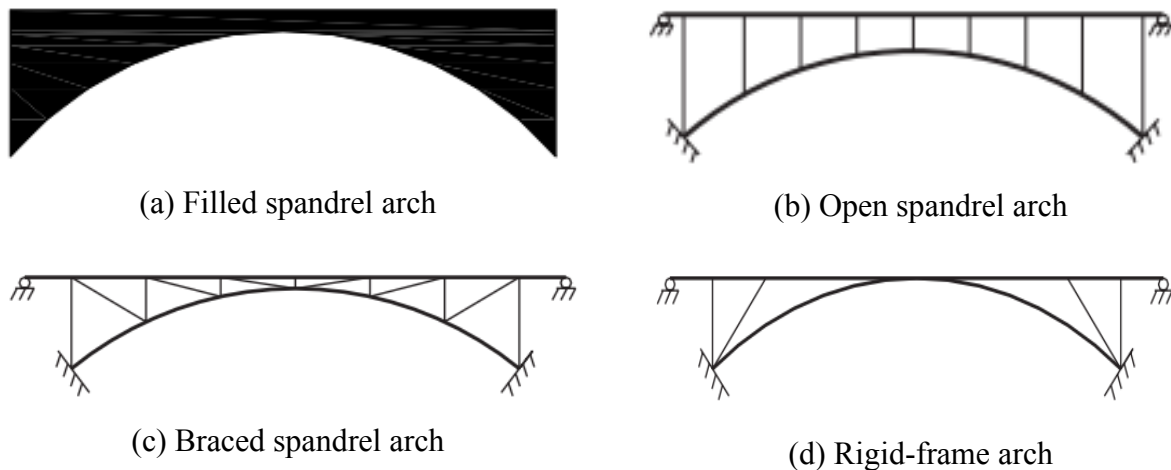


**Figure 1.20.** Deck arch bridges sub-types

### b. Through arch bridge

For an arch bridge in which the deck is at the arch base and passes through the arch, it is often called a through arch bridge. In this case, the deck's thrust is generally absorbed by a tie rod or girder connecting the two ends of the arch, resulting in a tied arch bridge, also called a bowstring arch bridge or Langer girder bridge (Figure 1.21a). It is usually adopted on sites with poor soil foundations. In a through arch, the loads from the deck are transferred to the arch through tension hangers. The tie rod is usually a steel plate girder, a steel box girder or sometimes a prestressed concrete girder.

Besides this first type, we distinguish many other types of through arch bridges. Amongst those we have the tied arch bridge shown in Figure 1.21b in which the arch rib rigidity is greater than that of the stiffened girder, so the rib mainly resists axial forces and bending moments and only axial forces are generated in the stiffened girder. There is another type known as the Lohse arch bridge (Figure 1.21c) having a structure in which the arch rib and the stiffening girder are connected with two elements with flexural stiffness at both ends, and are connected by vertical members that connect the arch rib and stiffening girder using hinges at both ends of the vertical members. Furthermore, an arch bridge with diagonal hangers is often called a Nielsen arch (Figure 1.21d) named after the engineer developed the underlying theory and founded a company of the same name. This is an arch type that uses cables as stayed struts to enhance the aesthetics of the bridge instead of using vertical members with flexural strength. When each of the diagonal hangers' crosses with others more than one time, the arch is also called a network arch (Figure 1.21e).

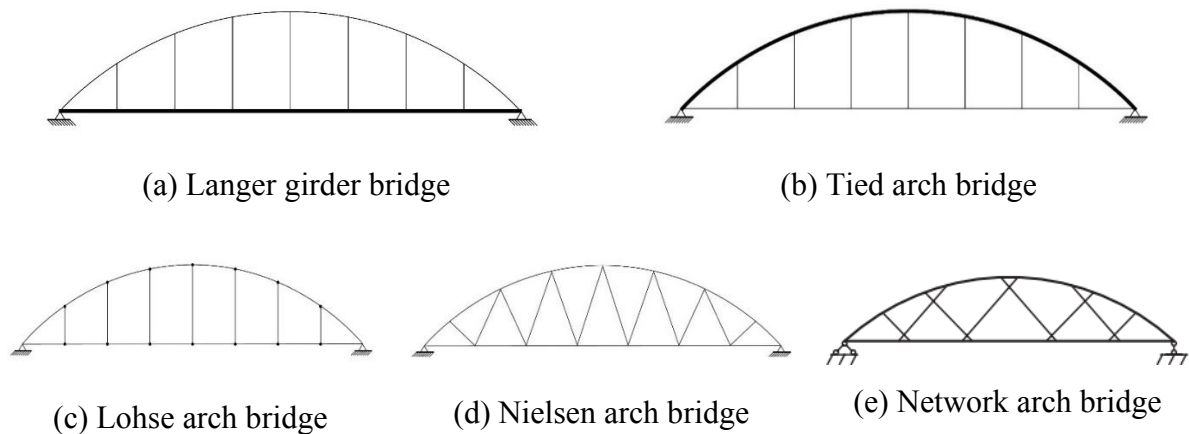


**Figure 1.21.** Various through arch bridges types (midasbridge.com)

**c. Half-through arch bridge**

This is an arch bridge which has a bridge deck located at an elevation between the crown of the arch and the springing line of the arch. It can be a true arch (Figure 1.22a) or a tied arch with flanking spans. The flanking span can be further classified as a cantilever arch (Figure 1.22b) or a half through rigid-framed arch (Figure 1.22c). A cantilever arch is supported by bearings and tied by rigid girders. A half-through rigid-framed arch, nickname of flying-bird arch, is rigidly connected to the piers and tied by cables; an arrangement widely used in Concrete Filled Steel Tube (CFST) arch bridges in China.

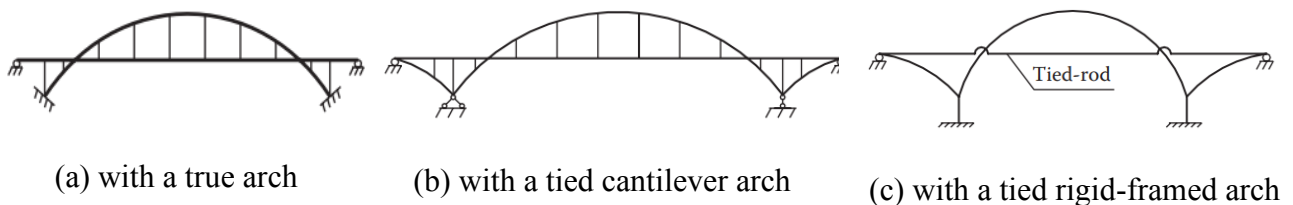


**Figure 1.22.** Half-through arch bridges types (Chen & Duan, 2014)

**1.1.3.2. According to structural systems**

An arch system can be grouped as a fixed arch, two-hinged arch, or three-hinged arch according to the number of hinges.

The fixed arch (or hingeless arch) as shown on Figure 1.23a is fixed at the abutments so that bending moments are transmitted to the abutment. The fixed arch has three redundancies, allows no rotation at the foundations. Fixed arch is a very stiff structure and suffers less deflection than other arches. However, as fixed arch is a structurally indeterminate structure, a

great deal of forces will be generated at the foundation. Therefore, fixed arch bridges can only be built where the ground is very stable. The fixed arch is most often used in reinforced concrete bridges, where the spans are short.

The hinged arches (Figure 1.23b) involve three hinge arrangements: single-hinged type, two-hinged type, and three-hinged type (Xanthakos, 1993). In arch bridges, two hinges or three hinges are frequently used. The two-hinged arch has pins at the end bearings, so that only horizontal and vertical components of force act on the abutment. The two-hinged arch is most often used to bridge long spans. The three-hinged arch has a hinge at the crown as well as the abutments, making it statically determinate and eliminating stresses due to temperature changes and rib shortening. In addition, the less complex forces on the bases can simplify the foundation design. Three-hinged arch also has obvious drawbacks. For example, three-hinged arch bridges have smaller rigidities and therefore experience much more deflection. In addition, the hinges are complex in fabrication. Steel arch bridge can be built as either hingeless (fixed) or hinged.

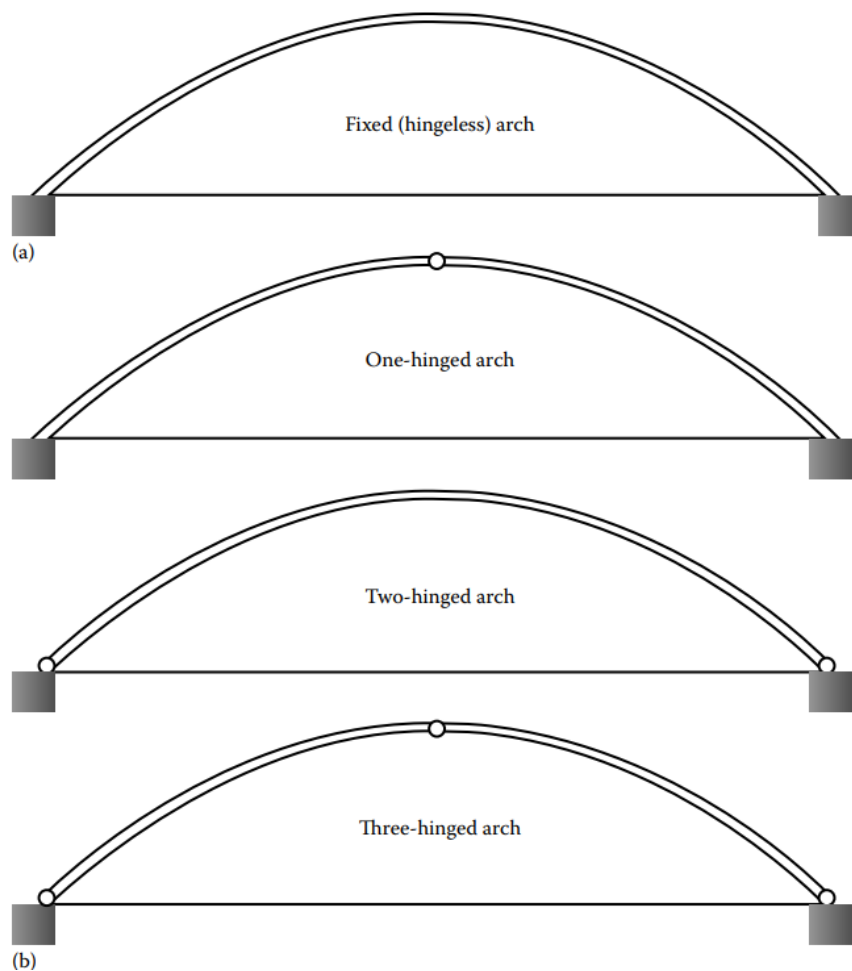


**Figure 1.23.** Fixed and hinged arch bridges (Fu & Wang, 2014)

### **1.1.3.3. According to construction materials**

Arch bridges have been built since ancient times due to easy accessibility of stone masonry, which is an appropriate material for sustaining compressive forces. The Aqueduct Bridge (or the Aqueduct of Segovia) in Spain is a Roman aqueduct and one typical and best-preserved ancient stone arch bridge. The Ponte Sant'Angelo in Rome (previously illustrated on Figure 1.3) is also a typical stone arch bridge. In China, the oldest existing stone arch bridge is the Zhaozhou Bridge of 605 AD. It was designed with perforated spandrels allowing a greater passage for floodwaters. Arch bridges designed in this type can be found worldwide, like the Stone Dock Bridge in China (Figure 1.24), the Bridge of Arta in Greece, and the Cenarth Bridge in Wales. In 1634, the Spectacle Bridge (a stone arch bridge) was constructed in Japan, as shown in Figure 1.25. The bridge gets its name from its resemblance to a pair of spectacles when the arches of the bridges are reflected as ovals on the surface of the river. Several stone bridges have been built in Japan and in the world following the construction of this bridge.



**Figure 1.24.** The Stone Dock Bridge in China  
(Owen, 2017)



**Figure 1.25.** The Spectacle Bridge in Nagasaki  
(Owen, 2017)

In addition, arch bridges can also be built with timber because of its high strength to density ratio, but special attention shall be given to its anisotropic behaviour. The Kintai Bridge in Japan is a model timber arch bridge, as shown in Figure 1.26.



**Figure 1.26.** The Kintai Bridge, Japan (wakuwaku.today)

In more modern times, stone and timber arch bridges continued to be built. In addition, other materials like cast iron, steel, and concrete were also increasingly used for the construction of arch bridges. By the end of the 18<sup>th</sup> century, arch bridges began to be built with iron. The Iron Bridge across the River Severn in England was opened in 1781, which became the first arch bridge in the world made of cast iron, as shown previously in Figure 1.8. However, more modern arch bridges are mainly built with reinforced concrete and structural steel, due to the benefits they give, namely the opportunity for slender, elegant arches, and make longer capacity become possible.

#### 1.1.4. Structural behaviour of arch bridges

This section will focus on the structural action of tied arch bridges providing us with a general overview of the structural behaviour of arch bridges. Figure 1.27 portrays the member, loading and displaced shape for a tied arch bridge. The uniform load acts on the concrete roadway deck that is ultimately transferred to the arch hangers.

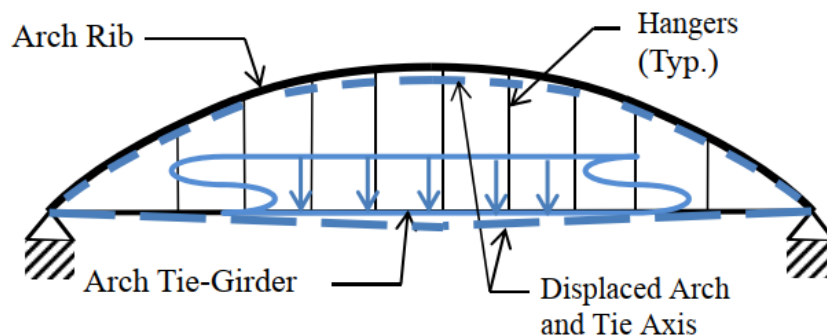


**Figure 1.27.** Tied Arch Structural Arrangement (Finke, 2016)

The loading places the hangers in tension and displaces the arch rib downward (Figure 1.28a). The arch rib is restrained at each end, which as for the two hinged arch, produced an axial shortening and develops a compressive thrust in the arch rib as illustrated on Figure 1.28b.

Finally, as the arch rib exerts an outward thrust on the supports, the arch tie pulls the supports into equilibrium loading the tie girder in tension as shown in Figure 1.28c.

From the standpoint of external statics, the single span tied arch behaves in a determinant manner and reacts on the supporting substructure as if it were a simply supported beam. Internally, however, the system is indeterminate with the behaviour being dependent on the ratio of the tie stiffness to the rib stiffness. In the classic bowstring arch the tie is predominantly a tension member with minimal bending stiffness. In this system the vertical loads are carried almost exclusively by the arch rib. The resulting proportions of the rib and lateral bracing are similar to what they would be if the system were in fact a “true” arch using a compression thrust block instead of a tension tie.

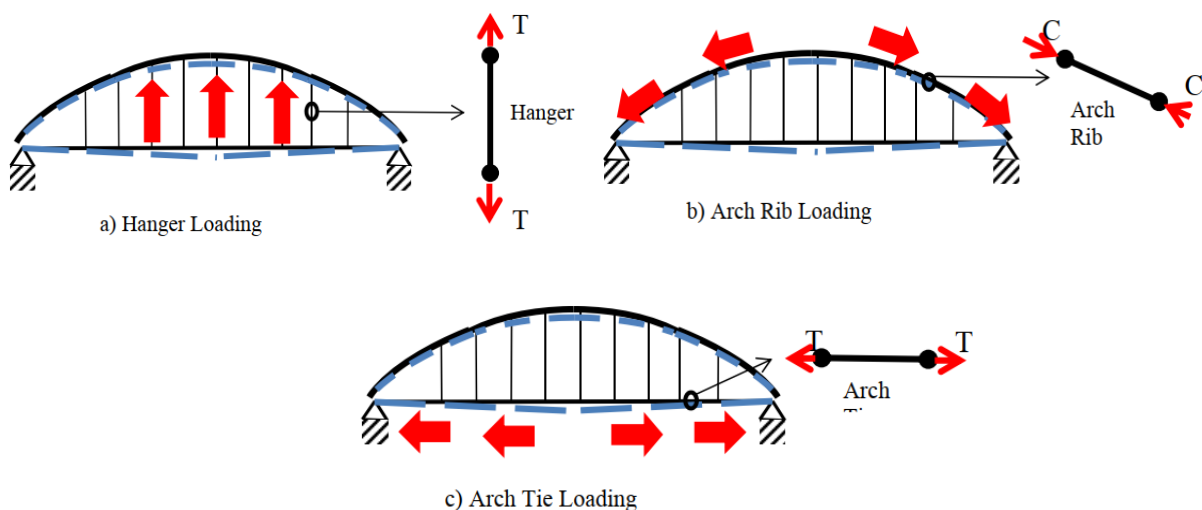


**Figure 1.28.** Tied Arch Structural Action (Finke, 2016)

### 1.1.5. Arch bridge design

The bridge design phase is probably the most fascinating and most difficult task for an experienced engineer if the design is original design and not an industrial or repetitive work. It is unnecessary to provide the definition of the bridge design process, list the various steps required, and detail the bureaucratic procedures involved in this context. Instead, it should be stated that the bridge is a complex structure that introduces into the surrounding landscape

relevant variations, dealing with a number of specialist fields: for example, hydraulic, geotechnical, landscaping, structural, architectural, economic, and socio-political considerations.

### 1.1.5.1. Bridge design methods

#### a. Allowable Stress Design

Allowable Stress Design (ASD) is also referred to as the service load design or working stress design (WSD). The basic conception (or design philosophy) of this method is that the maximum stress in a structural member is always smaller than a certain allowable stress in bridge working or service conditions. The allowable stress of a material determined according to its nominal strength over the safety factor. Therefore, the design requirements of the ASD method can be expressed as in equation (1.1).

$$\sum \sigma_i \leq \sigma_{all} = \frac{\sigma_n}{FS} \quad (1.1)$$

where  $\sigma_i$  is a working stress due to the design load, which is determined by an elastic structural analysis under the design loading conditions.  $\sigma_{all}$  is the allowable stress of the construction material. The  $\sigma_n$  is the nominal stress of the material, and  $FS$  denotes the safety factor specified in the design specification. Selection of allowable stress depends on several factors, such as the design code, construction materials, stress conditions.

The ASD method is very simple in use, but it cannot give a true safety factor against failure. All uncertainties in loads and material resistance are considered by using the safety factor in ASD. Although there are some drawbacks to ASD, bridges designed based on ASD have served very well with safety inherent in the system. Currently, ASD design method is still used in the bridge design specifications in Japan.

#### b. Load Factor Design

To overcome the drawbacks of the ASD design method, the ultimate load design method was developed in reinforced concrete design, which was modified as the Load Factor Method Design (LFD). In this method, different load multipliers were introduced, and the LFD design checks are generally be expressed in equation (1.2).

$$\sum \gamma_i Q_i \leq \phi R_n \quad (1.2)$$

where  $\gamma_i$  is a load factor and  $\phi$  is the strength reduction factor,  $Q_i$  and  $R_n$  are, respectively, load effect and nominal resistance.

### c. Load and Resistance Factor Design

Currently, limit state design (LSD) is the most popular design concept for bridge design and widely used for many countries in the world. In the United States, it is known as load and resistance factor design (LRFD). Load and Resistance Factor Design is a design methodology in which applicable failure and serviceability conditions can be evaluated considering the uncertainties associated with loads by using load factors and material resistances by considering resistance factors. The LRFD was approved by AASHTO in 1994, in the LRFD Highway Bridge Design Specifications. Equation (1.3) is the basis of LRFD methodology (AASHTO, 2007).

$$\sum \eta_i \gamma_i Q_i \leq \phi R_n = R_r \quad (1.3)$$

In this equation,  $\eta_i$  is the load modifier,  $\gamma_i$  is the load factor,  $\phi$  is the resistance factor,  $Q_i$  and  $R_n$  are load effect and nominal resistance respectively.

Several limit states, including strength limit state, service limit state, the fatigue and fracture limit state, and the extreme event limit state, are included in this design method. The strength and stability are considered in the strength limit state design. In service limit state design, the stress, deformation, and crack width in service condition should be carefully checked. Stress ranges, stress cycles, and toughness requirement are considered in the fatigue and fracture limit state, and the survival of a bridge during a major earthquake or flood is considered in extreme event limit state. Though the current design specification in Japan is based on the ASD design, the LRFD method is also used for designing the Tokyo Gate Bridge in Japan.

#### 1.1.5.2. Design of arch ribs and ties

Computers greatly facilitate preliminary and final design of all structures. They also make possible consideration of many alternative forms and layouts, with little additional effort, in preliminary design. Even without the aid of a computer, however, experienced designers can, with reasonable ease, investigate alternative layouts and arrive at sound decisions for final arrangements of structures.

**a. Rise-span ratio**

The generally used ratios of rise to span cover a range of about 1:5 to 1:6. The flatter rise is more desirable for through arches, because appearance will be better. Cost will not vary appreciably within the rise limits of 1:5 to 1:6. These rise ratios apply both to solid ribs and to truss arches with rise measured to the bottom chord.

**b. Panel length**

For solid-ribbed arches fabricated with segmental chords, panel length should not exceed 1/15 of the span. This is recommended for aesthetic reasons, to avoid large angular breaks at panel points. Also, for continuously curved axes, bending stresses in solid-ribbed arches become fairly severe if long panels are used. Other than this limitation, the best panel length for an arch bridge will be determined by the usual considerations, such as economy of deck construction.

**c. Ratio of depth to span**

In some arch bridges, the true arches (without ties) with constant depth solid ribs have depth–span ratios from 1:58 to 1:79. The larger ratio, however, is for a short span. A more normal range is 1:70 to 1:80. These ratios also are applicable to solid-ribbed tied arches with shallow ties. In such cases, since the ribs must carry substantial bending moments, depth requirements are little different from those for a true arch. For structures with variable-depth ribs, the depth–span ratio may be relatively small.

For tied arches with solid ribs and deep ties, rib depth may be small, because the ties carry substantial moments, thus reducing the moments in ribs. For a number of such structures, the depth–span ratio ranges from 1:140 to 1:190.

**d. Single-web or box girders**

For very short arch spans, single-web girders are more economical than box girders. Box girders can also be used for solid-ribbed arches. Welded construction greatly facilitates use of box members in all types of structures. For tied arches for which shallow ties are used, some examples in the world show use of members made up of web plates with diaphragms and rolled shapes with posttensioned strands. More normally, however, the ties, like solids ribs, would be box girders.

**e. Dead load distribution**

It is normal procedure for both true and tied solid-ribbed arches to use an arch axis conforming closely to the dead-load thrust line. In such cases, if the rib is cambered for dead load, there will be no bending in the rib under that load. The arch will be in pure compression. If a tied arch is used, the tie will be in pure tension. If trusses are used, the distribution of dead-load stress may be similarly controlled. Except for three-hinged arches, however, it will be necessary to use jacks at the crown or other stress-control procedures to attain the stress distribution that has been assumed. In an idealized uniformly loaded configuration, the thrust line would exhibit the shape of a funicular curve. Practically, even dead load is not perfectly uniform and is transmitted to the arch at panel points, resulting in a thrust line that deviates slightly from the idealized configuration.

**f. Live load distribution**

One of the advantages of arch construction is that fairly uniform live loading, even with maximum-weight vehicles, creates relatively low bending stresses in either the rib or the tie. Maximum bending stresses occur only under partial unbalanced loading not likely to be realized under normal heavy traffic flow. Maximum live-load deflection occurs in the vicinity of the quarter point with live load over about half the span.

**g. Wind stresses**

These may control design of long-span arches carrying two-lane roadways or of other structures for which there is relatively small spacing of ribs compared with span length. For a spacing–span ratio larger than 1:20, the effect of wind may not be severe. As this ratio becomes substantially smaller, wind may affect sections in many parts of the structure.

**h. Thermal stresses**

Temperature causes stress variation in arches. One effect sometimes neglected but which should be considered is that of variable temperature throughout a structure. In a through, tied arch during certain times of the day or night, there may be a large difference in temperature between rib and tie due to different conditions of exposure.

**i. Deflection**

For tied arches of reasonable rigidity, deflection under live load causes relatively minor changes in stress (secondary stresses). For a 220 m span with solid-ribbed arches 2.1 m deep at

the springing line and 1.2 m deep at the crown and designed for a maximum live-load deflection of 1/800 of the span, the secondary effect of deflections was computed as less than 2% of maximum allowable unit stress. For a true arch, however, this effect may be considerably larger and must be considered, as required by design specifications.

### **1.1.5.3. Design of other elements**

A few special conditions relating to elements of arch bridges other than the ribs and ties should be considered in design of arch bridges.

#### **a. Floor system**

Tied arches, particularly those with high-strength steels, undergo relatively large changes in length of deck due to variation in length of ties under various load conditions. Historically, it was considered necessary to provide deck joints at intermediate points to provide for erection conditions and to avoid high participation stresses. However, maintenance concerns regarding leaking of deck joints have resulted in a shift toward continuous decks. Proper detailing and erection sequencing can minimize these stresses.

#### **b. Bracing**

Various arrangements may be used for lateral bracing systems in arch bridges. For example, a diamond pattern, omitting cross struts at panel points, is often effective. Also, favourable results have been obtained with a Vierendeel truss.

In the design of arch bracing, consideration must be given to the necessity for the lateral system to prevent lateral buckling of the two ribs functioning as a single compression member. The lateral bracing thus is the lacing for the two chords of this member. The use of inclined ribs, referred to as a basket-handle configuration, can greatly influence the type and amount of lateral bracing required.

#### **c. Hangers**

These must be designed with sufficient rigidity to prevent adverse vibration under aerodynamic forces or as very slender members (wire rope or bridge strand). A number of long-span structures incorporate the latter type. Recently, post-tensioning strands have been demonstrated to be a viable alternative for hangers. Whereas arches using wire rope or bridge strand hangers are erected based on geometric control, hangers comprised of post-tensioning strands can be erected based on load control as the strands are tensioned. Vibration problems

have developed with some bridges for which rigid members with high slenderness ratios have been used. Corrosion resistance and provision for future replacement are other concerns which must be addressed in design of wire hangers. The use of inclined hangers has been employed for some tied arch bridges. This hanger arrangement can add considerable stiffness to the arch structure and cause it to function similar to a truss system with crossing diagonals. For such an arrangement, stress reversal, fatigue, and more complex details must be investigated and addressed.

### **1.1.6. Erection of arch bridges**

The construction process is an essential part of the conceptual design of any bridge. For an arch bridge, both its greatest advantage and biggest inconvenience are due to its shape. An arch shape has obvious advantages, but it has to be completed in order to be functional. A partial arch during construction of the arch has little to do with the final structure, and the construction method is always a concern when an arch is selected. Erection conditions vary so widely that it is not possible to cover many in a way that is generally applicable to a specific structure.

#### **1.1.6.1. Cantilever erection**

For arch bridges, except short spans, cantilever erection usually is used. This method is the most popular one for arch bridge building. With this method, halves of an arch rib are built separately from two springings to crown and finally closed at the crown. Because the arch before closure is not an efficient load-carrying structure, auxiliary members or structures are necessary during construction. This may require use of two or more temporary piers. Under some conditions, such as an arch over a deep valley where temporary piers are very costly, it may be more economical to use temporary tiebacks. Particularly for long spans, erection of trussed arches often is simpler than erection of solid ribbed arches. The weights of individual members are much smaller, and trusses are better adapted to cantilever erection. For many double-deck bridges, use of trusses for the arch ties simplifies erection when trusses are deep enough and the sections large enough to make cantilever erection possible and at the same time to maintain a clear opening to satisfy temporary navigation or other clearance requirements. According to the load-carrying structure composed of temporary members and the arch rib under erection, the cantilever method can be further categorized into free cantilever method, cable-stayed cantilever method, cantilever truss method, partial cantilever method, and so on

#### **1.1.6.2. Scaffolding method**

The scaffolding method is a classic construction method for arch bridges. All masonry arch bridges are built by this method. Large size of wood-and-steel composite centring was used in the construction of the New Danhe stone arch bridge with a record span of 146 m (Chen & Duan, 2014). Some important concrete arch bridges were also built using this method in history, such as the Albert Louppe (Plougastel) Bridge (see Figure 1.10), the Salginatobel Bridge with 90 m span built in 1930 in Switzerland, the Sandó Bridge, the Arrabida Bridge and the Gladesville Bridge (Troyano 2004). The scaffolding method is still used for various arch bridges today. However, this construction method loses its advantages for a long span bridge. The scaffolding may be formed of timber, bamboo or steel, as well as of combinations of these materials in various structural types. Since it is the main temporary support during the construction, it must have sufficient strength and stiffness to carry the whole or primary part of the weight of the arch, as well as construction loads. The deformation of scaffolding during the construction should be taken into account to ensure that the completed arch is centred with the designed arch axis. Moreover, the scaffolding must be carefully designed and constructed to avoid local or global buckling, and it must be simple to fabricate and erect and easily removed, transported, and reused.

#### **1.1.6.3. Swing method**

The swing method of arch bridge construction start from prefabrication of two half-arches or two half-bridge structures on each bank of the river. When completed, both are rotated into their final position for closure. This method transforms the construction work from a spatial work over the obstacle of the bridge crossing to a more accessible position above level ground. According to the direction of rotation, the swing method can be classified as horizontal swing method, vertical swing method, or a combination of these two methods, the hybrid swing method.

#### **1.1.6.4. Construction methods for tied arch bridges**

For a typical tied steel arch, the deck and steel tie can be erected on temporary erection bents. Once this operation is completed, the arch ribs, including bracings as well as hangers can be constructed directly on the deck. Alternatively, steel ties, and ribs may be erected simultaneously by means of tieback cables. A more spectacular erection scheme, that is economical when it can be used, involves constructing the tied arch span on the shore or on the

piles adjacent and parallel to the shore. When completed, the tied arch is floated on barges to the bridge site and then pulled up vertically to its final position in the bridge.

## **1.2. Redundancy**

In civil engineering, redundancy is a frontier concept. The terms redundancy and alternative load path are often regarded as synonyms, particularly in situations wherein the issues of accidental events and progressive collapse become apparent (Starossek, 2007). Redundancy typically stresses the ability of a structural system to redistribute among its members/connections the loads which can no longer be carried by some other damaged portions. To guarantee redundant structures, the availability of alternative load paths (or additional load-transfer mechanisms) is of paramount importance. Unlike structures exhibiting redundancy, non-redundant structures may fail immediately under local damage, such as loss of load carrying element(s). And for this very reason, redundancy means and also provides an availability of warning prior to system failure. In this section, the concept of redundancy of bridges will be presented starting with the various proposed definitions. Also, the classification of redundancy, its measures and influence will be presented.

### **1.2.1. Definitions**

The dictionary defines the word redundant as “exceeding what is necessary or normal” and provides “superfluous” as a synonym. Traditionally, bridge members have been classified as redundant or non-redundant by the designer by merely looking for alternative load paths (FHWA Bridge Design Handbook Vol. 9, 2012). A good, concise, universally accepted definition of redundancy does not currently exist in the bridge design or evaluation specifications. However, many past works have brought forward interesting definitions for this concept.

According to Ghosn & Moses (1998), bridge redundancy is the capability of a bridge to continue to carry loads after damage to or the failure of one or more of its members. Member failure can be either ductile or brittle. It can be caused by the application of large live loads, the sudden loss of one element due to brittle fracture, or an accident such as a collision by a truck, ship, or debris. The capability of a bridge to continue to carry loads after a member’s failure is due to its ability to redistribute these applied loads.

Similarly, McCullah & Gray (2005) define redundancy of a bridge structure as the capability of the structure system to continue to carry loads (vertical and lateral) after the failure of any of its components. Various non-natural, environmental, and natural hazards may cause the overloading or the damage of a structure. These hazards include vessel or vehicle collisions, overweight trucks, winds, earthquakes, and scouring. Depending on the nature of the load and the structural details involved, the failure can be either ductile or brittle. The failure types have drastically different consequences on the bridge system behaviour.

Moreover, Fu & Wang (2014) regard redundancy as the quality of a bridge to perform as designed in a damaged state because of the presence of multiple load paths. Conversely, non-redundancy is the lack of alternate load paths, meaning the failure of a single primary load-carrying member would result in the failure of the entire structure.

Lastly, according to Frangopol & Curley (1987), redundancy in a structure is generally defined as the absence of critical components whose failure would cause collapse of the structure. This implies that the problem of structural redundancy should be discussed in conjunction with "fail-safe" structures. However, there are considerable differences of opinion about the definition of structural redundancy.

Without being exhaustive, it can be noted that the various definitions of redundancy cited above are closely related and will enable anyone to have an insight of the concept.

### **1.2.2. Types of redundancy**

According to current engineering practice, redundancy should provide a structure with adequate alternative load paths in the case of excessive live loads or major component failures. According to the FHWA Bridge Design Handbook Vol. 9 (2012), three types of redundancy are defined as follows.

#### **1.2.2.1. Load path redundancy**

A member is considered load-path redundant if an alternative and sufficient load path is determined to exist. Load-path redundancy as defined by AASHTO Specifications is the type of redundancy that designers consider when they count parallel girders or load paths. A structure is non-redundant if it has only one or two load paths. For example, a bridge superstructure composed of only one or two parallel girders is regarded as non-redundant.

Failure of one girder of a system with one or two load paths is assumed to result in the collapse of the span, hence, the bridge is considered to be non-redundant.

However, merely determining the alternative load paths existence is not enough. The alternative load paths must have sufficient capacity to carry the load redistributed to them from an adjacent failed member. If the additional redistributed load fails the alternative load path, progressive failure occurs, and the members could, in fact, be fracture critical. In determining the sufficiency of alternative load paths, all elements present (primary and secondary members) should be considered.

#### **1.2.2.2. Structural redundancy**

This refers to the redundancy that exists as a result of the continuity within the load path. A member is considered structurally redundant if its boundary conditions or supports are such that failure of the member merely changes the boundary or support conditions but does not result in the collapse of the superstructure. Again, the member with modified support conditions must be sufficient to carry loads in its new configuration. For example, the failure of the negative moment region of a two-span continuous girder is not critical to the survival of the superstructure if the positive-moment region is sufficient to carry the load as a simply-supported girder.

Any statically indeterminate structure such as continuous beams and rigid frames would belong to this type. The Standard Specifications for Highway Bridges (AASHTO, 2002) usually does not assume structural redundancy to be sufficient. For example, even though a continuous two-span two-girder bridge is structurally indeterminate, the standard AASHTO criteria would technically classify it as non-redundant. However, if each critical section of a statically indeterminate system has sufficient ductility capacity against sudden rupture, the system would provide reserve strength allowing it to carry loads beyond the formation of the first plastic hinge.

#### **1.2.2.3. Internal redundancy**

A member is considered internally redundant if alternative and sufficient load paths exist within the member itself such as the multiple plies of a riveted steel member. Internal redundancy means that the failure of one element will not result in the failure of the other

elements of the member. For example, cracks that develop in one element do not spread to other elements.

### **1.2.3. Basis of bridge redundancy**

With respect to bridge structures, redundancy is the quality of a bridge to perform as designed in a damaged state because of the presence of multiple load paths. Conversely, non-redundancy is the lack of alternate load paths, meaning the failure of a single primary load-carrying member would result in the failure of the entire structure. In general, redundancy issue should exist for all types of bridges. However, of all bridge construction materials, only steel bridge members may have such designation as fracture critical, and with regard to the topic of structural redundancy, the non-redundant steel members are the fracture critical members (FCMs). FCMs are those in axial tension or tension components of bending members whose failure would result in the failure of the structure. These elements are labelled as such on the contract drawings and are subjected to more stringent design, testing, and inspection criteria than those that are part of a redundant system. Caltrans (2004) made a list of members or components, including but not limited to the following, identified as FCMs:

- Tension ties in arch bridges;
- Tension members in truss bridges;
- Tension flanges and webs in two-girder bridges;
- Tension flanges and webs in single or double box girder bridges;
- Tension flanges and webs in floor beams or cross girders;
- Tension braces in the cross frame of horizontally curved girder bridges;
- Attachments welded to an FCM when their dimension exceeds 100 mm in the direction parallel to the calculated tensile stress in the FCM;
- Tension components of bent caps;
- Splice plates of an FCM.

Moreover, Caltrans made a comprehensive flowchart for identifying FCMs of complex steel bridges in Figure 1.29. The definition of a narrow plate girder (PG) system varies slightly from that used in stability discussions when focusing on redundancy. Whereas the system could contain any number of closely spaced girders in stability discussions, twin girder systems alone constitute a narrow system in the context of redundancy. This is due to the fact that only two primary elements exist to transfer load. If one of these fails, the second would be unable to

support the entire weight of the structure, resulting in collapse. Other elements of the bridge, particularly the deck, could be able to carry additional loads encountered due to a non-redundant member failure and prevent collapse, which has been seen in the past. This built-in redundancy is difficult to predict, however, and is not explicitly recognized in the design. As such, for typical PG bridges, a minimum of three girders are required to provide alternate load paths and be considered system redundant.

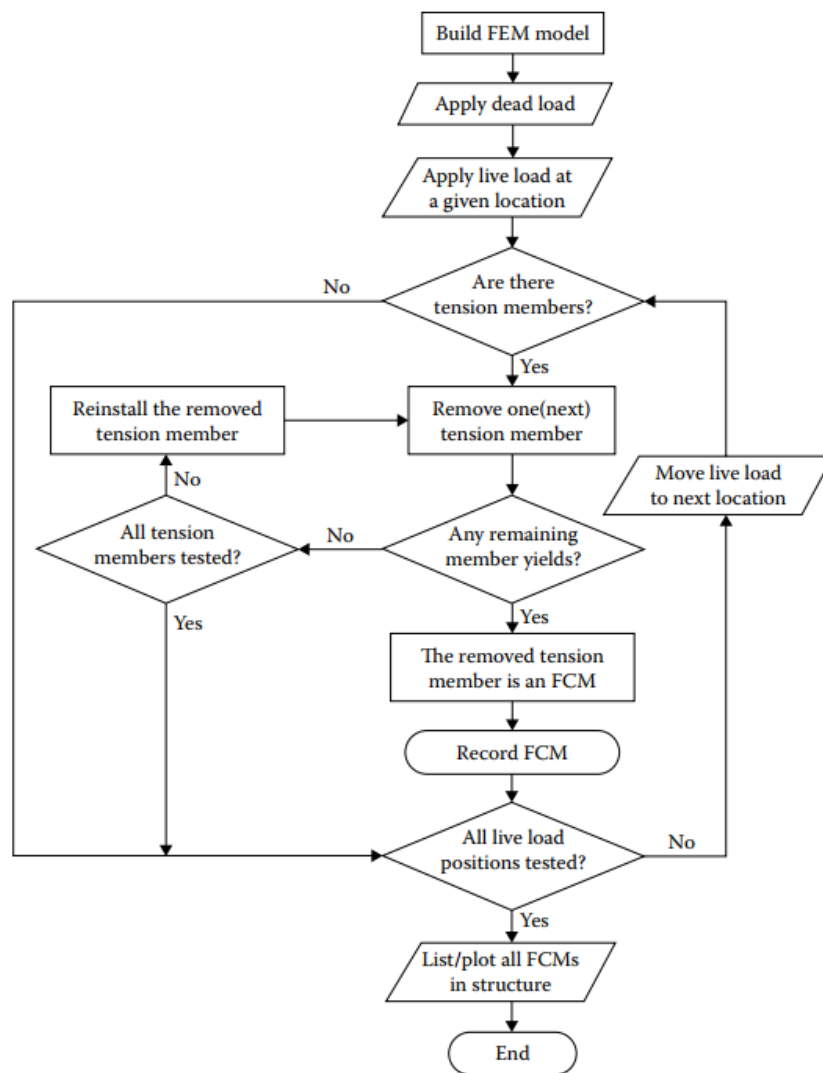


Figure 1.29. Flowchart for identifying FCMs of complex steel bridges (Caltrans, 2004)

#### 1.2.4. Measures of bridge redundancy

As redundancy is defined as the ability of a structural system to continue to carry load after the failure of one or several structural components. Although this concept is well understood, no consensus is currently available on non-subjective measures engineers should use to quantify structural redundancy and how to apply such measures to design adequately

redundant bridges. In an attempt to bridge this gap, several past works have developed different guidelines for the evaluation of redundancy in structural systems. In this section, after a review of the general behaviour of bridge systems, one of the most prevalent guidelines for measuring bridge redundancy will be presented.

#### 1.2.4.1. Typical behaviour of bridge systems

A first step in the process of evaluating bridge redundancy is to have a good understanding of the behaviour of bridge systems under applied loads. The performance of a bridge system can be represented as shown in Figure 1.30, which gives a conceptual representation of the response of a structure to different levels of applied loads and the different criteria that should be considered when evaluating member safety or system safety as well as system redundancy. The model is valid for representing the behaviour of systems under vertical loads or for systems under lateral loads. The green line in Figure 1.30 labelled “Intact system” may represent the applied load versus maximum displacement of a ductile bridge system when subjected to different levels of load. In this case, a load capacity evaluation is performed to study the behaviour of an intact system that was not previously subjected to any damaging load or event.

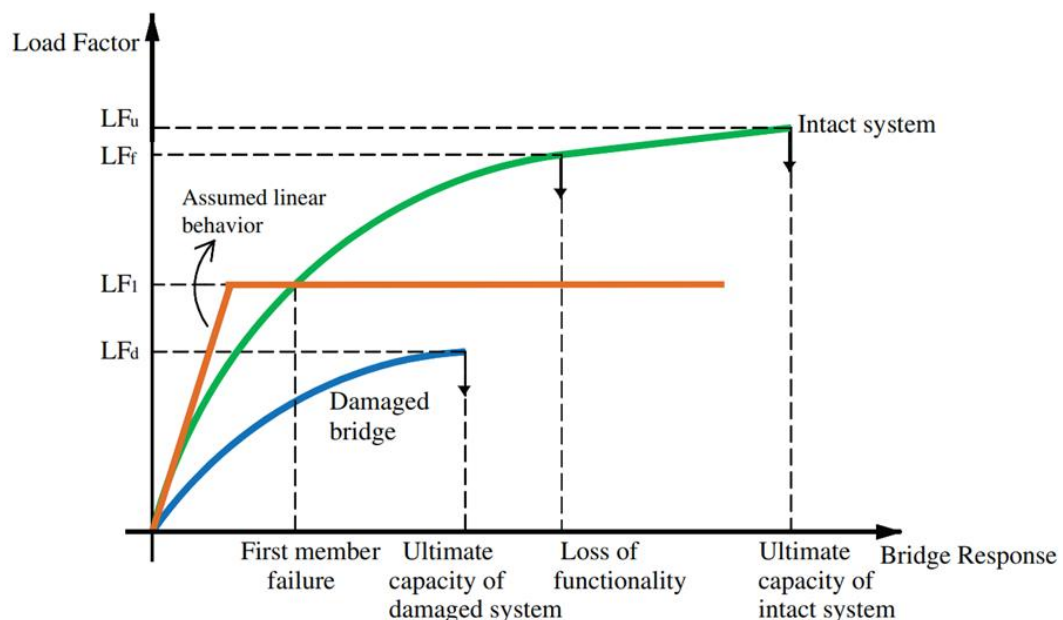


**Figure 1.30.** Representation of typical behavior of bridge systems (Ghosn et al., 2014)

To perform the load capacity analysis, the bridge is first loaded by the dead load and then the transient load is incrementally applied. The first structural member will fail when the transient load reaches  $LF_1$  (Load Factor 1).  $LF_1$  would then be related to member safety.  $LF_1$

may represent the actual load or the multiple of a basic load such as the number of design trucks that the system can carry before the first member reaches its limit capacity. Although  $LF_1$  should be evaluated using the actual response of the bridge accounting for material non-linearity, it has been common in structural design practice to assume linear-elastic response while evaluating the ability of the system to resist the failure of the most critical member as indicated using the bilinear brown curve in Figure 1.30.

Generally, the system will be able to carry additional load after  $LF_1$  is reached and the ultimate capacity of the entire bridge is not reached until the transient load reaches  $LF_u$ .  $LF_u$  would give an evaluation of system safety. Large deformations rendering the bridge unfit for use are reached when the transient load reaches  $LF_f$ .  $LF_f$  gives a measure of system functionality. A bridge that has been loaded up to this point is said to have lost its functionality.

Damage to bridge members leading to the loss in member and system capacity is also a concern. Bridge members are often subjected to fatigue stresses that may lead to the fracture and loss of the load carrying capacity of a main member. In addition, deterioration and corrosion, fire, or an accident, such as a collision by a truck, ship, or debris, could cause the reduction in the load carrying capacity of one or several main members. To ensure the safety of the public, bridges should be able to sustain these damages and still operate at a sufficient level of capacity. Although a damaged bridge cannot be expected to have the same capacity of an intact system, an adequately redundant system should still be able to carry its own weight and some level of transient load to allow for clearing the bridge before closure and the undertaking of necessary repairs. Therefore, in addition to verifying the safety of the intact structure, the evaluation of a bridge's safety and redundancy should consider the consequences of the failure of a critical bridge member. If the bridge has sustained major damage due to the brittle failure of one or more of its members, its behaviour can be represented by the blue curve labelled "Damaged bridge" in Figure 1.30. The ultimate capacity of the damaged bridge is reached when the transient load applied after the application of the dead load reaches  $LF_d$ .  $LF_d$  would give a measure of the remaining safety of a damaged system.

#### **1.2.4.2. Measure of the level of bridge redundancy**

Following the existing studies, it is clear that accounting for bridge redundancy during the safety analysis of new or existing bridges is of primary importance. However, the

mechanisms and the criteria that should be used to quantify bridge redundancy and consider it during the evaluation of bridge safety still have not been fully established.

Nonetheless, the AASHTO Load and Resistance Factor Design (LRFD) Bridge Design Specifications propose to consider redundancy during bridge design by using load modifiers that reflect the ductility, redundancy, and operational importance of the structure. However, the values of the load modifiers provided in the AASHTO LRFD were determined by judgment rather than through a calibration process.

Because redundancy is defined as the capability of a structure to continue to carry loads after the failure of one main member, a comparison between the overall capacity of originally intact and damaged bridge systems as represented by  $LF_u$ ,  $LF_f$ ,  $LF_d$ , in Figure 1.30, compared to the capacity of the most critical member represented by  $LF_1$ , would provide a measure of the level of bridge redundancy. In this context, the researchers define a “system reserve ratio” or “redundancy ratio” for the ultimate limit state as  $R_u$ . For the serviceability limit state, the redundancy ratio is defined as  $R_f$ . For the damaged bridge condition, the redundancy ratio is defined as  $R_d$ . These redundancy ratios are calculated as illustrated in equations (1.4) to (1.6).

$$R_u = \frac{LF_u}{LF_1} \quad (1.4)$$

$$R_f = \frac{LF_f}{LF_1} \quad (1.5)$$

$$R_d = \frac{LF_d}{LF_1} \quad (1.6)$$

The redundancy ratios,  $R_u$ ,  $R_f$ , and  $R_d$ , provide non-subjective deterministic measures of bridge redundancy. For example, when the ratio  $R_u$  is equal to 1.0 ( $LF_u = LF_1$ ), the ultimate capacity of the bridge system is equal to the capacity of the bridge to resist failure of its most critical member; such a bridge is non-redundant. As  $R_u$  increases, the level of bridge redundancy increases. Similar observations can be made about  $R_f$  and  $R_d$ . Although the redundancy ratio  $R_u$  cannot fall below 1.0, the two ratios  $R_f$  and  $R_d$  may, under certain circumstances, have values less than 1.0. A value of  $R_f$  less than 1.0 means that the bridge will exhibit large deformations at a load level smaller than the load that will cause the first member failure. This situation might occur in certain bridges because  $LF_1$  is calculated with a linear-

elastic model, whereas  $LF_1$  accounts for the nonlinear behavior of the bridge. A value for  $R_d$  less than 1.0 means that a damaged bridge may fail at a lower live load than the load that will cause the first member failure in the originally intact linear-elastic system. Thus, the minimum value that  $R_u$  can take is normally 1.0, indicating that some bridge systems may collapse when only one member reaches its load carrying capacity. However,  $R_d$  can be as low as 0.0, indicating that a bridge system may collapse under its own dead weight if a certain damage scenario takes place.

The measures given in equations (1.4), (1.5) and (1.6) indicate that structural systems are associated with different levels of redundancy. This is different than current convention that stipulates that a system is either redundant or non-redundant. The measures of redundancy set in the above equations are normalized, which makes them independent of the bridge specifications being followed and whether the bridge system is overdesigned or under designed. This makes the proposed measures valid for the evaluation of existing bridges as well as new designs. The measures also are valid whether the bridge is deficient or up to standards.

To check whether a bridge system has adequate levels of redundancy, it is sufficient to use a nonlinear structural analysis program to calculate  $LF_u$ ,  $LF_f$ ,  $LF_d$ , and  $LF_1$ , and to verify that  $R_u$ ,  $R_f$ , and  $R_d$  are adequate. If the system configuration does not provide sufficient levels of redundancy, the bridge configuration may need to be changed. Note that even if the levels of redundancy  $R_u$ ,  $R_f$ , and  $R_d$  are lower than expected, the bridge may still have high overall levels of member and system safety with high values for  $LF_u$ ,  $LF_f$ ,  $LF_d$ , and  $LF_1$ . Alternatively, a redundant system with high  $R_u$ ,  $R_f$ , and  $R_d$  values may have low overall system safety levels. Thus, a bridge with adequate redundancy levels may still be unsafe for certain applications if its member safety level  $LF_1$  is too low. Therefore, the goal of any bridge design specifications should not be limited to providing adequate redundancy levels but to assure adequate system safety levels. Thus, if a bridge system does not provide an adequate level of redundancy, the bridge members could be conservatively designed to increase  $LF_1$  as well as  $LF_u$ ,  $LF_f$ , and  $LF_d$ , and reduce the probability of member failures and, more importantly, reduce the probability of system collapse.

## **1.2.5. Redundancy and progressive collapse**

### **1.2.5.1. Generalities**

Another type of redundancy is the structural behaviour under dynamic loads, such as earthquake loading or blast loading. The effect of blast loading is more localized than earthquake's global effect. The ability to sustain local damage without total collapse (structural integrity) is a key similarity between seismic-resistant and blast-resistant designs. In general, the term progressive collapse has constantly been used in the redundancy analysis. As stated in ASCE/SEI 7-10 (2010), progressive collapse is defined as the spread of an initial local failure from element to element, eventually resulting in the collapse of an entire structure or disproportionately large part of it. To achieve targeted integrity during blast, the redundancy of the gravity load-carrying structural system takes centre stage in tackling the issue of progressive collapse. This is not explicitly addressed in any code. However, ASCE/SEI 7-10 (2010) implies a desired alternate load path in the event one or more beams and/or columns of a building fail as a result of a blast. The structure should be able to remain stable by redistributing the gravity loads to other members and subsequently to the foundation through an alternate load path, while keeping building damage somewhat proportional to the initial failure. For performance-based designs, factors considered include life safety issues, progressive collapse mechanisms, ductility of certain critical components, and redundancy of the whole structure. Blast load damages structures through propagating spherical pressure waves, which can be simulated by a series of equivalent loads. Performance of bridge elements under equivalent static loads can be considered as reasonably similar to that under the original dynamic blast loads. For the evaluation of the existing bridges under blast loading, the structural performance levels, the immediate occupancy (IO) level, life safety (LS) level, and the collapse prevention (CP) level, adopted in the FEMA 310 (1998) for the seismic evaluation of buildings, are used here.

### **1.2.5.2. Redundancy and progressive collapse analysis**

In general, a static redundancy and progressive collapse analysis of bridges includes three steps (Khuyen, 2016) as shown in the flow chart in Figure 1.31.

Step 1 checks the performance of the intact bridge before assumptions of any sudden breakage of members. The event of a member fracture relates two types of loadings, including primary loading and impact loading. The primary loading is used to cause the initial member fracture. It may be overweight trucks, traffic collision, corrosion or fatigue cracks.

Step 2 assumes the fractured scenario for the bridge. The fractured members in the fractured scenario are candidates of FCMs. The FCMs usually are members causing one or some remaining members to yield due to its loss. In a real bridge, damage scenario can appear on more than one member. However, under the continual inspection of the bridge’s owners, the probability of the presence of two or more member fractures is much lower than the probability of a member fracture. In addition, the case of more than one-member fracture can be a combination of single-member fractures. Mastering the case of one member fracture can achieve background to the further study of redundancy analysis with fractures beyond single member as well as to connections.

Step 3 analyses the model with fractured scenario in step 2. The static analyses such as linear analysis and nonlinear analysis are the most common approaches in this procedure. These static approaches deal with factors such as material elastic or inelastic, geometric first order or second order. These static methods are well known less complicated than dynamic analysis and yet accurate analysis. In the conventional method, the bridge is analysed by linear elastic analysis, then the safety of structure is checked by demand-ratio capacity.

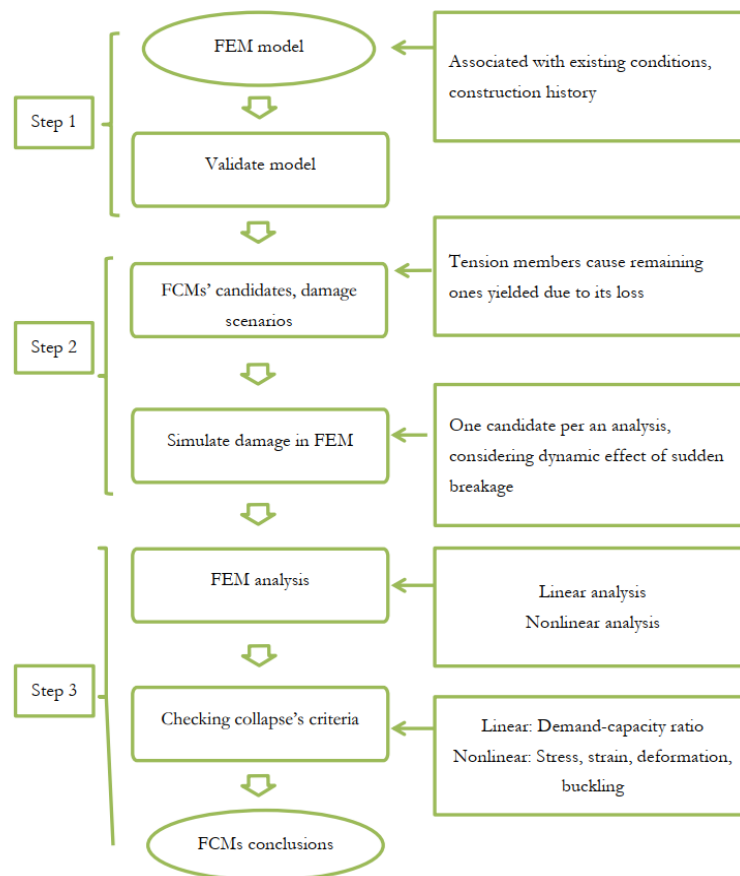
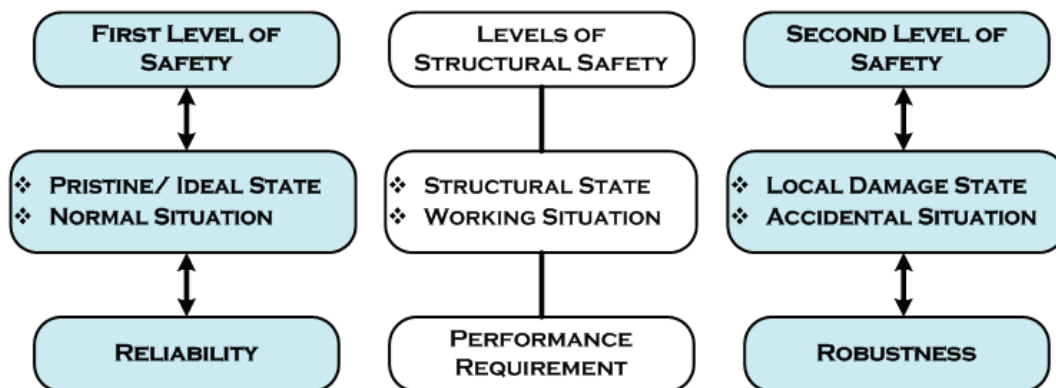


Figure 1.31. Redundancy and progressive analysis procedure (Khuyen, 2016)

### 1.2.6. Redundancy and structural safety

As regards the influence of redundancy, pilot studies customarily paid attention to its positive significance, and appraisal indexes as well, in terms of residual strength, failure probability, or reliability. Nevertheless, practical experience as well as several benchmark studies has shown that: (1) redundancy’s role in an intact structure can be rather limited; (2) increased degree of redundancy may bring with it increased uncertainty (Fang & Fan, 2011). By contrast, little effort has been dedicated to obtain holistic understanding of the redundancy’s role, among which pointed out that redundancy may reduce structural sensitivity to abnormal loadings, but improve structural reliability under design loads. This statement provides insights into redundancy, though it does not take note of the distinct working situations involved in structural safety.

From the life-span point of view, structural safety consists of two levels (as shown on Figure 1.32): firstly, a structure shall withstand loads reliably under normal situations and pristine state; secondly, the structure, or a major part of it, shall remain stable and avoid disproportionate failure under accidental situations and local damage state (Fang & Fan, 2011).



**Figure 1.32.** Different levels of structural safety (Fang & Fan, 2011)

From Figure 1.32, the first level corresponds to the pristine or intact state of a structure together with its reliability requirement, as covered in current reliability-based design/analysis. The second level, however, deals with local damage state and robustness requirement which used to be ignored within the conventional design/analysis envelope. It is thereby evident that principle differences exist between these levels, and this background implies that the role of redundancy ought to be explored in concert with the two underlying safety levels.

Within the present scenario, the significance of redundancy remains two-fold. At the reliability level, redundancy (i.e. the existence of alternative load paths) contributes to the safety

margin of a structure in its intact state; at the robustness level, however, redundancy (i.e. the development of alternative load paths) assists in mitigating the sensitivity/vulnerability of the structure to accidental scenarios. On the other hand, note that structural robustness, otherwise known as ‘structural integrity’ in North America, highlights the tolerance of a structural system to accidental scenarios. The requirement of robustness thus coincides with the objective of hazard mitigation in the sense that “under accidental scenarios, the risk of disproportionate failure should be mitigated to an acceptably low extent”. Undoubtedly, redundancy serves as a key factor for structural robustness because it offers the possibility of avoiding an unacceptable failure (e.g., cascading or progressive collapse) by means of alternative load paths.

### **1.2.7. Enhancing redundancy**

#### **1.2.7.1. Design of new bridges**

The concept of acceptable new bridge designs with varying levels of redundancy as championed by the LRFD Specifications has not found favour among practicing bridge engineers. Tradition has led to designers thinking of a bridge as redundant or nonredundant without varying degrees. As demonstrated (though obtusely) by NCHRP Report 406, bridges traditionally deemed redundant, multi-girder bridges, can be demonstrated to exhibit varying quantifiable degrees of redundancy based upon the number of girders and their spacing. Yet, if designers think of non-redundancy versus redundancy analogously to black versus white, the concept of enhancing redundancy in one way or the other equates to turning non-redundant bridges into redundant ones. The easiest and most effective manner to enhance the performance of non-redundant bridges is the selection of high-performance steels with their inherent enhanced fracture toughness. Non-redundant bridge members, those classified as such and those proven to be quasi-redundant by analysis should be fabricated from high-performance steel. Redundant members need not be fabricated from high-performance steel, unless warranted by unusually special conditions.

Structural redundancy relies on a variety of factors, including structural form/configuration, member sizes, material properties, member/connection properties (like resistance, deformation, or ductility), applied loads and load sequence, and so on (Fang & Fan, 2011). Designing for redundancy, in principle, should take these factors into account. The point lies in deciding when and how to incorporate them into practice. Major aspects of ensuring redundancy will be discussed herein based on different phases of the life cycle of a structure.

**Table 1.1.** Consideration of redundancy enhancement in different phases (Fang & Fan, 2011)

	Structural Form	Material Property	Member Ductility	Continuity
Conceptual Design	● ●	● ●	●	●
Detailing Design		●	● ●	● ●
Construction		●	●	●
Maintenance		●	●	

Considering four phases, i.e. conceptual design, detailing design, construction, and use/maintenance, Table 1.1 has sought to indicate the identified major aspects of ensuring redundancy together with associated phases. Note that a single circle denotes medium level of correlation while two circles denote high correlation. By way of analogy, structural continuity needs to be addressed in conceptual design, for example, by setting settlement and aseismic joints rationally; in course of construction, however, the key to continuity lies in analysing where to set concrete construction joints. For general structural systems, redundancy realisation may be conducted by consideration of the following means: (1) ensuring hyperstatic vertical and/or lateral load-bearing systems; (2) employing ductile materials and connections; (3) providing resistance to load/moment reversals, for example, by setting continuous/symmetrical reinforcement through beam to column connections; (4) providing sufficient tying of structural elements (like edge beams and adjoining slabs).

Finally, it is important to point out that redundancy is not always necessary for improvement of the safety of structural systems. There are certain situations where redundancy does not guarantee an appropriate robustness, and damage propagation needs to be prevented effectively by means of weak links, a strategy analogous to the ‘segmentation’ as proposed in (Starossek, 2007). Under the circumstances, reduced continuity and non-ductile failure modes may be more desirable.

### 1.2.7.2. Rating and retrofit of existing bridges

The application of the system factors suggested in the AASHTO Manual for Bridge Evaluation to the rating of existing bridges could lead to inadequate ratings for bridges with non-redundant members such as two-girder bridges. For example, a two-girder bridge designed without the application of system factors would be rated with a system factor of 0.85 reducing

its resistance by 15%. If this bridge does not rate now, is it significant? The bridge has not changed, but our thoughts on reliability and safety have. Prior to posting or retrofitting, the bridge system (primary and secondary members including the deck and appurtenances) should be analysed to determine if it can be classified as quasi-redundant. Two-girder bridges (or arches or trusses) designed in accord with the LRFD Specifications will actually be more reliable or safer than those designed in accordance with the older AASHTO Standard Specifications for Highway Bridges. The calibration of the LRFD Specifications “set the bar” at the level of safety in multi-girder bridges where the increased load distribution of more refined lateral live-load distribution factors compensated for the increased live load of the HL-93 notional live-load model. Two-girder bridges do not enjoy the load distribution enhancement. This little-recognized fact should be factored into the considerations of rating a bridge with non-redundant members but designed to the LRFD Specifications.

### **1.3. Resilience**

Assessment of the performance of bridges during extreme events has been an issue of concern for engineers and decision makers who are involved with the operation and management of such civil infrastructure systems. A major aspect of arch bridges is the particularity of their geometry. This aspect has made such bridges more and more sensitive to the consequences of extreme or accidental events hazards, as the disruption of only a few components may result in detrimental effects on the performance of the entire bridge. Furthermore, any pronounced damage of the structure components may potentially cause firstly the collapse of the whole structure and secondly extensive human and socioeconomic losses, some of which cannot even be properly measured. It is then necessary to understand and improve the behaviour of bridge structures when exposed to some extreme events.

#### **1.3.1. Definitions**

Resilience is becoming a driving concept for new generations of Building Codes and Standards, particularly in United States and Europe, informing innovative trends and practical policies for design, assessment, monitoring, and maintenance of strategic structures and infrastructure facilities. Several definitions of resilience can be found in literature, based on the epistemological orientation and theoretical background of the reference discipline (Alipour, 2017). This concept can be applied to a variety of systems, such as buildings, bridges,

facilities, infrastructure, network, economics, and communities. The general concept of resilience was first put forth by ecologists more than 40 years ago.

According to Holling, resilience is the perturbation that can be absorbed before the system converges to another state of equilibrium. Primm redefined resilience to be a measure of the speed at which engineering systems return to the equilibrium condition. Another study considered resilience to be the intrinsic ability of a system to adjust its functioning before, during, or after changes and disturbances so that it can sustain required operations under both expected and unexpected conditions (Alipour, 2017).

Bruneau et al. (2003) also conducted a comprehensive analysis of various aspects of resilience at the community level and suggested four dimensions of resilience, called the four R's, which include robustness, redundancy, rapidity, and resourcefulness. According to Bruneau et al., robustness is the ability of the system or system components to withstand external shocks without a significant loss of performance. As previously seen in section 1.2, Redundancy, as previously seen, is the extent to which the system satisfies and sustains functional requirements in the event of a disturbance. Rapidity is the speed at which recovery is accomplished. Resourcefulness is the ability to diagnose and prioritize problems and to initiate a solution through the identification and monitoring of all resources, including economic, technical, and social information. According to this definition of resilience, the implementation of resilience can enhance the performance of the system through reduction of the probability of failure, reduction of the consequences of failure, and reduction of the time to recovery.

In civil engineering, resilience can be defined as the capability of the system to withstand the effects of extreme events and to recover promptly and efficiently the pre-event performance and functionality (Bruneau et al., 2003). Moreover, resilience of a civil infrastructure system is defined in literature as a function that indicates the capability of the system to sustain a level of functionality over a period decided by owners or the society.

### **1.3.2. Illustration of resilience in a system**

To better illustrate the concept of resilience, a system performance curve is defined here. System performance can be measured according to different measures and factors depending on the system considered (bridges in our case). For further illustration, Figure 1.33 depicts the changes in an arbitrary system performance measure,  $Q(t)$ , over time.

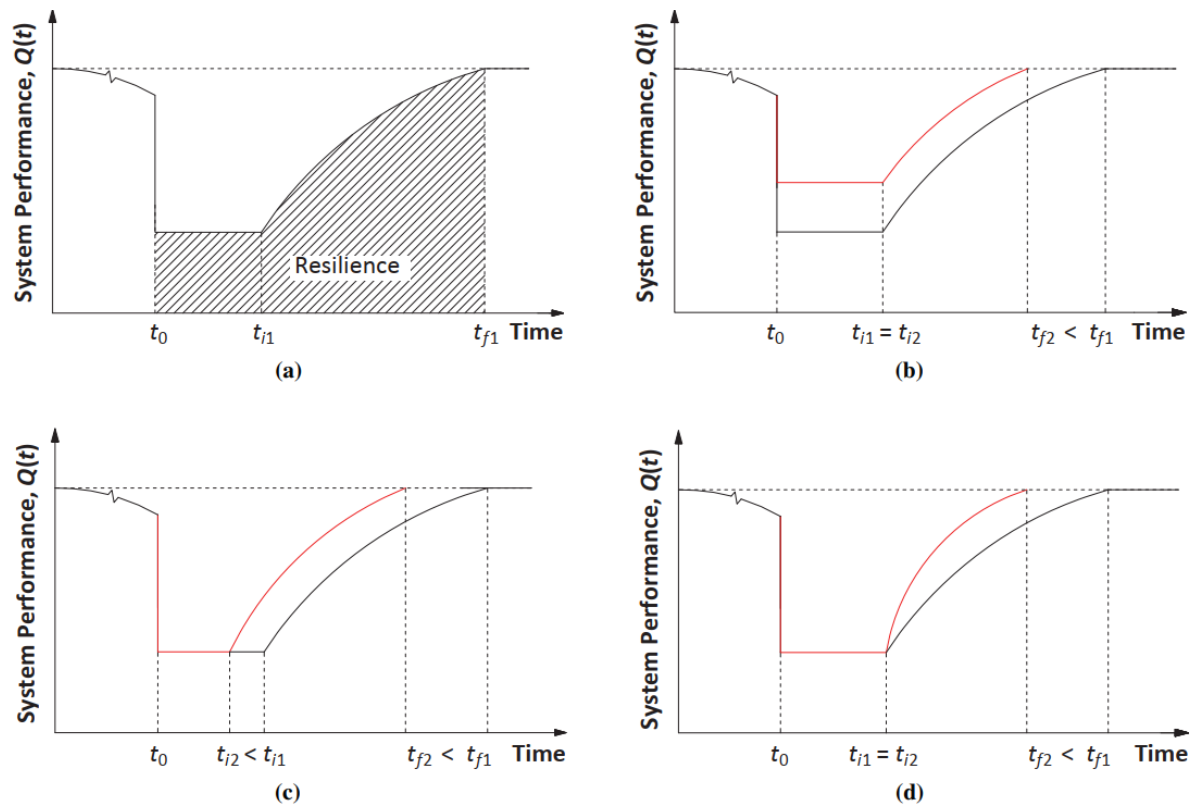


**Figure 1.33.** Estimation of resilience measures through absorptive, adaptive, and restorative capacity of a system (Alipour, 2017)

A major drop in the performance measure is seen when an extreme event occurs, which is considered time zero ( $t_0$ ). On the basis of the state of robustness, the absorptive capacity of the system is affected and the performance that remains may become less than what was expected for a system with no degradation. The cross-hatched area under the performance curve in Figure 1.33a can be considered an indicator of the resilience of the system. After the occurrence of an extreme event, the role of adaptive capacity can be recognized on the basis of the amount of time that it takes for the recovery of the system to begin ( $t_i$ ). This parameter is an indicator of the state of redundancy and the rapidity of the system. Finally, the restorative capacity of the system can be evaluated by the amount of time that it takes for the pre-disaster performance level to be fully regained ( $t_f$ ). This parameter reflects the state of resourcefulness of the system (Figure 1.33).

All the mitigation and recovery efforts planned for a large-scale system require the expenditure of resources. Hence, in addition to the time-based measures, cost-based measures are investigated to obtain reliable estimates of the resilience of deteriorating systems.

### 1.3.3. Framework for estimating resilience

Resilience is generally quantified as a dimensionless quantity representing the rapidity of the system to revive from a damaged condition to the pre-damaged functionality level. System performance following an extreme event (commonly referred to as system vulnerability), resulting losses, and post event system recovery are the three major components used to quantify the disaster resilience of a civil infrastructure system see (Figure 1.34).

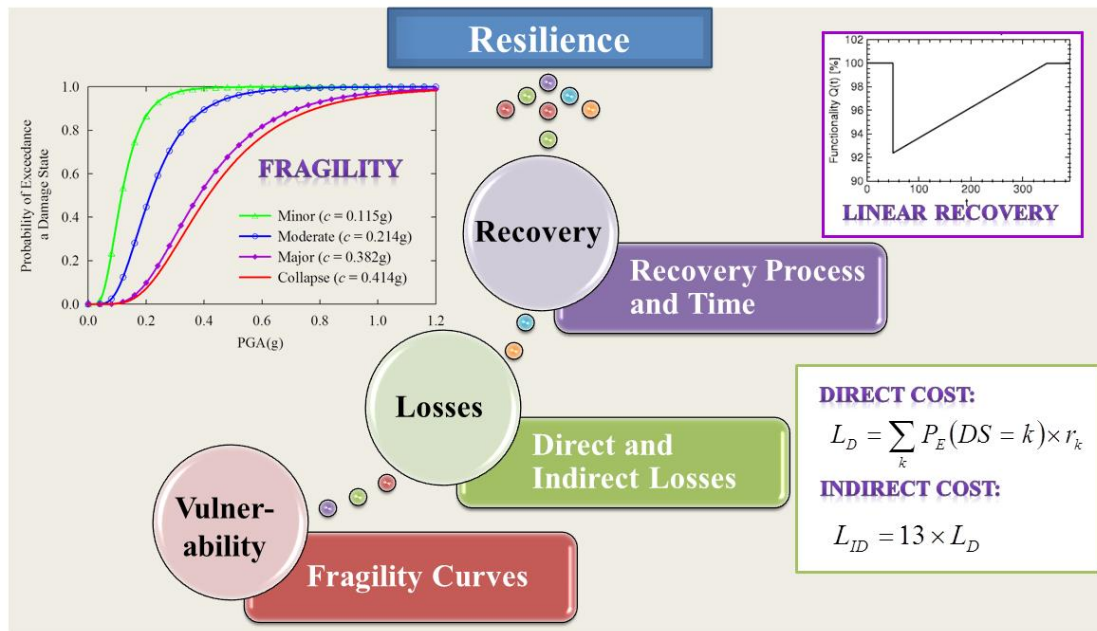


**Figure 1.34.** Proposed framework for resilience quantification (UTCP, 2014)

The vulnerability model was developed from structural analysis under extreme events like natural disasters. This model is expressed in the form of fragility curves that provide probabilities of exceeding various performance levels for different hazard intensities.

The loss model incorporates direct and indirect losses from a post event degraded system over the period of system restoration. The direct loss arises due to system restoration after the event and the indirect loss arises due to post event disrupted functionality of the system. For highway transportation systems, indirect losses consist of rental, relocation, business interruptions, traffic delay, loss of opportunity, losses in revenue, etc.

The recovery model describes a path following which post-event restoration of systems is expected to take place. This model considers the time required to complete system restoration, which greatly depends on the severity of structural damage of systems due to extreme events.

Resilient bridges have the capability to withstand unusual or extreme forces without collapse or loss of lives. They are able to recover from distress or major damage with minimal disruption to traffic and essential services. Three key factors affect the resilience of bridges: ductility, redundancy, and operational importance.

- Ductility in a structural system is characterized by development of significant and visible inelastic deformations before failure.
- Redundancy previously defined as the capability to continue to carry loads after the failure of one of its components. In other words, a redundant bridge system has multiple load paths for distributing the loads when a component fails.
- Operational importance relates to the consequences of loss of use of the bridge. Rapid emergency response is important for the survival of people and the security of the incident scene.

The AASHTO LRFD Bridge Design Specifications recognizes the significant effects of ductility, redundancy, and operational importance on the resilience of bridges. The LRFD Specifications accounts for these effects on the load side of the limit states equation. It recommends the use of multiple load paths and continuous bridges, unless there are compelling reasons for not doing so.

#### **1.3.4. Extreme events**

The performance of bridges under damage and emergency conditions induced by sudden extreme events, such as earthquakes, can be assessed based on the concept of resilience. Resilience of structure and infrastructure systems is generally investigated considering damage and disruptions caused by sudden extreme hazards, such as earthquakes, collisions and explosions. It is therefore necessary to have a basic understanding of extreme events in order to be able to evaluate the resilience of bridges.

##### **1.3.4.1. Definition**

The definition, classification, and diagnosis of extreme events are far from simple. No universal unique definition of what an extreme event is exists. From a mathematical point of view, to define an extreme value, a statistical distribution or a historical distribution is required. Extreme values based on observational data are important in assessments of the safety and life cycles of structures. The prediction of future conditions, especially extreme conditions, is

necessary in bridge design and is performed on the basis of an extrapolation from previously observed data combined with engineering judgment.

Bier et al. (1999) defined “extreme events” to be events that are extreme in terms of both their low frequency and their high degree of severity. Ghosn et al. (2003) defined extreme events to be manufactured or environmental hazards with a high potential for the production of structural damage that are associated with a relatively low rate of occurrence. AASHTO introduced the concept of extreme event limit states to deal with the performance of bridges during earthquakes, scour or other hydraulic events, ice loads, or ship collisions but did not necessarily provide clear definitions of extreme events. The Load and Resistance Factor Design specification adopted a limit state philosophy, or the state beyond which a component ceases to satisfy the provisions for which it was designed. The idea of the limit state provides a systematic approach to ensure the satisfactory short and long-term performance of bridges. Alipour & Shafei (2016) defined extreme events to be those high-intensity events with a lower probability of occurrence that could push the structure beyond its expected response (that is, the response for which the engineer designed the structure).

#### **1.3.4.2. Holistic consideration of extreme events**

In line with those definitions, a holistic definition of an extreme event requires the following (Alipour, 2017):

- An objective and unambiguous identification of the event,
- Definition of the intensity of the event as a function of its features and the risk that it generates for the built environment, and
- Definition of an intensity–frequency probability density function that represents the statistics on the occurrence of the event for each class of intensity.

Here it is believed that for a more holistic definition of the extreme event, three main factors should be considered:

- The definition of the extreme event is a function of space and time: (a) events that are extreme in one area of the world may not be so in another one, and (b) events that are extremes at one time may not be so in the future or may not have been in the past.
- The characterization of an extreme event should take into account the spatial and temporal scales of the event, in addition to its intensity. For instance, the flooding of a

river may result in erosion of the foundations of many of the bridges downstream that would require full or partial closure until full inspections and repairs are conducted.

- The definition of an extreme event is a function of its consequences and the impacts that it has on the safety of the human and the built environment (here, transportation assets).

Table 1.2 shows the likelihoods of different hazards identified by bridge engineers in the United States (US). After follow-up interviews with engineers ranking winds to have a high likelihood of occurrence, it was found out that wind events do not necessarily result in the structural failure of bridges. They had ranked wind to be an event with a high likelihood of causing failure because the secondary effects of the high winds.

**Table 1.2.** Expected likelihood of different hazards across U.S. States identified by state bridge and hydraulic engineers (Alipour, 2017)

Respondent and Hazard Type	Probability (percent)			
	Highly Likely	Likely	Possible	Unlikely
<b>Bridge Engineers</b>				
Collision	34	39	24	3
Scour	20	54	26	0
Wind	18	27	31	24
Floods and debris flow	16	53	29	2
Landslide	14	16	34	36
Fire	5	11	46	38
Storm surge and waves	2	20	18	59
Earthquake	2	11	31	56
Blast	0	0	16	84
Liquefaction	0	5	30	65
<b>Hydraulic Engineers</b>				
Floods and debris flow	28	44	28	0
Scour	28	35	35	2
Storm surge and waves	2	23	26	49

NOTE: Highly likely = almost 100% probability in next year; likely = between 10% and 95% probability in next year; possible = between 1% and 10% probability in next year; unlikely = 1% probability in next year.

It is necessary to precise that these data are only based on the US and thus could considerably be different in other parts of the world

For the purpose of this work, explosions (blast) will be considered due to their severity, dynamic properties and due to the vulnerability of bridge structures to such events.

### **1.3.5. Blast event characterisation**

An explosion can be defined as a very fast chemical reaction involving a solid, dust or gas, during which a rapid release of hot gases and energy takes place. The phenomenon lasts only some milliseconds and it results in the production of very high temperatures and pressures. Blast wave propagation depends on several parameters such as its impulse, the stand-off distance, weight of explosive. All these parameters will be presented below.

#### **1.3.5.1. Ideal blast wave characteristics**

During detonation the hot gases that are produced expand in order to occupy the available space, leading to wave type propagation through space that is transmitted spherically through an unbounded surrounding medium.

The blast wave contains a large part of the energy that was released during detonation and moves faster than the speed of sound. Figure 1.35 shows the idealised profile of the pressure in relation to time for the case of a free-air blast wave, which reaches a point at a certain distance from the detonation. The pressure surrounding the element is initially equal to the ambient pressure  $P_o$ , and it undergoes an instantaneous increase to a peak pressure  $P_{so}$  at the arrival time  $t_A$ , when the shock front reaches that point. The time needed for the pressure to reach its peak value is very small and for design purposes it is assumed to be equal to zero. The peak pressure  $P_{so}$  is also known as side-on overpressure or peak overpressure. The value of the peak overpressure decreases with increasing distance from the detonation centre. After its peak value, the pressure decreases with an exponential rate until it reaches the ambient pressure at  $t_A+t_o$ ,  $t_o$  being called the positive phase duration. After the positive phase of the pressure-time diagram, the pressure becomes smaller (referred to as negative) than the ambient value, and finally returns to it. The negative phase is longer than the positive one, its minimum pressure value is denoted as  $P_{so}^-$  and its duration as  $t_o^-$ . During this phase the structures are subjected to suction forces, which is the reason why sometimes during blast loading glass fragments from failures of facades are found outside a building instead in its interior.

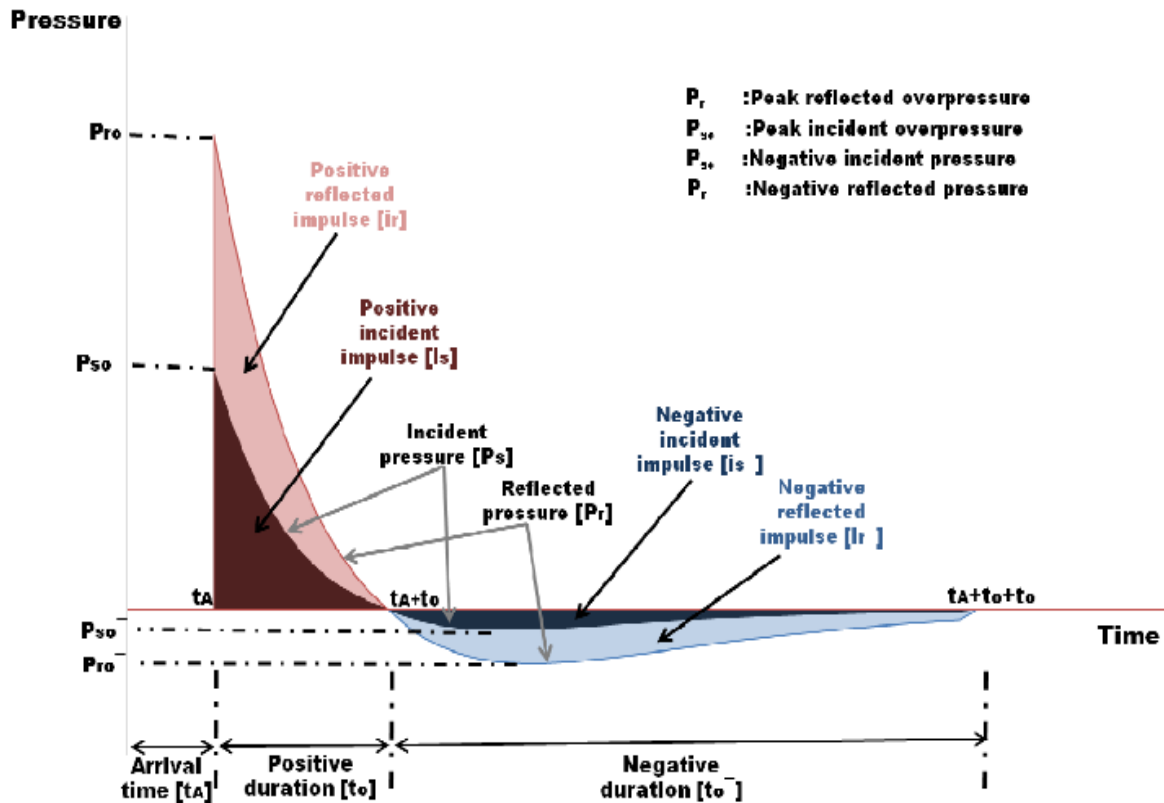


Figure 1.35. Blast pressure distribution over time (Karlos et al., 2016)

The negative phase of the explosive wave is usually not taken into account for design purposes as it has been verified that the main structural damage is connected to the positive phase. As it can be seen from Figure 1.35, the positive incident pressure decreases exponentially. The following form of Friedlander’s equation (1.7) has been proposed and is widely used to describe this rate of decrease in pressure values.

$$P_s(t) = P_{s0} \left(1 - \frac{t}{t_0}\right) e^{-b\frac{t}{t_0}} \tag{1.7}$$

Where:  $P_{s0}$  is the peak overpressure

$t_0$  is the positive phase duration

$b$  is a decay coefficient of the waveform

$t$  is the time elapsed, measured from the instant of blast arrival

The decay coefficient  $b$  can be calculated through a non-linear fitting of an experimental pressure time curve over its positive phase. Besides the peak pressure, for design purposes an

even more important parameter of the blast wave pulse is its impulse because it relates to the total force (per unit area) that is applied on a structure due to the blast. It is defined as the shaded area under the overpressure-time curve of Figure 1.35. The impulse is distinguished into positive  $i_s$  and negative  $i_s^-$ , according to the relevant phase of the blast wave time history. Equation (1.8) gives the expression in the case of the positive impulse, which is more significant than its negative counterpart in terms of building collapse prevention.

$$i_s = \int_{t_A}^{t_A+t_o} P_s(t) dt \quad (1.8)$$

From equation (1.9), the positive impulse can be analytically calculated as:

$$i_s = \frac{P_{so} t_o}{b^2} [b - 1 + e^{-b}] \quad (1.9)$$

This equation constitutes an alternative way for solving iteratively for the decay parameter  $b$  when the values of  $i_s$ ,  $P_{so}$  and  $t_o$  are known from experimental data.

### 1.3.5.2. Blast parameters

The principal blast loads parameters are stand-off distance and explosive type and weight.

#### a. Stand-off distance

One of the most critical parameters for blast loading computations is the distance of the detonation point from the structure of interest. The peak pressure value and velocity of the blast wave, which were described earlier, decrease rapidly by increasing the distance between the blast source and the target surface (Figure 1.36). In the figure, only the positive phases of the blast waves are depicted, whose durations are longer whenever the distance from the detonation point increases.

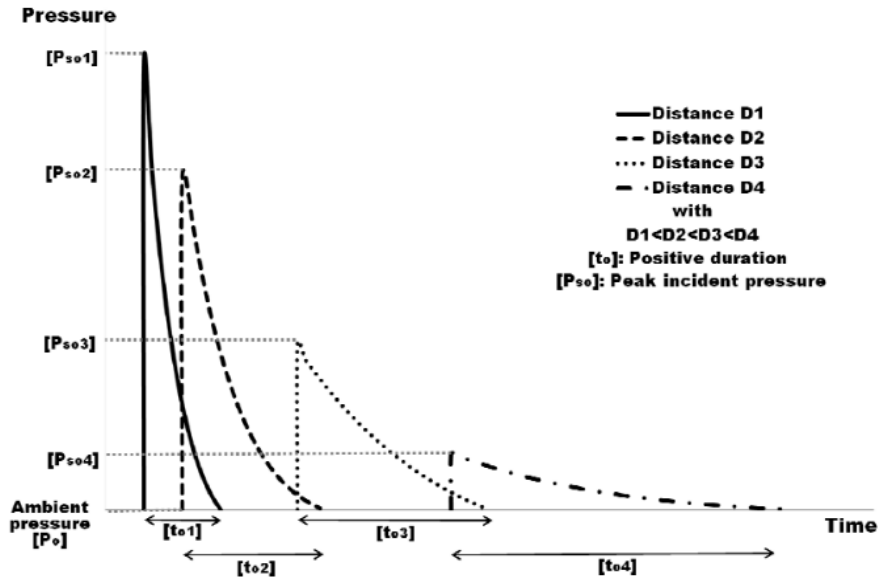


Figure 1.36. Influence of distance on the blast positive pressure phase (Karlos et al., 2016)

The effect of distance on the blast characteristics can be taken into account by the introduction of scaling laws. According to Hopkinson-Cranz law, a dimensional scaled distance is introduced as described by equation (1.10).

$$Z = \frac{R}{\sqrt[3]{W}} \tag{1.10}$$

Where:  $R$  is the distance from the detonation source to the point of interest

$W$  is the weight of the explosive used

**b. Explosive type and weight**

The wide variety of explosives has led to the adoption of a universal quantity, which is used for all necessary computations of blast parameters. TNT (Trinitrotoluene) was chosen as its blast characteristics resemble those of most solid type explosives. An equivalent TNT weight is computed according to equation (1.11) that links the weight of the chosen design explosive to the equivalent weight of TNT by utilizing the ratio of the heat produced during detonation:

$$W_e = W_{exp} \frac{H_{exp}^d}{H_{TNT}^d} \tag{1.11}$$

Where:

$W_e$  is the TNT equivalent weight

$W_{exp}$  is the weight of the actual explosive

$H_{exp}^d$  is the heat of detonation of the actual explosive

$H_{TNT}^d$  is the heat of detonation of the TNT

### 1.3.5.3. Blast pressure determination

There are various relationships and approaches for determining the incident pressure value at a specific distance from an explosion. All the proposed relationships entail computation of the scaled distance, which depends on the explosive mass and the actual distance from the centre of the spherical explosion.

Kinney and Graham presents a formulation that is based on chemical type explosions (Karlos & Solomos, 2013). It is described by equation (1.12) and has been used extensively for computer calculation purposes.

$$P_{so} = P_o \frac{808 \left[ 1 + \left( \frac{Z}{4.5} \right)^2 \right]}{\left\{ \left[ 1 + \left( \frac{Z}{0.048} \right)^2 \right] \left[ 1 + \left( \frac{Z}{0.32} \right)^2 \right] \left[ 1 + \left( \frac{Z}{1.35} \right)^2 \right] \right\}^{0.5}} \quad (1.12)$$

Where:  $Z$  is the scaled distance

$P_o$  is the ambient pressure

Other relationships for the peak overpressure for spherical blast include those of (Brode, 1955) shown in Equations (1.13a) and (1.13b). The pressure  $P_{so}$  in bars is given as:

$$P_{so} = \begin{cases} \frac{6.7}{Z^3} + 1 & , \text{for } P_{so} > 10 \text{ bar} \\ \frac{0.975}{Z} + \frac{1.455}{Z^2} + \frac{5.85}{Z^3} - 0.019 & , \text{for } 0.1 < P_{so} < 10 \text{ bar} \end{cases} \quad (1.13a)$$

$$(1.13b)$$

Another formulation, that is widely used for computing peak overpressure values for ground surface blast has been proposed by Newmark (equation 1.14) and does not contain categorization according to severity of the detonation.

$$P_{so} = 6784 \frac{W}{R^3} + 93 \sqrt{\frac{W}{R^3}} \quad (1.14)$$

$P_{so}$  is in bars

$W$  is the charge mass in metric tons (=1000kg) of TNT and

$R$  is the distance of the surface from the centre of a spherical explosion in  $m$ .

Mills has also introduced an expression of the peak overpressure in kPa (Karlos & Solomos, 2013), in which  $W$  is expressed in kilograms of TNT and the scaled distance  $Z$  is in  $m/kg^{1/3}$  represented in equation (1.15).

$$P_{so} = \frac{1772}{Z^3} - \frac{114}{Z^2} + \frac{108}{Z} \quad (1.15)$$

#### 1.3.5.4. Explosion and blast-loading types

As shown in Figure 1.37, they can be distinguished in three basic types, which depend on the relative position of the explosive source and the structure to be protected i.e., on the height  $H^*$  above ground, where the detonation of a charge  $W$  occurs, and on the horizontal distance  $RG$  between the projection of the explosive to the ground and the structure. These three explosion types are:

- (a) Free-air bursts: The explosive charge is detonated in the air; the blast waves propagate spherically outwards and impinge directly onto the structure without prior interaction with other obstacles or the ground.
- (b) Air bursts: The explosive charge is detonated in the air, the blast waves propagate spherically outwards and impinge onto the structure after having interacted first with the ground: a Mach wave front is created.

- (c) Surface bursts: The explosive charge is detonated almost at ground surface; the blast waves immediately interact locally with the ground and they next propagate hemispherically outwards and impinge onto the structure.

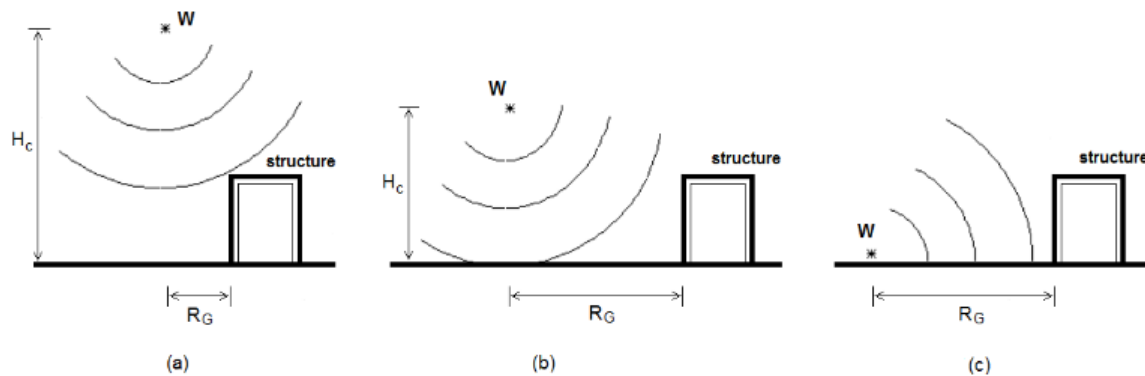


**Figure 1.37.** Types of external explosions and blast loadings (Karlos & Solomos, 2013)

## Conclusion

The foremost objective of this chapter was to have to general overview on arch bridges and the inherent concepts of resilience and redundancy. Thus, arch bridges history and generalities were presented. In order to know how those bridges can be design, some design procedures of arch bridges and main design guidelines have been defined. After that, a presentation of their advantages and disadvantages have been made as well as the comparison with other bridge types. Afterwards, the concept of redundancy in the framework of bridge design was presented. Finally, to completely get in touch with the subject, resilience and extreme events were highlighted. The next chapter presents the method and theories involved in the design of a typical steel arch bridge and the procedure for eventual evaluation of its redundancy and resilience.

## **CHAPTER 2: METHODOLOGY**

---

### **Introduction**

The previous chapter enabled us to have an overview on arch bridges and to understand the concepts of resilience and redundancy in relation to bridge structures. This chapter will focus on the description of the methodology work. This is the part of the study that establishes the research procedure after the definition of the problem, so as to achieve the set of objectives. It is partitioned in different sections, the first being a general recognition of the site done by documentary research. This is followed by data collection that will enable the modelling and analysis of the arch bridge. Thereafter, this chapter will focus on the description of the verification procedures and the governing equations used by analytical and numerical procedures which are intended to be used for performing redundancy and resilience analysis. The modern software makes it possible to analyse ever increasing number of structural problems. However, the results of this analysis are strongly dependent on the assumptions made and the understanding of the working principles of the software used, so care is always recommended when adopting numerical solutions.

### **2.1. General site recognition**

Based on documentary research of the site to be studied, the recognition of the site will be done. It will enable one to have knowledge of physical parameters of the site, that is, the geographical location, the climate, the relief, hydrology, geology and on the other hand, socio-economic parameters such as demographics, economic activities and transport means in the region.

### **2.2. Data collection**

The data collected are the related to the geometry of the arch bridge and its different constituent structural elements as well as the data taking into consideration the properties of the material used on site.

### **2.2.1. Geometrical data**

The geometrical data will be taken from structural plans that show the disposition of the different views and structural elements of the arch bridge and their geometrical dimensions. These data constitute structural details and contain sections of structural elements such as girders, cross-beams, arch ribs, hangers, bracing elements and deck of the bridge.

### **2.2.2. Material properties**

A good knowledge of material properties will help to determine the structural resistances of the bridge elements to the applied loads and therefore the global behaviour of the structure. Some of the material characteristics needed for the steel and concrete elements are the structural classes, yield strengths, densities, Young's modulus and Poisson ratio.

## **2.3. Design codes and actions on the structure**

One of the most important things to be carefully considered in the design of any structure are load actions on the structure. The decision about the design codes and standards to be used is crucial because of this since they give the different guidelines for determination actions and eventually determination of the resistances. As a result, this section illustrates firstly the various codes used for arch bridges design, then the loads they take into account and lastly the different load combinations necessary for proper design.

### **2.3.1. Design codes**

Depending on where the construction takes place, a good design should follow certain precise standards. There are many kinds of norms in use across the world, including the Chinese code, American code and European norm. The European Committee for Standardization recommends using Eurocode, a standardized code. Different sections of the Eurocodes are used depending on the project location, the material used, and the sort of structure to be done. The main sections of Eurocodes considered for this work are:

- EN 1990 Eurocode 0: Basis of structural design
- EN 1991 Eurocode 1: Actions on structures
- EN 1992 Eurocode 2: Design of concrete structures
- EN 1993 Eurocode 3: Design of steel structures
- EN 1994 Eurocode 4: Design of composite steel and concrete structures

### 2.3.2. Actions on the structure

The computation of the loads acting on the bridge is the main objective of this section. These loads include permanent and live loads. Additionally, the determination of accidental actions (blast load in this case) will be presented.

#### 2.3.2.1. Permanent loads

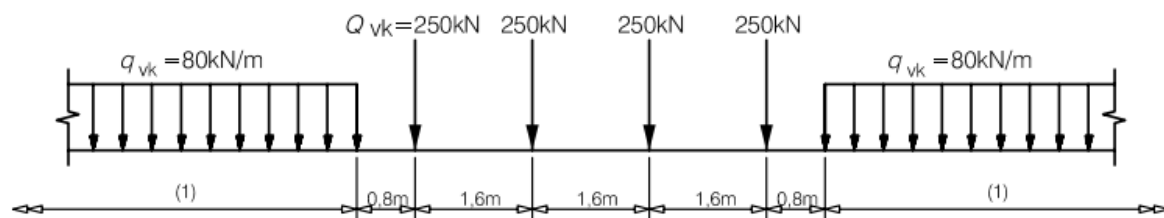
Also known as static or dead loads, these are actions that act on the structure during its whole nominal life with a negligible variation of their intensity in time. These include the self-weight of the structural elements ( $G_1$ ) and the self-weight of the non-structural elements ( $G_2$ ) present in the nominal life of the structure but which do not take part in the load bearing mechanism. The former can be computed using the density and the geometry of the structural element while the latter which could be computed in a similar manner are contributed mainly by: weight of the slab, weight of rails, sleepers and ballast.

#### 2.3.2.2. Live loads

Also known as variable loads, these are loads for which the variation in magnitude with time is neither negligible nor monotonic. These imposed loads are those arising during the service life of the bridge. For this study, the live load considered include traffic, wind, temperature and shrinkage effect loading.

##### a. Traffic load

For the complete analysis of the vertical forces, the rail traffic Load Model 71 (LM 71) has been considered. This Load Model represents the static effect of vertical loading due to normal rail traffic (EN 1991-2, 2003) as illustrated on Figure 2.1.



##### Key

(1) No limitation

**Figure 2.1.** Load Model 71 and characteristic values for vertical loads (EN 1991-2, 2003)

The characteristic values given in Figure 2.1 shall be multiplied by a factor, on lines carrying rail traffic which is heavier or lighter than normal rail traffic. When multiplied by the factor the loads are called "classified vertical loads". This factor shall be one of the following:

$$0,75 - 0,83 - 0,91 - 1,00 - 1,10 - 1,21 - 1,33 - 1,46$$

To find the design values in this project,  $\alpha = 1,33$  is on the safe side (1,0 is for normal traffic).

### b. Wind load

The general expression of linearly distributed wind force  $F_w$  acting on a structure or a structural component can be determined directly by using equation (2.1).

$$F_w = c_s \cdot c_d \cdot c_f \cdot q_p(z_e) \cdot d_{tot} \quad (2.1)$$

Where:

$q_p(z_e)$  is the peak velocity pressure at reference height  $z_e$

$d_{tot}$  is the total depth of the structural element  $z_e$

$c_s \cdot c_d$  is the structural factor

$c_f$  is the force coefficient

The peak velocity pressure at height  $z$  is expressed by equation (2.2).

$$q_p(z) = \frac{1}{2} \cdot (1 + 7 \cdot I_v(z)) \cdot \rho \cdot v_m^2(z) = c_e(z) \cdot q_b \quad (2.2)$$

Where:

$\rho$  is the air density

$v_m(z)$  is the mean wind velocity at height  $z$  and is given by equation (2.3)

$$v_m(z) = c_r(z) \cdot c_o(z) \cdot v_b \quad (2.3)$$

$c_r(z)$  is the roughness coefficient

$c_o(z)$  is the orography coefficient

$v_b$  is the basic wind velocity given by equation (2.5)

$I_v(z)$  is the turbulence intensity and can be obtained from equation (2.4)

$$I_v(z) = \frac{k_l}{c_o(z) \cdot \ln(z/z_o)} \quad (2.4)$$

$k_l$  is the turbulence factor

$z_o$  is the roughness length obtained from Table 2.1

$$v_b = c_{dir} * c_{season} * v_{b,0} \quad (2.5)$$

$c_{dir}$  is the directional factor

$c_{season}$  is the season factor

It is important to note that the fundamental value of the basic wind velocity is the characteristic 10 minutes mean wind velocity having the probability  $p$  of an annual exceedance. It is determined by multiplying the basic wind velocity by the probability factor determined from equation (2.6).

$$c_{prob} = \left( \frac{1 - K \ln(-\ln(1 - p))}{1 - K \ln(-\ln 0.98)} \right)^n \quad (2.6)$$

Where:

$K$  is the shape parameter taken from the National Annex (the recommended value is 0.2)

$n$  is the exponent taken from the National Annex (the recommended value is 0.5)

The recommended procedure for the determination of the roughness factor  $c_r$  at height  $z$  is based on a logarithmic velocity profile as shown in equation (2.7).

$$c_r(z) = \begin{cases} k_r \ln\left(\frac{z}{z_o}\right) & \text{for } z_{min} \leq z \leq z_{max} \\ c_r(z_{min}) & \text{for } z \leq z_{min} \end{cases} \quad (2.7)$$

Where:

$z_0$  is the roughness length that is obtained from Table 2.1

$k_r$  is the terrain factor which is calculated using equation 2.8

$$k_r = 0.19 \left( \frac{z_0}{z_{0,II}} \right)^{0.07} \quad (2.8)$$

**Table 2.1.** Table of terrain categories and terrain parameters (EN 1991-1-4, 2005)

Terrain category		$z_0$ m	$z_{min}$ m
0	Sea or coastal area exposed to the open sea	0,003	1
I	Lakes or flat and horizontal area with negligible vegetation and without obstacles	0,01	1
II	Area with low vegetation such as grass and isolated obstacles (trees, buildings) with separations of at least 20 obstacle heights	0,05	2
III	Area with regular cover of vegetation or buildings or with isolated obstacles with separations of maximum 20 obstacle heights (such as villages, suburban terrain, permanent forest)	0,3	5
IV	Area in which at least 15 % of the surface is covered with buildings and their average height exceeds 15 m	1,0	10
NOTE: The terrain categories are illustrated in A.1.			

### c. Temperature load

The action of temperature rise or fall on steel structures is characterised by expansion or contraction respectively. Consequently, for bridges, representative values of thermal actions will be assessed for the uniform temperature component and the temperature difference components.

#### i. Uniform temperature component

It depends on the minimum and maximum temperature which a bridge will achieve. This results in a range of uniform temperature changes which, in an unrestrained structure would result in a change in element length. Having the minimum shade air temperature ( $T_{min}$ ) and maximum shade air temperature ( $T_{max}$ ) for the site, we can derive minimum and maximum uniform bridge temperature components  $T_{e,min}$  and  $T_{e,max}$  using the graph on Figure 2.2.

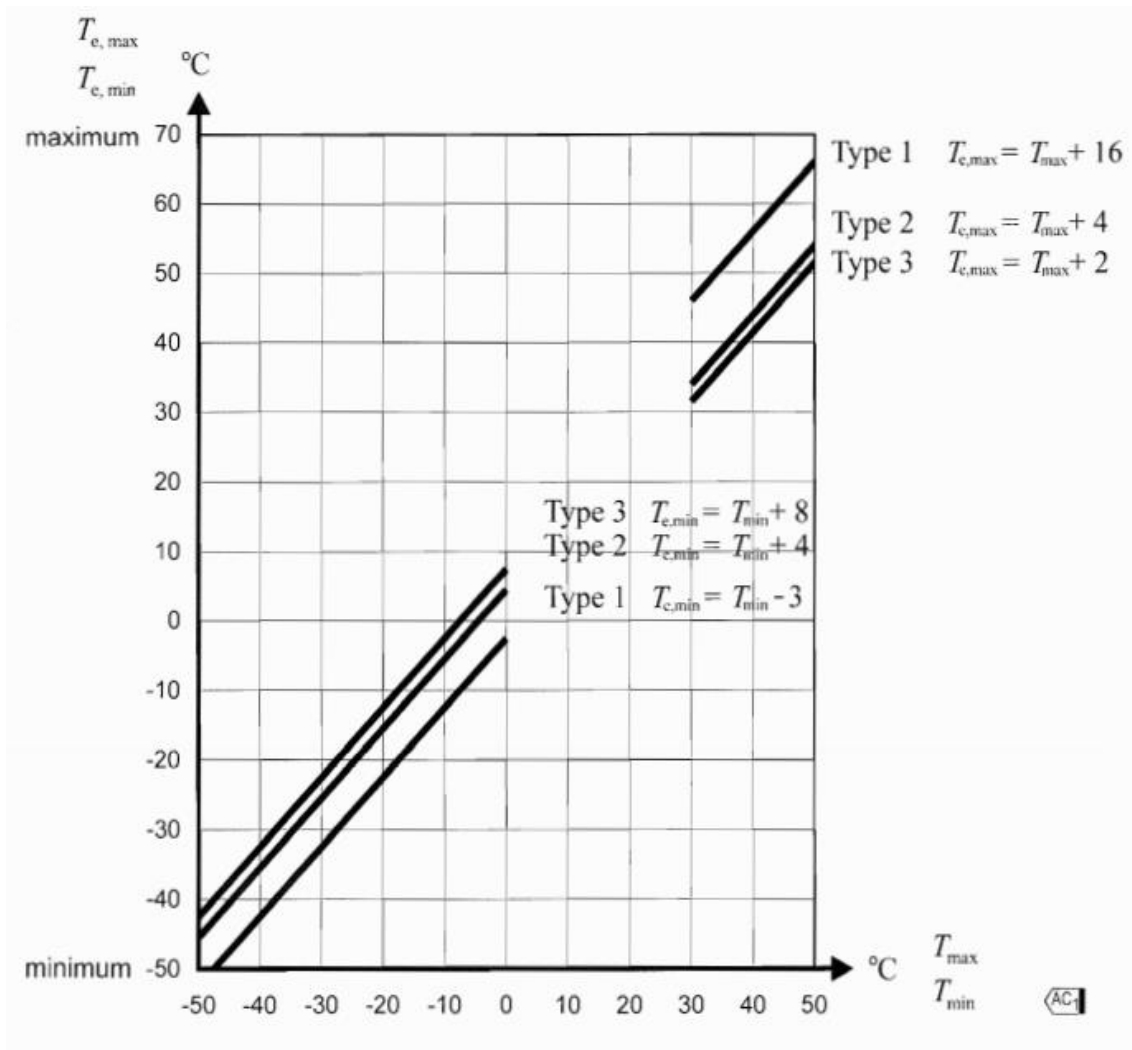


**Figure 2.2.** Correlation between minimum/maximum shade air temperature and minimum/maximum uniform bridge temperature component (EN 1991-1-5, 2003)

The initial bridge temperature  $T_0$  is important for calculating contraction down to the minimum uniform bridge temperature component and expansion up to the maximum uniform bridge temperature component. Thus, the characteristic value of the maximum contraction range of the uniform bridge temperature component,  $\Delta T_{N,con}$  should be taken as computed in equation (2.9).

$$\Delta T_{N,con} = T_0 - T_{e,min} \quad (2.9)$$

Also, the characteristic value of the maximum expansion range of the uniform bridge temperature component,  $\Delta T_{N,exp}$  should be taken as calculated in equation (2.10).

$$\Delta T_{N,exp} = T_{e,max} - T_0 \quad (2.10)$$

The overall range of the uniform bridge temperature component is the obtained from equation (2.11).

$$\Delta T_N = T_{e,max} - T_{e,min} \quad (2.11)$$

## ii. Temperature difference component

Over a prescribed time period heating and cooling of a bridge deck's upper surface will result in a maximum heating (top surface warmer) and a maximum cooling (bottom surface warmer) temperature variation. The vertical temperature difference may produce effects within a structure due to:

- Restraint of free curvature due to the form of the structure (like portal frame and continuous beams);
- Friction at rotational bearings;
- Non-linear geometric effects (2nd order effects).

Two approaches exist for the determination of the temperature difference load component on a bridge deck (EN 1991-1-5, 2003) which are vertical linear component (Approach 1) and the vertical temperature components with non-linear effects (Approach 2). In this study we will use the first approach.

In this approach, the effect of vertical temperature differences will be considered by using an equivalent linear temperature difference component with  $\Delta T_{M,heat}$  and  $\Delta T_{M,cool}$ . These values obtained from Table 2.2 will be applied between the top and the bottom of the bridge deck.

**Table 2.2.** Recommended values of linear temperature difference component for different types of bridge decks for road, foot and railway bridges (EN 1991-1-5, 2003)

Type of Deck	Top warmer than bottom	Bottom warmer than top
	$\Delta T_{M,heat}$ (°C)	$\Delta T_{M,cool}$ (°C)
Type 1: Steel deck	18	13
Type 2: Composite deck	15	18
Type 3: Concrete deck: - concrete box girder - concrete beam - concrete slab	10 15 15	5 8 8

The values given in the Table 2.2 are based on a depth of surfacing of 50 mm for road and railway bridges. For other depths of surfacing, these values should be multiplied by the factor  $k_{sur}$ . Recommended values for the factor  $k_{sur}$  are given in Table 2.3.

**Table 2.3.** Recommended values of  $k_{sur}$  to account for different surfacing thickness (EN 1991-1-5, 2003)

Road, foot and railway bridges						
Surface Thickness	Type 1		Type 2		Type 3	
	Top warmer than bottom	Bottom warmer than top	Top warmer than bottom	Bottom warmer than top	Top warmer than bottom	Bottom warmer than top
[mm]	$k_{sur}$	$k_{sur}$	$k_{sur}$	$k_{sur}$	$k_{sur}$	$k_{sur}$
unsurfaced	0,7	0,9	0,9	1,0	0,8	1,1
water-proofed <sup>1)</sup>	1,6	0,6	1,1	0,9	1,5	1,0
50	1,0	1,0	1,0	1,0	1,0	1,0
100	0,7	1,2	1,0	1,0	0,7	1,0
150	0,7	1,2	1,0	1,0	0,5	1,0
ballast (750 mm)	0,6	1,4	0,8	1,2	0,6	1,0
<sup>1)</sup> These values represent upper bound values for dark colour						

The load ( $T_k$ ) due to thermal variation across the deck is expressed by equation (2.12).

$$T_k = A_c \cdot \varepsilon \cdot E_{cm} \quad (2.12)$$

Where:

$A_c$  is the slab area

$\varepsilon$  is a thermal coefficient

$E_{cm}$  is the concrete elastic modulus with  $E_{cm} = 22000 \cdot (f_{cm}/10)^{0.3}$

The resultant thermal load can be redistributed on the different girders. The force  $T_{beam}$  on each girder that will be considered is evaluated according to equation (2.13).

$$T_{beam} = \frac{T_k}{n}, \quad (2.13)$$

where  $n$  is the number of girders.

#### d. Shrinkage effect

In steel-concrete composite bridges, the slab is restrained by steel beam. The shear connectors resist the force arising out of shrinkage, by inducing a tensile force on the slab (global effect). This reduces the apparent shrinkage of composite structure with respect to the free shrinkage of concrete. Shrinkage effect is combined to the creep effect; the latter is evaluated at infinite time.

##### i. Creep

The effects of creep are taken into account by reducing concrete elastic modulus  $E_{cm}$  thus increasing the modular ratio. The maximum modular ratio at infinite time  $n_L$  is given by equation (2.14).

$$n_L = n_0(1 + \psi_L \rho_t) \quad (2.14)$$

Where:

$n_0$  is the modular ratio  $E_s/E_{cm}$  for the short-term loading

$\rho_t$  is the creep coefficient depending on the age  $t$  of concrete and the age  $t_0$  at loading

$\psi_L$  is the creep multiplier depending on the type of loading; to be taken as 1,1 for permanent loads; 0,55 for primary and secondary effects of shrinkage; 1,5 for prestressing by imposed deformations.

In order to determine the creep coefficient  $\rho_t(t, t_0)$ , we have to consider the following data:

Relative humidity  $RH = 70\%$

Reference zero time  $t_0 = 3 \text{ days}$

Fictitious dimension  $h = 2A_c/u$  (2.15)

Where  $A_c$  is cross sectional area of the concrete slab and  $u$  is the perimeter of concrete exposed to drying.

The value of  $\rho_t(t, t_0)$  total shrinkage at  $t = \infty$  will be found with software MIDAS/Civil as illustrated on Figure 2.3.

The screenshot shows the 'Add/Modify Time Dependent Material (Creep / Shrinkage)' dialog box. The 'Name' field contains 'Creep/Shrink C32/40' and the 'Code' is set to 'European'. Under the 'European' section, the following parameters are defined:
 

- Characteristic compressive cylinder strength of concrete at the age of 28 days (fck): 32 N/mm<sup>2</sup>
- Relative Humidity of ambient environment (40 - 99): 70 %
- Notional size of member: 613 mm
- Formula for notional size:  $h = 2 * A_c / u$  (Ac : Section Area, u : Perimeter in contact with atmosphere)
- Type of cement:  Class N,  Class S,  Class R
- Type of code:  EN 1992-2 (Concrete Bridge),  EN 1992-1 (General Structure),  Use of silica-fume
- Age of concrete at the beginning of shrinkage: 3 day

 At the bottom, the 'Show Result...' button is highlighted with a red rectangular box, along with 'OK', 'Cancel', and 'Apply' buttons.

**Figure 2.3.** Time dependent concrete creep and shrinkage (MIDAS/Civil software)

**ii. Shrinkage**

The total shrinkage is composed of two components:

- Drying shrinkage strain  $\varepsilon_{cd}$ : it develops slowly, since it is a function of the migration of the water through the hardened concrete;
- Autogenous shrinkage strain  $\varepsilon_{ca}$ : it develops during hardening of the concrete, therefore the major part.

The total long-term shrinkage  $\varepsilon_{cs}(\infty)$  is calculated through equation (2.16).

$$\varepsilon_{cs}(\infty) = \varepsilon_{ca}(\infty) + \varepsilon_{cd}(\infty) \quad (2.16)$$

Equations (2.17) to (2.20) used for the computation of shrinkage strain components are reported in Table 2.4.

**Table 2.4.** Formulae of various shrinkage strain components

$\varepsilon_{ca} = 2.5. (f_{ck} - 10). 10^{-6}$	(2.17)
$\varepsilon_{cd}(\infty) = k_h. \varepsilon_{c0}$	(2.18)
$\varepsilon_{c0} = 0.85. ((220 + 110. \alpha_{ds1}). e^{(-\alpha_{ds2}. f_{cm}/f_{cm0})). 10^{-6}. \beta_{RH}$	(2.19)
$\beta_{RH} = 1.55. (1 - \left(\frac{RH}{RH_0}\right)^3)$	(2.20)

Where:  $\varepsilon_{cd}(\infty)$  is the long-term dry shrinkage strain

$\varepsilon_{ca}(\infty)$  is the long-term autogenous shrinkage.

The remaining parameters needed for the computation of the shrinkage effect are obtained from section 3.1.4 of Eurocode 2 (EN 1992-1-1, 2004).

Shrinkage of concrete is taken into account by applying an axial force at slab ends. The corresponding axial force is given by equation (2.21).

$$N_{c,r\infty} = \varepsilon_{cs}(\infty). E_{c,eff}. A_c \quad (2.21)$$

Where  $E_{c,eff}$  is the reduced modulus of elasticity of concrete and obtained from equation (2.22).

$$E_{c,eff} = \frac{E_{cm}}{1 + \rho(\infty, t_0)} \quad (2.22)$$

The resultant shrinkage load can be redistributed on the different girders of the bridge. The force  $N_{beam}$  on each girder is evaluated according to equation (2.23):

$$N_{beam} = N_{c,r\infty}/n \quad (2.23)$$

Where  $n$  is the number of beams.

### 2.3.2.3. Blast load

Blast loads are intrinsically complex. However, in this section, charts have been supplied to compute the blast load parameters for a given charge weight and stand-off distance using experimental data and scaling rules.

#### a. Scaled distance

Equation (2.24) presents the empirical formula for calculating the scaled distance  $Z$  (m), which is one of the most important blast load parameters.

$$Z = \frac{R}{\sqrt[3]{W}} \quad (2.24)$$

Here,  $R$  = Standoff distance (m),  $W$  = Equivalent TNT weight of explosion (kg).

#### b. Stand-off distance

The method used to compute the blast load parameters at point A as shown in Figure 2.4 is discussed below.

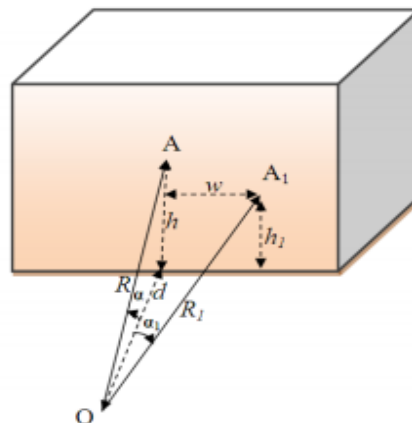


**Figure 2.4.** Illustration of some key blast parameters (Mbakop, 2020)

The blast origin is shown in Figure 2.5 as point O, and point A is where the blast parameters need to be computed. It is placed at a horizontal distance  $d$  and a height  $h$  from point O. The angle of incidence  $\alpha$  is defined as the angle formed by the shock wave and the perpendicular line to the target surface. The expressions of  $R$  and  $\alpha$  are given by equations (2.25) and (2.26) respectively.

$$R = \sqrt{(d^2 + h^2)} \tag{2.25}$$

$$\alpha = \cos^{-1}(d/h) = \tan^{-1}(h/d) \tag{2.26}$$

**c. Arrival time**

Figure 2.5 depicts all of the necessary positive phase parameters in metric units depending on the scaled distance  $Z$ . As a result, the arrival time  $t_A$  can be determined.

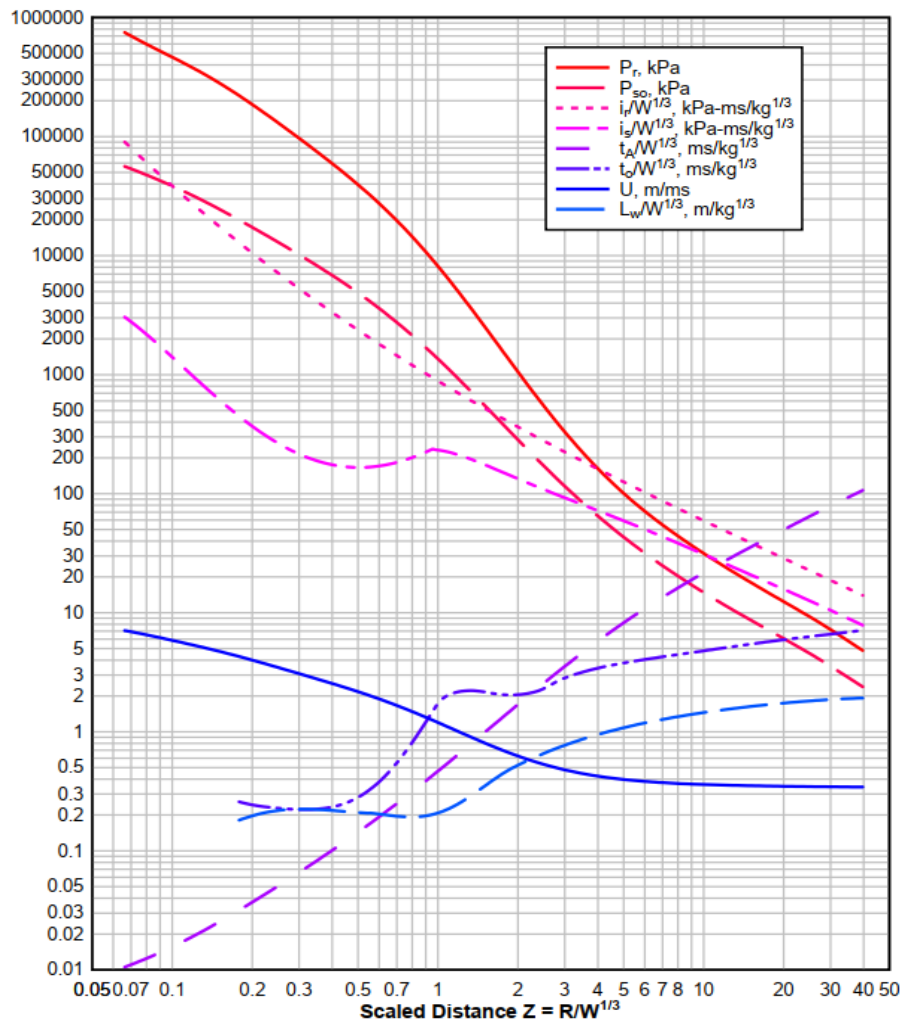


**Figure 2.5.** Parameters of positive phase of shock spherical wave of TNT charges from surface bursts (Karlos & Solomos, 2013)

#### d. Blast pressure distribution

Eric Jacques, an assistant professor at Virginia Tech, created RC Blast, a computer software that calculates blast loads for known values of charge weight and stand-off distance using the scaled distance  $Z$  and the tables in U.S. Department of the Army Technical Manual 5-1300. The RC Blast program is commonly used to calculate the equivalent blast pressure distribution caused by an explosion. Moreover, Mills equation (2.27) is used to calculate the peak pressure,  $P_{s0}$ .

$$P_{s0} = \frac{1}{Z} \left( 108 + \frac{1772}{Z^2} - \frac{114}{Z^2} \right) \quad (2.27)$$

#### 2.3.3. Load combinations

The following rules are considered for the combination of loads with regard to static loads imposed in a structure, as specified by Eurocode 0 (EN 1990, 2002). When it comes to bridges, we have static load cases for static loads and dynamic load cases which consider accidental and dynamic loads.

##### 2.3.3.1. Static load cases

This section presents the different ways of combining the effects of static loads on a structure.

##### a. Fundamental combination

This combination is used for Ultimate Limit State (ULS) associated to determining of structure resistance and is given by equation (2.28).

$$\sum_j \gamma_{G,j} * G_{k,j} + \gamma_{Q,1} * Q_{k,1} + \sum_{i>1} \gamma_{Q,i} * \psi_{0,i} * Q_{k,i} \quad (2.28)$$

Where:

$G_{k,j}$ : are the permanent loads

$Q_{k,1}$ : is the leading variable load

$Q_{k,i}$ : are the accompanying variable loads

$\gamma_{G,j}$ : are the partial safety factors applied to permanent loads

$\gamma_{Q,i}$ : are the partial safety factors applied to variable loads

$\psi_{0,i}$ : are the combination coefficients for the live loads

The coefficients  $\gamma_{G,j}$  and  $\gamma_{Q,i}$  are partials factors which minimize the loads, which tend to reduce the solicitations and maximise the ones that increase them. The recommended values preconized by the Eurocode 0 for the partial safety factors are given in Table 2.5.

**Table 2.5.** Recommended values of partial safety factors for ULS combination (EN 1990, 2002).

Partial safety factor	Favourable load	Unfavourable load
$\gamma_{G,j}$	1.35	1.00
$\gamma_{Q,1}$	1.50	0.00
$\gamma_{Q,i}$	1.50	0.00

A load envelope is obtained from ULS combinations to have the most unfavourable condition for an element.

**b. Characteristic combination (rare)**

Usually used for non-reversible Serviceability Limit States (SLS), this combination shown in equation (2.29) has to be used in the verifications with the allowable stress method.

$$\sum_j G_{k,j} + P + Q_{k,1} + \sum_{i>1} \psi_{0,i} * Q_{k,i} \tag{2.29}$$

**c. Frequent combination**

Frequent combination in equation (2.30) is recommended for reversible SLS.

$$\sum_j G_{k,j} + P + \psi_{1,1} * Q_{k,1} + \sum_{i>1} \psi_{2,i} * Q_{k,i} \tag{2.30}$$

#### d. Quasi-permanent combination

Generally used for long-term effects, it is given by equation (2.31).

$$\sum_j G_{k,j} + P + \sum_{i \geq 1} \psi_{2,i} * Q_{k,i} \quad (2.31)$$

The values recommended for the reduction factors for the actions on railway bridges are given in Table 2.6.

**Table 2.6.** Recommended values of  $\psi$  factors for railway bridges (EN 1990 Annex A2, 2005)

	Temperature load	Wind load	Railway traffic load
$\psi_0$	0.6	0.75	0.8
$\psi_1$	0.5	0.5	0.8 if 1 track is loaded 0.7 if 2 tracks are loaded
$\psi_2$	0.5	0	0

#### 2.3.3.2. Dynamic load cases

Accidental explosions and fires can occur throughout the nominal life of a structure. EN 1990 formulates a combination used at the ULS related to the design of accidental actions in anticipation of such an event. The accidental load combination is shown in equation (2.32).

$$G + P + A_d + (\psi_1 \text{ or } \psi_2)Q_{k,1} + \sum \psi_2 Q_{k,i} \quad (2.32)$$

Where:

$G$ : is the self-weight of the structure

$A_d$ : is the design value of the accidental load (blast load for this work)

$Q_{k,1}$ : is the characteristic value of the leading live load

$Q_{k,i}$ : are the characteristic values of the accompanying variable loads

The values of  $\psi_1$  and  $\psi_2$  depend on the relevant accidental design situation.

## **2.4. Structural analysis and design**

Structural analysis is a set of processes used to assess how design actions affect structures. The analysis type used for the assessment of the arch bridge is the linear static analysis. In this type of analysis, a linear relation exists between applied forces and displacements, which is applicable to structural problems where stresses remain in the linear elastic range of the used material. The structure will be designed according to the corresponding limit states in such a way to sustain all actions acting upon it during its intended service life. This indicates that it will be designed with appropriate structural stability (ultimate limit states) and will continue to be fit for the purpose for which it is designed (serviceability). Before designing any element, it must be classified based on its ability to generate plastic hinges and rotational deformations. In this section, the numerical modelling softwares and structural analysis made will be presented.

### **2.4.1. Numerical modelling**

Numerical modelling in civil engineering is used as a tool that facilitates the engineers to evaluate the behaviour of structures. The numerical methods are convenient, and less time-consuming for the analysis of redistribution of stresses and designing of structures. The modelling of the structure will be done entirely in MIDAS/Civil 2022, the modelling of the blast load behaviour in RCblast, scientific representation, post processing and verifications in Microsoft Excel 2019. Modelling will consist of creating the appropriate material, section properties, loads cases and combinations. The steel elements shall be drawn according to structural plans and the supports conditions assigned accordingly. The structure shall be loaded with respect to specific load patterns discussed in section 2.3.2. The load combinations will be defined prior to the analyses to satisfy the ULS and SLS conditions as discussed in section 2.3.3.

#### **2.4.1.1. MIDAS/Civil 2022 description**

MIDAS/Civil is a bridge design and analysis software that combines powerful pre-and post-processing features with an extremely fast solver, which makes bridge modelling and analysis simple, quick, and effective. It enables creation of nodes and elements as if drawings were made using the major functions of CAD programs. It provides linear and nonlinear structural analysis capabilities and is capable of handling different types of analysis notably

time-history analysis, construction stage analysis, heat of hydration analysis, moving load analysis, modal analysis and many more. The program's efficient analysis algorithms yield exceptional versatility and accurate results appropriate for practical design applications. MIDAS/Civil also provides results for different structures like reinforced concrete structures, metallic frame structures and other types that are compatible with Microsoft Excel, which enables the user to review all analysis and design results systematically.

#### **2.4.1.2. Bridge modelling procedure**

A three-dimensional computational model of the bridge will be created in MIDAS/Civil. The structural elements (arch ribs, main girders, cross beams and hangers) for numerical simulation are modelled using 1D fibre beam element. In the analysis, those elements are connected to each other by a fixed joint (rigid links) with zero degrees of freedom as is done in the practice of such bridges.

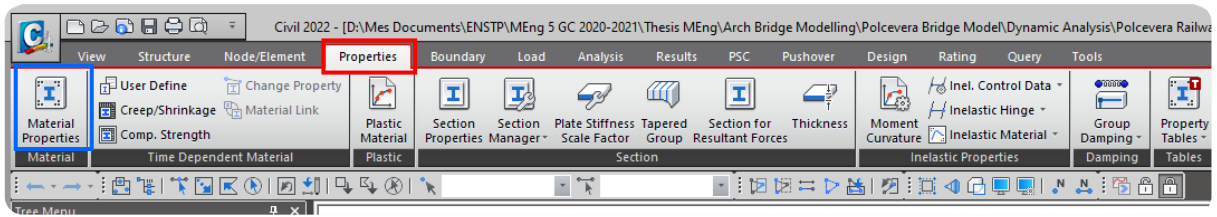
The slab is modelled as a 2D plate element with the corresponding thickness. Hangers and slab bracings are modelled as truss elements with linear elastic behaviour since they are meant to resist only axial forces.

The superstructure of the bridge is connected to the abutments or pier with bearings. Abutments will be replaced by fixed constraints and elastic links with high vertical stiffness will be used as bearing at both bridge end.

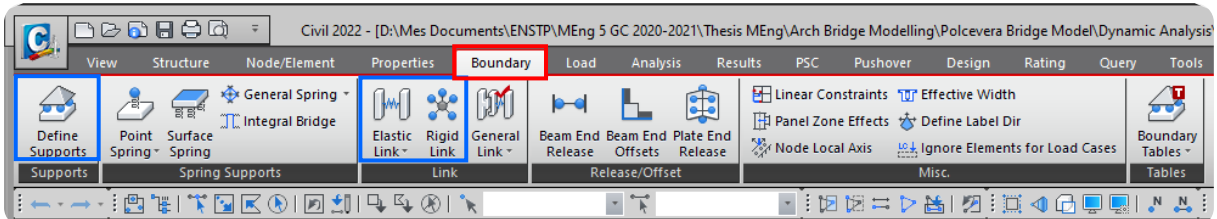
In sum, to do the static analysis of the bridge under permanent and live loads in MIDAS/Civil, the following main menus to be used are presented as follows:

- Properties: this section is meant for definition of material and section properties of different elements such as the arch rib, main girder, cross bracings, hangers and slab bracings;
- Boundary: here, the definition of boundary restrains, rigid and elastic links of our bridge;
- Loads: loads cases are defined here (self-weight, live loads, dynamic loads);
- Results: different results (displacements, stresses, moments, axial, shear forces...) can be displayed.

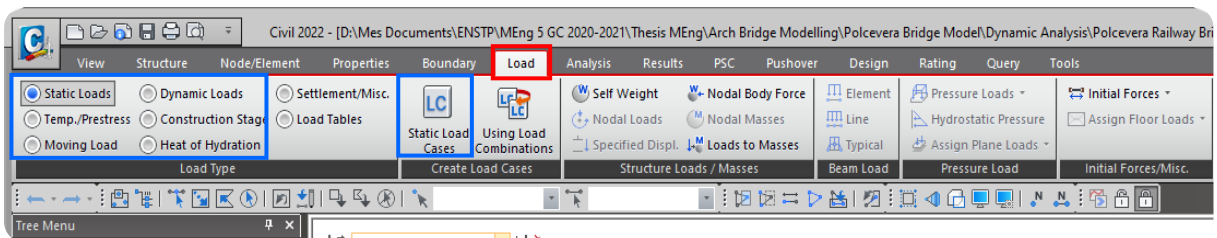
These various menus of the FEM software are presented in Figure 2.6.



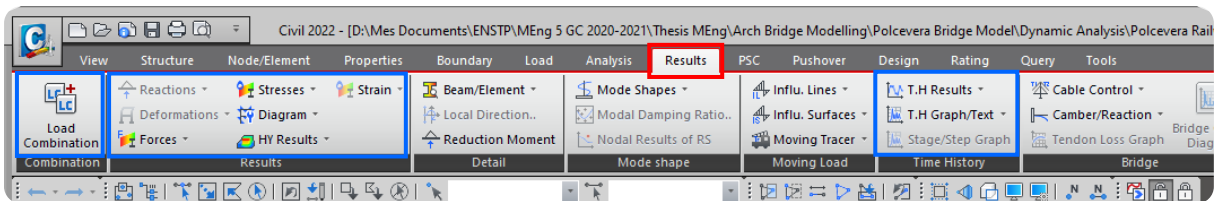
a) Properties menu



b) Boundary conditions menu



c) Load menu



d) Results menu

Figure 2.6. MIDAS/Civil 2022 menus

## 2.4.2. Steel sections classification

The classification of a steel section depends principally on its geometrical properties. The sections of the members to be design are going to be classified as class 1, 2, 3, or 4 following the Eurocode 3 (EN 1993-1-1, 2005). The code defines these classes as follows:

- Class 1 cross-sections are those which can form a plastic hinge with the rotation capacity required from plastic analysis without reduction of the resistance.
- Class 2 cross-sections are those which can develop their plastic moment resistance, but have limited rotation capacity because of local buckling.

- Class 3 cross-sections are those in which the stress in the extreme compression fibre of the steel member assuming an elastic distribution of stresses can reach the yield strength, but local buckling is liable to prevent development of the plastic moment resistance.
- Class 4 cross-sections are those in which local buckling will occur before the attainment of yield stress in one or more parts of the cross-section.

The sections are going to be classified following the guidelines provided in Table 2.7, Table 2.8 and Table 2.9.

**Table 2.7.** Maximum width-to-thickness ratios for internal compression parts (EN 1993-1-1, 2005)

Internal compression parts						
				Axis of bending		
				Axis of bending		
Class	Part subject to bending	Part subject to compression		Part subject to bending and compression		
1						
	$c/t \leq 72\epsilon$	$c/t \leq 33\epsilon$		when $\alpha > 0,5$ : $c/t \leq \frac{396\epsilon}{13\alpha - 1}$ when $\alpha \leq 0,5$ : $c/t \leq \frac{36\epsilon}{\alpha}$		
2						
	$c/t \leq 83\epsilon$	$c/t \leq 38\epsilon$		when $\alpha > 0,5$ : $c/t \leq \frac{456\epsilon}{13\alpha - 1}$ when $\alpha \leq 0,5$ : $c/t \leq \frac{41,5\epsilon}{\alpha}$		
3						
	$c/t \leq 124\epsilon$	$c/t \leq 42\epsilon$		when $\psi > -1$ : $c/t \leq \frac{42\epsilon}{0,67 + 0,33\psi}$ when $\psi \leq -1^*)$ : $c/t \leq 62\epsilon(1 - \psi)\sqrt{-\psi}$		
$\epsilon = \sqrt{235/f_y}$	$f_y$	235	275	355	420	460
	$\epsilon$	1,00	0,92	0,81	0,75	0,71

\*)  $\psi \leq -1$  applies where either the compression stress  $\sigma \leq f_y$  or the tensile strain  $\epsilon_y > f_y/E$

**Table 2.8.** Maximum width-to-thickness ratios for outstand flanges (EN 1993-1-1, 2005)

Outstand flanges						
		Rolled sections		Welded sections		
Class	Part subject to compression	Part subject to bending and compression				
		Tip in compression		Tip in tension		
Stress distribution in parts (compression positive)						
1	$c/t \leq 9\epsilon$	$c/t \leq \frac{9\epsilon}{\alpha}$	$c/t \leq \frac{9\epsilon}{\alpha\sqrt{\alpha}}$			
2	$c/t \leq 10\epsilon$	$c/t \leq \frac{10\epsilon}{\alpha}$	$c/t \leq \frac{10\epsilon}{\alpha\sqrt{\alpha}}$			
Stress distribution in parts (compression positive)						
3	$c/t \leq 14\epsilon$	$c/t \leq 21\epsilon\sqrt{k_\sigma}$ For $k_\sigma$ see EN 1993-1-5				
$\epsilon = \sqrt{235/f_y}$	$f_y$	235	275	355	420	460
	$\epsilon$	1,00	0,92	0,81	0,75	0,71

**Table 2.9.** Maximum width-to-thickness ratios for angle compression part (EN 1993-1-1, 2005)

Angles						
Refer also to "Outstand flanges" (see sheet 2 of 3)					Does not apply to angles in continuous contact with other components	
Class	Section in compression					
Stress distribution across section (compression positive)						
3	$h/t \leq 15\epsilon : \frac{b+h}{2t} \leq 11,5\epsilon$					
Tubular sections						
Class	Section in bending and/or compression					
1	$d/t \leq 50\epsilon^2$					
2	$d/t \leq 70\epsilon^2$					
3	$d/t \leq 90\epsilon^2$					
<b>NOTE</b> For $d/t > 90\epsilon^2$ see EN 1993-1-6.						
$\epsilon = \sqrt{235/f_y}$	$f_y$	235	275	355	420	460
	$\epsilon$	1,00	0,92	0,81	0,75	0,71
	$\epsilon^2$	1,00	0,85	0,66	0,56	0,51

### 2.4.3. Steel members design at Ultimate Limit States

The ultimate limit states are those that involve the failure of a structural element or the entire structure. Ultimate limit state verifications are design verifications that pertain to the safety of individuals on and around the structure. The design verifications will be carried out in accordance with Eurocode 3 standard (EN 1993-1-1, 2005).

#### 2.4.3.1. Design of members subjected to axial force

The design of a steel member in tension or compression is done in such a way that the design actions are lower than the resisting axial forces.

##### a. Member in tension

For a member in tension, the design value of the tension force  $N_{Ed}$  at each cross section shall satisfy the condition in equation (2.33).

$$\frac{N_{Ed}}{N_{t,Rd}} \leq 1 \quad (2.33)$$

Where  $N_{Ed}$  is the design tension force and  $N_{t,Rd}$  is the design resisting tensile force of the element and is the minimum between the design plastic resistance of the gross cross-section  $N_{pl,Rd}$  and the design ultimate resistance of the net cross-section at holes for fasteners  $N_{u,Rd}$  which are given in equations (2.34) and (2.35).

$$N_{pl,Rd} = \frac{A \cdot f_y}{\gamma_{M0}} \quad (2.34)$$

$$N_{u,Rd} = \frac{0.9 \cdot A_{net} \cdot f_u}{\gamma_{M2}} \quad (2.35)$$

##### b. Member in compression

When a steel member is subjected to compressional force, there are two principal verifications to be made. Firstly, the axial compressional resistance and then the buckling resistance.

### i. Compressional resistance

For a member in compression, the design value of the compression force  $N_{Ed}$  at each cross section shall satisfy the condition in equation (2.36):

$$\frac{N_{Ed}}{N_{c,Rd}} \leq 1 \quad (2.36)$$

The value of the design resistant compression force  $N_{c,Rd}$  is determined with the help of equations (2.37) and (2.38).

$$N_{c,Rd} = \frac{A \cdot f_y}{\gamma_{M0}} \quad \text{for class 1, 2 and 3 cross sections} \quad (2.37)$$

$$N_{c,Rd} = \frac{A_{eff} \cdot f_y}{\gamma_{M0}} \quad \text{for class 4 cross sections} \quad (2.38)$$

### ii. Buckling resistance

The steel element in compression will also be checked for buckling. To do so, the design compressive force  $N_{Ed}$  should be lower than the buckling resistance force  $N_{b,Rd}$  as pointed out by equation (2.39).

$$\frac{N_{Ed}}{N_{b,Rd}} \leq 1 \quad (2.39)$$

The design buckling resistances of the members in compression according to the various element classes are given by equations (2.40) and (2.41).

$$N_{b,Rd} = \frac{\chi \cdot A \cdot f_y}{\gamma_{M1}} \quad \text{for class 1, 2 and 3 cross sections} \quad (2.40)$$

$$N_{b,Rd} = \frac{\chi \cdot A_{eff} \cdot f_y}{\gamma_{M1}} \quad \text{for class 4 cross sections} \quad (2.41)$$

Where,  $\chi$  is the buckling factor which reduces the resisting axial force of the whole element. To determine  $\chi$ , the appropriate buckling curve is first selected from the buckling curves on Figure 2.7 which is given according to Table 2.10 with respect to the section's characteristics and steel type.

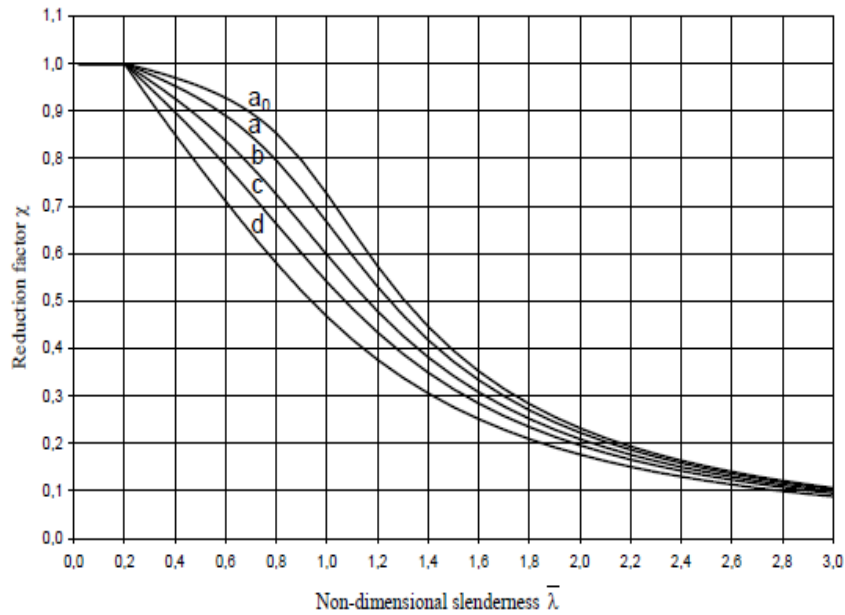


Figure 2.7. Buckling curves (EN 1993-1-1, 2005)

Table 2.10. Selection of buckling curve for a cross section (EN 1993-1-1, 2005)

Cross section		Limits	Buckling about axis	Buckling curve		
				S 235 S 275 S 355 S 420	S 460	
Rolled sections		$h/b > 1,2$	$t_f \leq 40$ mm	y-y z-z	a b	a <sub>0</sub> a <sub>0</sub>
			$40 \text{ mm} < t_f \leq 100$	y-y z-z	b c	a a
		$h/b \leq 1,2$	$t_f \leq 100$ mm	y-y z-z	b c	a a
			$t_f > 100$ mm	y-y z-z	d d	c c
Welded I-sections		$t_f \leq 40$ mm	y-y z-z	b c	b c	
		$t_f > 40$ mm	y-y z-z	c d	c d	
Hollow sections		hot finished	any	a	a <sub>0</sub>	
		cold formed	any	c	c	
Welded box sections		generally (except as below)	any	b	b	
		thick welds: $a > 0,5t_f$ $b/t_f < 30$ $h/t_w < 30$	any	c	c	
U-, T- and solid sections			any	c	c	
L-sections			any	b	b	

The non-dimensional slenderness,  $\bar{\lambda}$  necessary for the determination of the buckling factor is computed using equation (2.42) and equation (2.43).

$$\bar{\lambda} = \sqrt{\frac{Af_y}{N_{cr}}} = \frac{l_{cr}}{i} \left( \frac{1}{\lambda_1} \right) \quad \text{for class 1, 2 and 3 cross sections} \quad (2.42)$$

$$\bar{\lambda} = \sqrt{\frac{A_{eff} \cdot f_{yk}}{N_{cr}}} = \frac{l_{cr}}{i} \frac{\sqrt{\frac{A_{eff}}{A}}}{\lambda_1} \quad \text{for class 4 cross sections} \quad (2.43)$$

Where:

$l_{cr}$  is the buckling length in the buckling plane considered

$i$  is the radius of gyration about the relevant axis

$$\lambda_1 = 93.9\varepsilon.$$

$N_{cr}$  is the elastic critical force for the relevant buckling mode based on the gross cross-sectional properties and is given by Euler's equation (2.44).

$$N_{cr} = \frac{\pi^2 EJ}{l_0^2} \quad (2.44)$$

### iii. Arch buckling resistance

Given that a curved rib of the arch bridge is subject to a high axial force, the chance of a failure due to buckling of the rib cannot be ignored and must be accounted for. The subject of stability of arches is very well handled by Trahair (1989). Values to use in formulas for critical buckling loads are listed in tables for many different cases of loading and various arch configurations. The maximum horizontal buckling force  $H$  and uniform load causing buckling are computed according to equations (2.45) and (2.46)

$$H = C_1 \frac{EI}{L^2} \quad (2.45)$$

$$q = C_2 \frac{EI}{L^3} \quad (2.46)$$

Where  $C_1$  and  $C_2$  are coefficients obtained from Table 2.11. Also, the other parameters  $E$ ,  $I$  and  $L$  are described below Table 2.11.

**Table 2.11.** Critical-Load Parameter and Critical Horizontal Reaction Parameter for Uniform Elastic Arches in Pure Compression (Trahair, 1989)

$\frac{h}{L}$	Three-Hinged Arch		Two-Hinged Arch		Fixed Arch	
	$qL^3/EI$	$HL^2/EI$	$qL^3/EI$	$HL^2/EI$	$qL^3/EI$	$HL^2/EI$
<i>Parabolic arches subjected to vertical load uniformly distributed on a horizontal projection</i>						
0.10	22.5	28.1	29.1	36.3	60.9	76.2
0.15			39.5	32.9	85.1	70.9
0.20	39.6	24.8	46.1	28.8	103.1	64.5
0.25			49.2	24.6	114.6	57.3
0.30	49.5	20.6	49.5	20.6	120.1	50.0
0.35			47.8	17.1	120.6	43.1
0.40	45.0	14.1	45.0	14.1	117.5	36.7
0.50	38.2	9.6	38.2	9.6	105.3	26.3

<sup>a</sup> $h$ , rise;  $L$ , span;  $q$ , critical intensity of distributed load;  $H$ , critical horizontal reaction at supports;  $E$ , Young's modulus of elasticity;  $I$ , moment of inertia of the cross section.

#### 2.4.3.2. Design of beam elements

The design procedure for the beam elements involves firstly the design for pure bending, bending moment and axial force interaction, then, shear verification and the control of interaction between shear force and bending moment.

##### i. Design for pure bending

The design value of bending moment at each cross-section shall satisfy the condition in equation (2.47):

$$\frac{M_{Ed}}{M_{C,Rd}} \leq 1 \quad (2.47)$$

Where  $M_{Ed}$  is the design value of the bending moment acting on the element and  $M_{C,Rd}$  is the design resisting bending moment which is computed using equations (2.48), (2.49) and (2.50).

$$M_{C,Rd} = M_{pl,Rd} = \frac{W_{pl} \cdot f_y}{\gamma_{M0}} \quad \text{for class 1 or 2 sections} \quad (2.48)$$

$$M_{C,Rd} = M_{el,Rd} = \frac{W_{el,min} \cdot f_y}{\gamma_{M0}} \quad \text{for class 3 sections} \quad (2.49)$$

$$M_{C,Rd} = M_{el,Rd} = \frac{W_{eff,min} \cdot f_y}{\gamma_{M0}} \quad \text{for class 4 sections} \quad (2.50)$$

Where:

$f_y$  is the yielding strength

$W_{pl}$  is the plastic section modulus

$W_{el,min}$  is the elastic section modulus

$W_{eff,min}$  is the effective section modulus

## ii. Bending moment and axial force interaction

As earlier defined, beams can be subjected to axial and flexural load. In a more conservative approach, the design proposal states that the condition given by the Navier's equation (2.51) should hold.

$$\frac{N_{Ed}}{N_{c,Rd}} + \frac{M_{Ed}}{M_{c,Rd}} \leq 1 \quad (2.51)$$

In which  $N_{Ed}$  is the design axial force and  $M_{Ed}$  the design moment acting on the element at the cross-section under consideration,  $N_{c,Rd}$  is the cross-section axial resistance, and  $M_{c,Rd}$  is the cross-section moment resistance. Equation (2.52) gives the relationship that design axial force and the design cross section resistance should follow:

$$\frac{N_{Ed}}{N_{c,Rd}} \leq 1 \quad (2.52)$$

Here  $N_{c,Rd}$  is given by equation (2.53):

$$N_{c,Rd} \leq \frac{Af_y}{\gamma_{M0}} \quad (2.53)$$

For a given section, there is no reduction to the major axis plastic moment resistance provided the conditions presented in (2.54) and (2.55) are satisfied:

$$N_{Ed} \leq 0.25 N_{pl,Rd} \quad (2.54)$$

$$N_{Ed} \leq \frac{0.5 h_w t_w f_y}{\gamma_{M0}} \quad (2.55)$$

### iii. Shear design

The design value of the design acting shear force,  $V_{Ed}$  at each cross-section of the beam element must satisfy equation (2.56).

$$\frac{V_{Ed}}{V_{c,Rd}} \leq 1 \quad (2.56)$$

For plastic design (which shall be the one considered),  $V_{c,Rd}$  is the design plastic shear resistance,  $V_{pl,Rd}$  given by equation (2.57)

$$V_{pl,Rd} = \frac{A_v \left( \frac{f_y}{\sqrt{3}} \right)}{\gamma_{M0}} \quad (2.57)$$

Where:  $f_y$  is the yielding strength of the steel

$A_v$  is the shear area

### iv. Shear and bending moment interaction

In case the shear force is less than half the plastic shear resistance ( $V_{Ed} < 0.5V_{pl,Rd}$ ), its effect on the moment resistance may be neglected. Otherwise, if  $V_{Ed}$  exceeds 50% of  $V_{pl,Rd}$ , the reduced plastic shear resistance of the beam section is calculated using a reduced yield strength  $f'_y$  of the steel is given by equation (2.58).

$$f'_y = (1 - \rho)f_y \quad (2.58)$$

$$\text{Where: } \rho = \left( \frac{2V_{Ed}}{V_{pl,Rd}} - 1 \right)^2 \quad (2.59)$$

#### 2.4.4. Serviceability Limit States (SLS) verifications

The serviceability limit states are concerned with the structure's behaviour under normal operation, the comfort of those who use the structure, and its appearance. The serviceability limit states may be irreversible or reversible.

Irreversible limit states occur when some consequences persist after the actions that exceeded the limit have been removed, such as permanent girder deformation or cracking in some bridge members. On the other hand, reversible limit states are witnessed when none of the consequences of the actions that exceeded the limit remain after the actions that exceeded the limit have been removed, so the member stresses are within its elastic region.

The following criteria are taken into account during serviceability limit state design checks:

- Deflections that affect the structure's appearance, user comfort, and functionality;
- Vibrations that may limit the structure's functionality and cause discomfort to structure users;
- Damages that may have an impact on the structure's appearance or durability and;
- Stress limitation in the section.

The Eurocodes do not specify any serviceability criteria limits, but these limits may be specified in the National Annexes. The limits for each project should be defined based on the member's use and the client's requirements. The following SLS checks will be considered for our bridge structure and requirements:

- For the stress limitation in steel members, the stress  $\sigma$  in the element is limited by equation (2.60),

$$\sigma \leq 0.8f_y \quad (2.60)$$

- For beam elements, the control of the deflection  $d$  in millimetres shall be done following equation (2.61)

$$d < l/500 \quad (2.61)$$

where,  $l$  is the span length in millimetres.

## **2.5. Redundancy analysis**

As can be extracted from the previous chapter that, apart from the pristine state, redundancy stresses the desired global behaviour of a structure under accidental failure scenarios. Taking this fact into consideration, it can be said herein that: redundancy is an essential property of a structural system concerning existence and subsequent development of alternative load path(s) or multiple load-transfer mechanisms. Owing to the wide variability of accidental scenarios, redundancy shall nominally be viewed as a property of a structural system alone and being independent of the possible accidental scenarios.

The structural components of a bridge do not behave independently but interact with other components to form one structural system. Current bridge specifications ignore this system effect and deal with individual components. Because redundancy is connected to system behaviour, this study will attempt to assess the response of an arch bridge following accidental and unpredicted failure situations in the bridge.

For the purpose of this work, the accidental failure of the hangers will be assumed in different configurations and the global behaviour of the structure assessed. To do so, 10 hanger loss cases will be assumed. Being mindful of the infinite numbers of scenarios that could arise, it was decided to split the cases into symmetric and asymmetric hanger failure configuration in order to have a wider view of the possible situations. The structural analysis of the structure in all the 10 cases will be carried out and important values of stress redistribution in the hangers, arch and girder compared. Also, the global deflection of the bridge will be assessed.

## **2.6. Resilience analysis**

To analyse the resilience of a bridge, the ideal situation would be to use a structural model and a finite element analysis package that consider the elastic and inelastic behaviour of the bridge members. This program could evaluate intact bridges under the effect of heavy loads as well as consider different damage scenarios. The program could be used to check the structure to verify whether acceptable behaviour, unserviceable conditions, or collapse states occur under maximum expected loading conditions.

To analyse the resilience of the arch bridge in this work, the definition of the dynamic accidental load will be first done. Then the FEM software will be used to predict the response of the bridge to the dynamic load.

### **2.6.1. Explosive weight and positions of explosion**

The following considerations will be made:

- Blast will occur at 2 different positions. The considered cases are: blast at start off the bridge (at the position Hanger 1) and blast at middle of bridge (at Hanger 15).
- Assuming that the bomb is transported on the railway by a train have considered a size that this vehicle can carry. A blast from 500 kg of TNT will be used.

### **2.6.2. Blast loading**

The minimum height above which the blast can happen will be 1 m. The effect of explosion diminishes as the scaled distance increases. Thus, the maximum stand-off distance of 3 m is considered. The charges are blasted on the bridge side at 1 m from the hangers. This is done in order to see the maximum effect on the hangers. Blast wave considered dispersing in all directions and affect all girders surrounded by the blast.

The blast parameters (weight 500 kg and stand-off distance 1 m) will be input in the software RCBlasT to determine the blast wave properties that will then be applied as dynamic load in MIDAS/Civil.

### **2.6.3. Eigen value analysis**

An eigen value analysis provides dynamic properties of a structure by solving the characteristic equation composed of mass matrix and stiffness matrix. The dynamic properties include natural modes (or mode shapes), natural periods (or frequencies) and modal participation factors.

- **Natural mode:** A natural mode pertains to free vibration in an undamped system. 1st mode, 2nd mode... and nth mode represent the order in which least energy is required to deform the structure.
- **Natural Period:** A natural period is the time that it takes to freely vibrate the structure into the corresponding natural mode one full cycle.

- **Modal Participation Factor:** The ratio of the influence of a specific mode to the total modes.

It is necessary to point out the fact that an eigen value analysis must precede dynamic analyses such as time history analysis or response spectrum analysis.

#### 2.6.4. Non-linear time-history analysis

When extreme loadings like blast are applied to a structure thereby resulting in high stresses in the range of non-linear stress-strain relationship, material non-linear behaviours are encountered. Highly stressed elements like hangers enter in a domain of non-linear behaviour due to the high stresses. In order to assess the resilience of the structure it necessary to be able to predict the evolution of stresses with time in the structure which influence the time of recovery of the structure or the damage of this one locally or globally. Resilience in this case is regarding a global point of view and not the failure of only one element.

##### 2.6.4.1. Non-linear behaviour of elements

Prior to this analysis, it is necessary to describe the non-linear properties the materials will portray while in the plastic range.

The non-linear behaviour is achieved when the linear elastic behaviour of a material is surpassed. In fact, the bridge is modelled with elements having linear elastic properties. Therefore, the non-linearity of the materials must be taken into account especially for extreme dynamic loading such as blast. The behaviour laws defined by the Park model were considered and the properties will be automatically computed in the software.

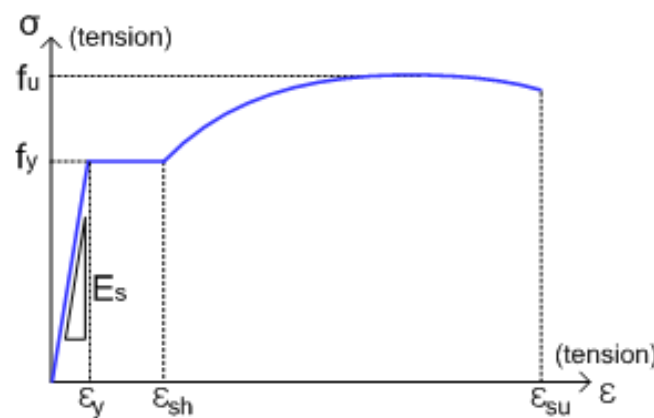


**Figure 2.8.** Park model for non-linear behaviour of elements

Where:

$f_y$	is the yielding stress of the material	$\epsilon_y$	is the yielding strain of the material
$f_u$	is the ultimate stress of the material	$\epsilon_{sh}$	is the strain at the onset of strain hardening
$E_s$	is the elastic modulus of the material	$\epsilon_{su}$	is the rupture or ultimate strain of the material

#### 2.6.4.2. Dynamic equilibrium consideration

For a time-history analysis, the dynamic equilibrium equations to be solved are given by equation (2.62).

$$[M]\ddot{u}(t) + [C]\dot{u}(t) + [K]u(t) = p(t) \quad (2.62)$$

Where:

$[K], [C], [M]$  are the stiffness matrix, the damping matrix and the diagonal mass matrix respectively

$u, \dot{u}$ , and  $\ddot{u}$ : are the displacement, velocity and acceleration of the structure respectively

$p(t)$  represents the applied load (blast in this case).

Modal-superposition is a good procedure to the non-linear problems. Therefore, it will be to solve the dynamic equilibrium equation in order to obtain the time-history response of the bridge against blast load.

## Conclusion

The aim of this chapter was to give detailed step-by-step procedures used all through the thesis work. Accordingly, the chapter started by recognising the site through physical and geographical parameters. Subsequently, the procedure for collecting data, assessing codes and standards used in this study, as well as determining the different actions and actions combinations necessary for the structural verification of the arch bridge, was detailed. Also, the different analysis tools that were used for the work were presented. After that, the various analysis steps were made using ideal modelling tools in order to firstly, do a static verification of the structure, then analyse the behaviour of the bridge following an accidental hanger failure and finally, the response of the bridge to dynamic accidental loading.

## **CHAPTER 3: RESULTS AND DISCUSSIONS**

---

### **Introduction**

This chapter presents the results of the step-by-step procedure detailed in the previous chapter. It starts by presenting the results of the research on the site where the case study is found and the various data collected. Secondly, the results of the various load computations performed are presented as well as those of the verification of the structural model both at ultimate and at serviceability limit states. Subsequently, it presents the results of the redundancy analysis that was conducted considering different configurations of hanger failure in the arch bridge. Furthermore, the main results of the dynamic time history analysis of blast load effect on the bridge are portrayed. The corresponding discussions proceed accordingly as the various results obtained are presented.

### **3.1. General site presentation**

In order to conduct an appropriate study, it is necessary to have a good knowledge of the context of the project which is at the centre of our attention. Thus, this section aims at presenting the site at which the bridge is located. To do so effectively, the physical parameters will firstly be presented as well as the human and socio-economic parameters, which influence the project of interest.

#### **3.1.1. Physical parameters**

Here, parameters like the geographical location, the climate, the hydrology and the topography of the city harbouring the project will be presented.

##### **3.1.1.1. Geographical location**

Genoa (Genova in Italian, Genua in Latin) is a very particular city and capital of the Liguria region in Italy. As it was the city of ancient Ligurians, its name probably originates from a word Genoa in Ligurian which means "knee", or in other words "angle" in reference to its geographical position on the map of Italy (see Figure 3.1). It is the sixth-largest city in Italy and is located in a narrow coastal strip between the sea and the mountains that forms the watershed with the Po Valley, more particularly at latitude  $44^{\circ} 24' 50.9940''$  N and  $8^{\circ} 56'$

31.8624" E. The municipality extends on a surface area of about 240 km<sup>2</sup>, mainly stretched for 30 km along the coast and, secondly, along the two main valleys of Bisagno and Polcevera rivers. The territory of Genoa is divided into 5 main areas: the centre, the west, the east, the Polcevera and the Bisagno valley.



**Figure 3.1.** Geographical location of Genoa on the map of Italy (roughguides.com)

Being a coastal city, the city of Genoa has a good number of major and minor water bodies throughout it. One of the major rivers crossing this city is the Polcevera River in the Polcevera valley shown on Figure 3.2. Located between Pontedecimo and the Ligurian Sea, the Polcevera is 11 kilometres long, but its total length including the Torrente Verde is 19 kilometres. Moving southwards towards the sea, after being crossed by the Ponte Morandi, a motorway bridge that partially collapsed in August 2018, the river ends its course in the Ligurian Sea between Sampierdarena and Cornigliano, two quarters of Genoa. Just about a couple of kilometres before entering the sea, it crossed by a railway arch bridge which is our case study.

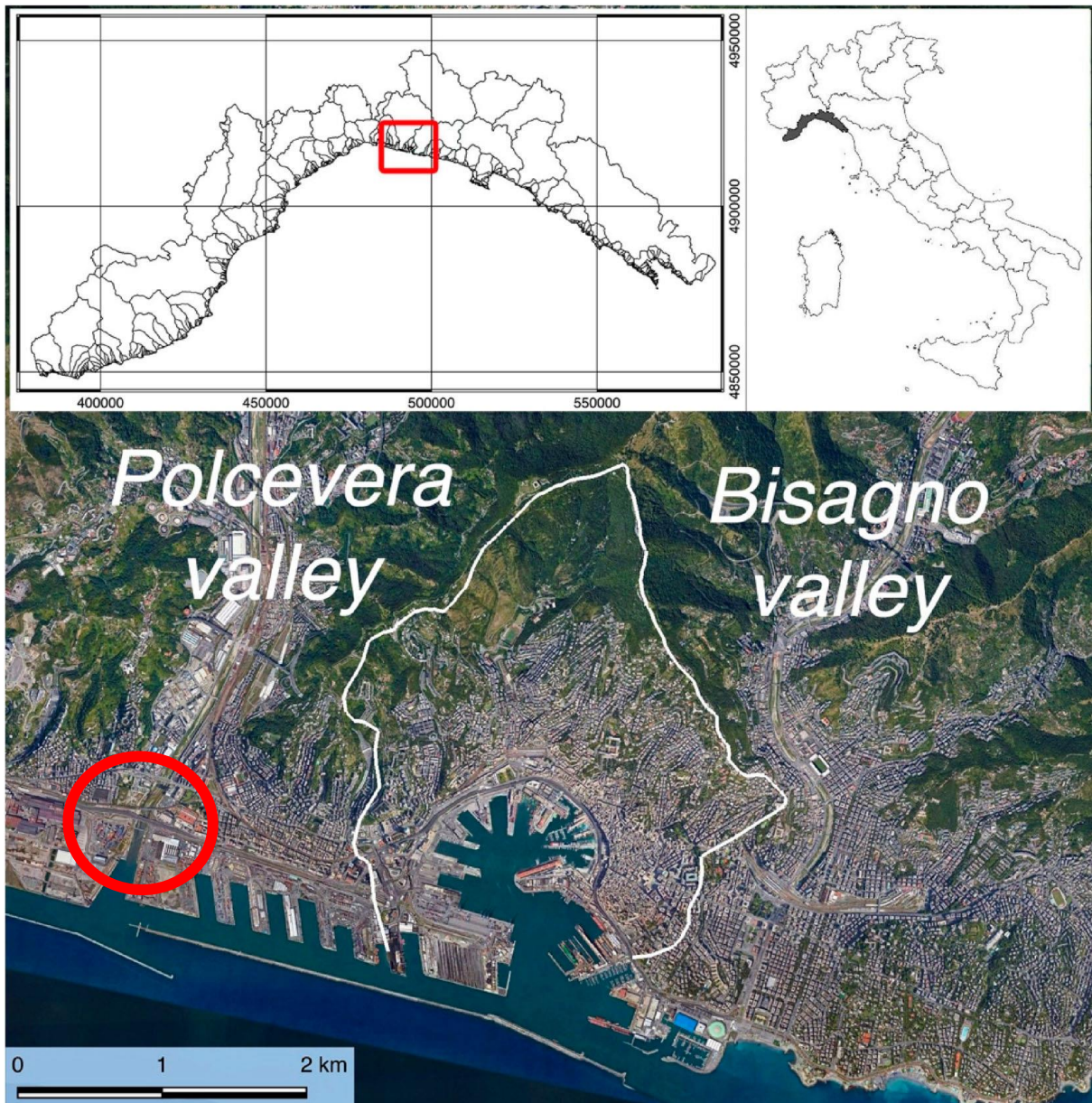


**Figure 3.2.** Location of the project (Faccini et al., 2021)

### 3.1.1.2. Climate

The climate of the area is characterized by a mild winter and hot summer with a wet autumn and spring. The medium annual rainfall is about 1300 mm per year (Paliaga et al., 2019) but mostly concentrated in the humid seasons as during the summer, the mean monthly rainfall is less than 40 millimetres. The diagram in Figure 3.3 highlights the medium-high rainfall values in October and November during which events of floods and shallow landslides often occur. Also, the annual average relative humidity is 68%, ranging from 63% in February to 73% in May.

The average yearly temperature is around 19 °C during the day and 13 °C at night. In the coldest months: December, January and February, the average temperature is 12 °C during the day and 6 °C at night. In the warmest months: July and August, the average temperature is 27.5 °C during the day and 21 °C at night. The mean monthly temperatures in the city of Genoa are presented on Figure 3.3. The daily temperature range is limited, with an average range of about 6 °C between high and low temperatures. Furthermore, being a coastal city, the average annual temperature of the sea is 17.5 °C, from 13 °C in the period January to March to 25 °C in August. In the period from June to October, the average sea temperature exceeds 19 °C.

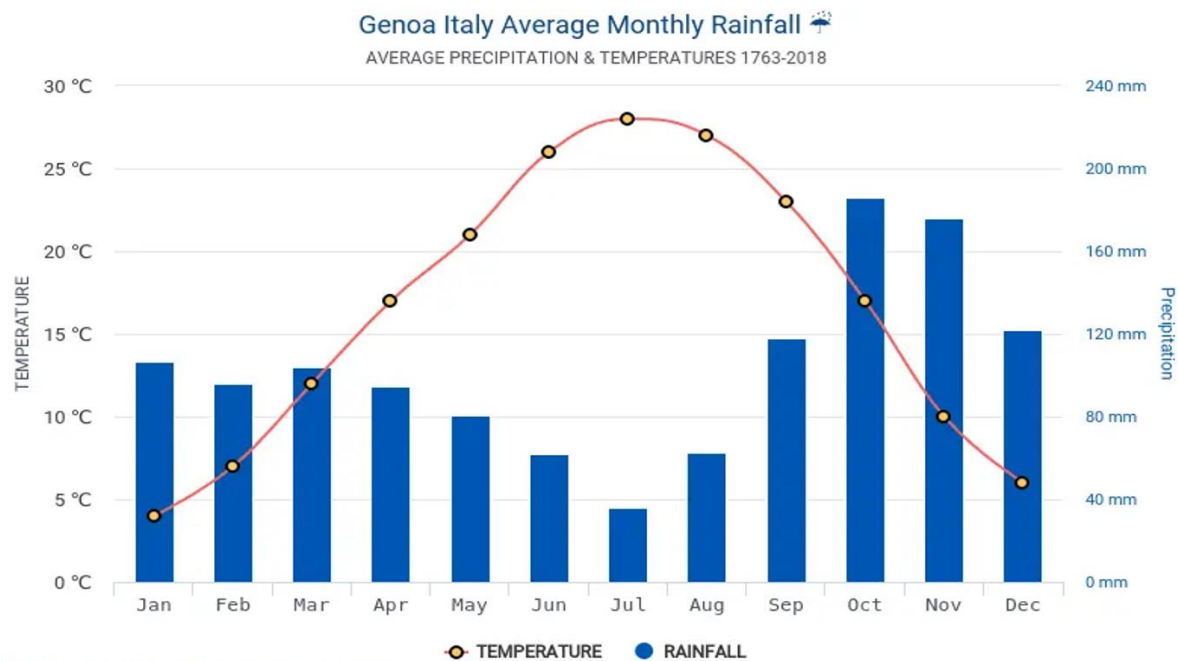


**Figure 3.3.** Mean monthly rainfall and temperatures in Genoa (climate-data.org)

Genoa is also a windy city, especially during winter when northern winds often bring cool air from the Po Valley (usually accompanied by lower temperatures, high pressure and clear skies).

### 3.1.1.3. Relief and hydrology

The maximum altitude of the studied area around the project is about 496 m at the Sperone Fortress, about 3 km from the coastline. The slope gradient is high particularly in the eastern part of the Municipality and in the western one, where values above 50% are widely spread. The slope angle varies between 20° and 40°, even though near the coastal strip it shows lower values than 10°. Such a morphometric feature is the main predisposing factor of the high geo-hydrological hazard in the area: in case of heavy rainfall the reduced time of concentration

of the small catchments causes the run-off to reach quickly the small floodplain, where the concentrated flow impacts an intensely urbanized territory. Within this territory, several small drainage basins (total area between 0.45 and 2.36 km<sup>2</sup>) as represented in the ‘Genova Zero’ map whose streams nowadays flow widely covered by urbanization. The two main rivers of the city of Genoa are the Polcevera river to the West and the Bisagno one to the East are previously presented on Figure 3.2.

#### **3.1.1.4. Geology**

The geological features of the area are another factor contributing to instability and then to geo-hydrological hazard. The geological sketch map of Genoa shows the presence of sedimentary bedrock in the eastern part of the Municipality and ophiolite in the western one, with a transition zone in the middle. A pervasive structural deformation, both fragile and ductile of the rock mass, together with a frequent alternation of different lithology, are often an important predisposing factor to instability processes. The geological setting of the area around the project is characterized by heterogeneous Flysch and Pliocene clay deposits. Some of the soils and rock types present are Marly limestone, marls with shale interlayers, siltstones and Ortovero clays.

#### **3.1.2. Human and socio-economic parameters**

This section is concerned with the description of parameters like population, economy, culture and transportation.

##### **3.1.2.1. Population**

Genoa is a coastal port city with a present population of about 600,000 inhabitants even though in the early 70s, when industrial activity was at its highest, it was more than 800,000 (as shown on Figure 3.4) and planners were imagining a 1 million citizens city. At the beginning of 2011, there were 608,493 people residing in Genoa, of whom 47% were male and 53% were female. The city is characterised by rapid aging and a long history of demographic decline, that has shown a partial slowdown in the last decade. Genoa has the lowest birth rate and is the most aged of any large Italian city. Minors (children with ages 18 and younger) totalled only 14.12% of the population compared to pensioners who number 26.67%. This compares with the Italian average of 18.06% (minors) and 19.94% (pensioners). The median age of Genoa's residents is

47, compared to the Italian average of 42. The current birth rate of the city is only 7.49 births per 1,000 inhabitants, compared to the national average of 9.45.

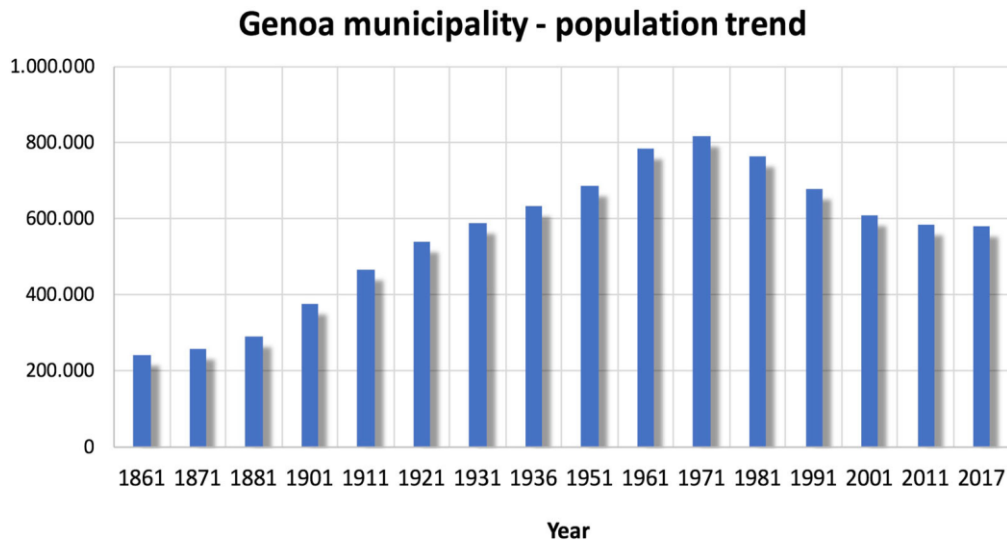


**Figure 3.4.** Population trend in the city of Genoa (Paliaga et al., 2019)

### 3.1.2.2. Economy

The first settlements and even the actual main industrial and transport activities are based on the port that is one of the main harbours in the Mediterranean Sea. This port was extended in the 1950s due to the industrial zones of Milan and Turin which needed supplies. There has been an increase in the container trans-shipment over years. The city is also an important exit point for the oil pipelines to Switzerland and Germany. The surrounding districts such as: Sampierdarena, Cornigliano and Multedo are important heavy industry centres. Other significant industrial sectors are papermaking, textiles and transport.

### 3.1.2.3. Transport

The city has highly developed transport infrastructure. Firstly, the Port of Genoa in which several cruise and ferry lines serve the passenger terminals, with a traffic of 3.2 million passengers in 2007. The quays of the passenger terminals extend over an area of 250,000 square metres, with 5 equipped berths for cruise vessels and 13 for ferries, for an annual capacity of 4 million ferry passengers, 1.5 million cars and 250,000 trucks. Also, due to its high population density, the city of Genoa has an extensive traffic network and is linked with the major cities of Italy, France and Switzerland by railway and highways. The city has several railway stations and a good railway network. The main railway stations are Genoa Brignole in the east and Genoa Principe in the west. From these two stations depart the main trains connecting Genoa

to France, Turin, Milan and Rome. Lastly, the city has an airport built over the sea, named the Christopher Columbus Airport, in reference to the famous explorer Christopher Columbus who was born in Genoa in 1451.

### **3.2. Presentation of the project**

The work is located in the locality of Sampierdarena in Genoa, more precisely in the area of the former ILVA Cornigliano plant at latitude  $44^{\circ} 24' 46.94''$  N and longitude  $8^{\circ} 52' 41.14''$  E and constitutes the railway crossing on the Polcevera stream. The construction is part of the redevelopment of the freight network of the Genoa junction, being the replacement of the metal girders of the railway bridge over the Polcevera stream at the kilometric point 0+995 of the Genoa-Ventimiglia line and the construction of the variant route of the section of line affected from kilometric point 0 + 730 to kilometric point 1+335 approximately to solve the interference with the new road layout of the Canepa seafront.

#### **3.2.1. Geometrical and structural characteristics**

An aerial view of the project is presented on Figure 3.5.



**Figure 3.5.** View of the Polcevera railway arch bridge

It is a steel arch bridge whose construction ended in 2011, having a total length of 179.5 m and made principally of two identical arches of spans 80 m each (see Figure 3.6). The structural typology adopted for the 80 m spans, that is from SPA to P2, is that of an eliminated thrust arch at the bottom and braced walls at the top.

The length of each beam, between the axes of the supports, is 78.50 m, while the distance between the walls (width of the bridge) is 10.80 m as shown on Figure 3.7. On each wall, the arch is connected to the main beam by means of 15 hangers with a 4 m pitch consisting of round bars in special S 460 NL steel with nominal diameter  $\Phi$  130 mm. The arch-deck connection takes place by means of the special end segment (“shoe”) which provides for a connection of the arch cores to the core of the beam-chain. The arch consists of a caisson section 2 m high, with an upper flange 1500 x 35 mm, a lower flange 1500 x 35 mm and two 30 mm cores; the height in the key of the arch is 18.70 m. The beams are made with a double T section of height 2.80 m, with upper flange 1000 x 40 mm, lower flange 1000 x 40 mm and 20 mm core, in correspondence with the joint with the arch the thickness of the core becomes equal to 40 mm.

The remaining span from P2 and SPB is made with a simple support deck whose length, between the axes of the supports, is 10.80 m. The beams are made with a double T section (like an I section) of height 2.80 m, with upper flange 1000 x 30 mm (segment 1) and 1000 x 35 mm (segment 2), lower plate 1000 x 30 mm (segment 1) and 1000 x 35 mm (segment 2) and core of 20 mm (segment 1) and 18 mm (segment 2). The support surface for the railway superstructure is made with a deck with HEB 600 steel beams embedded in a concrete slab with a minimum thickness of 650 mm; the extrados of the slab provides a waterproofing mantle with overlying protective screed. The retaining walls of the ballast and the slab have  $\Phi$  130 holes for water drainage.

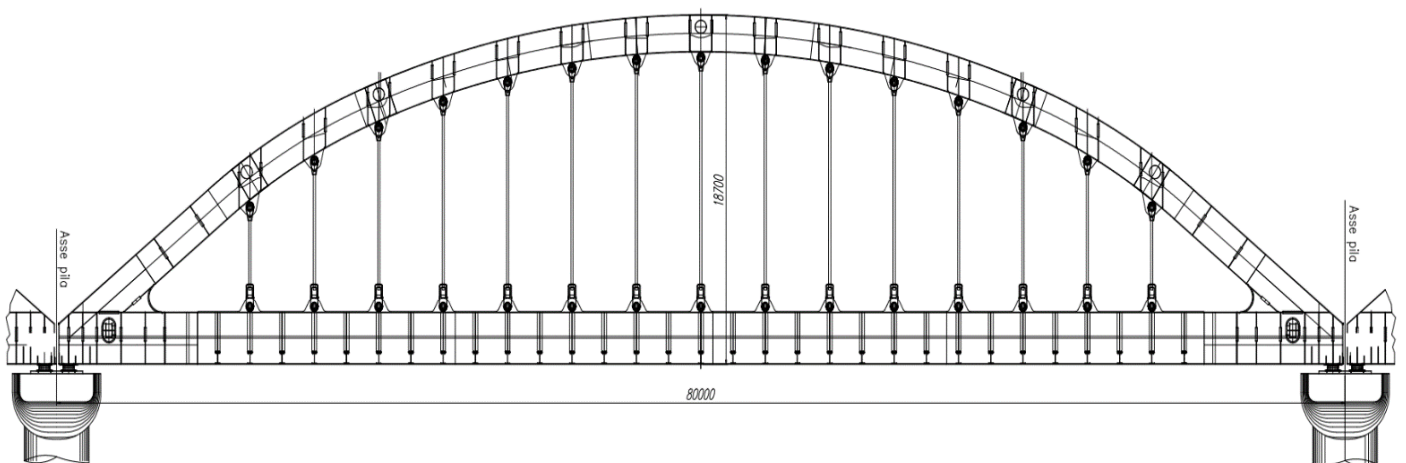


**Figure 3.6.** Longitudinal view plan of one arch of the Polcevera railway arch bridge

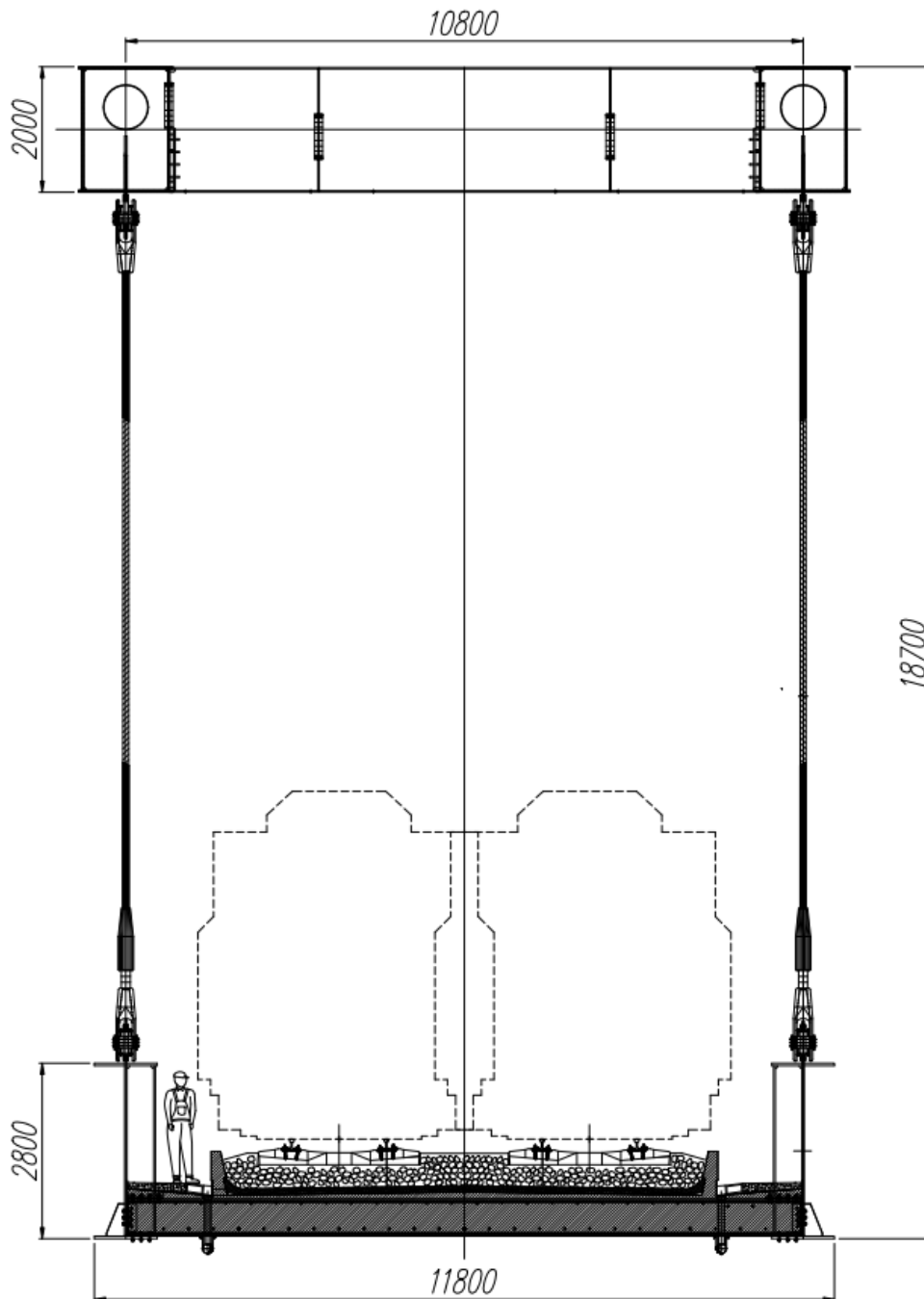


Figure 3.7. Cross sectional view in the midspan of the bridge

### 3.2.2. Materials characteristics

The structure is made of steel as the main material with a S420 grade for all the main structural elements (arch rib, girder beam, cross beam, cross bracings) while the hangers are made of steel class S460 NL, the characteristics of which, are presented on Table 3.1 and Table 3.2 respectively. Moreover, the slab concrete belongs to C32/40 resistance class with normal

setting (N). For steel reinforcement, B450C was considered. The principal characteristics of concrete and steel reinforcement used are reported in Table 3.3 and Table 3.4 respectively.

**Table 3.1.** Mechanical characteristics of main structural steel used

<b>Structural Steel</b>			
<b>Designation</b>	<b>S 420 (EN 10025-3)</b>		<b>Units</b>
Characteristic Ultimate Strength	$f_{uk}$	520	MPa
Characteristic Yield Strength	$f_{yk}$	420	MPa
Elastic Modulus	$E_s$	210000	MPa
ULS Safety Factor	$\gamma_s$	1.05	
Design Yield Strength	$f_{yd}$	400.00	MPa
Density	$\rho$	7850	kg/m <sup>3</sup>
Unit weight	$\gamma$	78.5	kN/m <sup>3</sup>
Shear modulus	$G$	80769.23	MPa
Poisson's ratio in elastic range	$\nu$	0.3	
Coefficient of linear thermal expansion	$\alpha$	0.000012	°K <sup>-1</sup>

**Table 3.2.** Mechanical characteristics of steel used for hangers

<b>Steel for Hangers</b>			
<b>Designation</b>	<b>S 460 N/NL (EN 10025-3)</b>		<b>Units</b>
Characteristic Ultimate Strength	$f_{uk}$	540	MPa
Characteristic Yield Strength	$f_{yk}$	460	MPa
Elastic Modulus	$E_s$	210000	MPa
ULS Safety Factor	$\gamma_s$	1.05	
Design Yield Strength	$f_{yd}$	438.10	MPa
Density	$\rho$	7850	kg/m <sup>3</sup>
Unit weight	$\gamma$	78.5	kN/m <sup>3</sup>
Shear modulus	$G$	80769.23	MPa
Poisson's ratio in elastic range	$\nu$	0.3	
Coefficient of linear thermal expansion	$\alpha$	0.000012	°K <sup>-1</sup>

**Table 3.3.** Mechanical characteristics of concrete

<b>Concrete for deck slab</b>			
<b>Designation</b>		<b>C32/40</b>	<b>Units</b>
Cylindrical Characteristic Strength	$f_{ck}$	32	MPa
Average Cylindrical Strength	$f_{cm}$	40	MPa
Average Tensile Strength	$f_{ctm}$	3.02	MPa
Average Flexural Strength	$f_{ctfm}$	3.63	MPa
Elastic Modulus	$E_{cm}$	33345.76	MPa
Cracked Elastic Modulus	$E_{cracked}$	16672.88	MPa
Cylindrical Design Strength	$f_{cd}$	18.13	MPa
Design Tensile Strength	$f_{ctd}$	1.41	MPa

**Table 3.4.** Mechanical characteristics of concrete slab steel reinforcement

<b>Steel reinforcements for concrete</b>			
<b>Designation</b>		<b>B450C</b>	<b>Units</b>
Characteristic Ultimate Strength	$f_{uk}$	540	MPa
Characteristic Yield Strength	$f_{yk}$	450	MPa
Elastic Modulus	$E_s$	210000	MPa
Design Yield Strength	$f_{yd}$	391.30	MPa

### 3.3. Load determination and combinations

Eurocodes and principles illustrated in section 2.3 were used to calculate the different load values, do the load combinations and conduct the static analysis verifications of the arch bridge model. This section presents the results of the load computation and the eventual load combinations.

#### 3.3.1. Load determination

Here the different loads acting on the structure calculated using the guidelines provided in the section 2.3.2 are presented.

### 3.3.1.1. Permanent actions

The different permanent actions present on the bridge include the self-weight of the structural members and the ones of the non-structural members. The self-weight of the structural elements was automatically computed by the software using the properties of the sections and densities of the defined materials. It should be noted that a load increment factor of 15% was added to take into account the weight of the connections, steel plates and other minor structural elements. Also, for simplicity of the model, the concrete slab self-weight was also computed and applied on the main girders. The results for the structural elements are presented on Table 3.5.

**Table 3.5.** Self-weight of structural elements

Permanent loads	Values	Units
Self-weight of steel structural elements (+15%)	78.5	kN/m <sup>3</sup>
Self-weight of concrete slab	25	kN/m <sup>3</sup>

With regards to the non-structural elements, the ones considered are the self-weights of the rail structure (ballast, sleepers, rails...). It should be noted that there's no footway on our railway bridge, nor guardrails since the girders have a sufficient height to act directly as guardrails. The results are presented on Table 3.6.

**Table 3.6.** Self-weight of non-structural elements

Elements	Number	Weight density (kN/m <sup>3</sup> )	Width (m)	Thickness / height(m)	Characteristic value (kN/m)
Ballast	1	20	8	0.35	56
Sleepers (spacing = 0.6 m)	2 (Lanes 1&2)	24 (Concrete sleepers)	2.6	0.15 x 0.24 (cross section)	3.96
Rails	4 (2 per lane)	/	/	/	2.4

### 3.3.1.2. Live loads

#### a. Traffic load

The number of notional lanes in this case is 2, each of width 3 m and axle spacing (approximately the standard rail spacings used) of 1435 mm prescribed for normal railways. It is necessary to recall that, the railway traffic model adopted for the design is the standard Load Model 71 (LM 71) for normal rail traffic on railway bridges with an adjustment factor of 1.33. The model is predefined in the software MIDAS/Civil and so was just calibrated as illustrated on Figure 3.8.

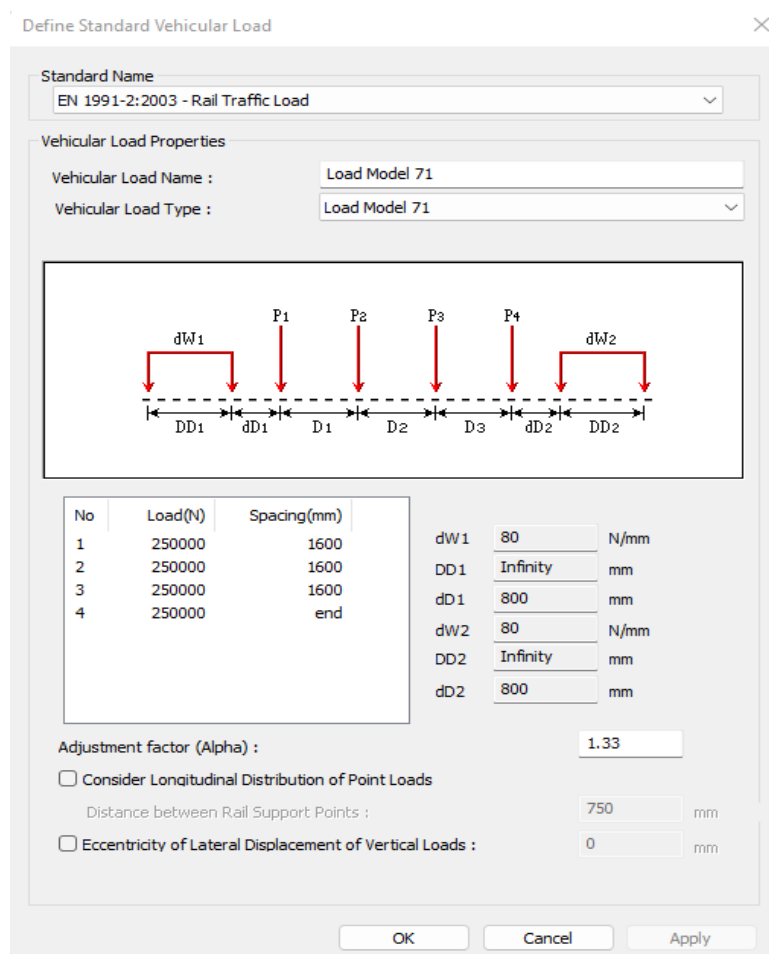


Figure 3.8. Load Model 71 rail traffic vehicle load definition in MIDAS/Civil

#### b. Wind Load

With the information on wind load determination given in section 2.3.2.2 well known, proceeding to an excel implementation permits to find the wind force acting on the structure and then distribute it to the wind braces. This project faces a terrain of category 0 ( $z_0 = 0.003$  m

and  $z_{\min} = 1$  m). The fundamental reference velocity considered is  $V_{b,0} = 28$  m/s according to Figure 3.9 and Table 3.7.



Figure 3.9. Wind map zones of Italy (Sonda, 2019)

Table 3.7. Basic wind reference velocity for wind zones in Italy (Sonda, 2019)

Zona	Descrizione	$v_{b,0}$ [m/s]	$a_0$ [m]	$k_a$ [1/s]
1	Valle d’Aosta, Piemonte, Lombardia, Trentino Alto Adige, Veneto, Friuli Venezia Giulia (con l’eccezione della provincia di Trieste)	25	1000	0,010
2	Emilia Romagna	25	750	0,015
3	Toscana, Marche, Umbria, Lazio, Abruzzo, Molise, Puglia, Campania, Basilicata, Calabria (esclusa la provincia di Reggio Calabria)	27	500	0,020
4	Sicilia e provincia di Reggio Calabria	28	500	0,020
5	Sardegna (zona a oriente della retta congiungente Capo Teulada con l’Isola di Maddalena)	28	750	0,015
6	Sardegna (zona a occidente della retta congiungente Capo Teulada con l’Isola di Maddalena)	28	500	0,020
7	Liguria	28	1000	0,015
8	Provincia di Trieste	30	1500	0,010
9	Isole (con l’eccezione di Sicilia e Sardegna) e mare aperto	31	500	0,020

The wind force coefficient and parameters are computed and presented on Table 3.8.

**Table 3.8.** Computed wind coefficients and parameters

Distance between Girders	$d$	10.8	m
Total Width of Bridge	$b$	10.8	m
Total Length of Bridge	$L$	78.5	m
Return Period (Years)	$T$	100	years
Reference Height for external Wind Action (m)	$z_e$	27.7	m
Air Density	$\rho_a$	1.25	kg/m <sup>3</sup>
Fundamental Basic Wind Velocity	$v_{b,0}$	28	m/s
Roughness Length (m)	$z_0$	0.003	m
Reference Roughness Length	$z_{0, ref}$	0.003	m
Minimum Height (m)	$z_{min}$	1	m
Directional Factor	$c_{dir}$	1	
Season Factor	$c_{season}$	1	
Orography Factor	$c_o(z_e)$	1	
Turbulence Factor	$k_l$	1	
Probability of Exceedance	$p$	0.01	
Probability Factor	$c_{prob}$	1.04	
Terrain Factor	$k_r$	0.19	
Roughness Factor	$c_r(z_e)$	1.2	
Basic Wind Velocity (m/s)	$v_b$	28	m/s
Mean Wind Velocity (m/s)	$v_m$	33.6	m/s
Turbulence Intensity	$I_v(z_e)$	0.158	
Peak Velocity Pressure (kPa)	$q_p(z_e)$	1.38	kPa

Using the above parameters, the wind force is computed and reported on Table 3.9

**Table 3.9.** Wind force computation

Parameter	Symbol	Value	Unit
Depth of Velocity Pressure (m)	$d_{tot}$	2.8	m
Width to Depth Ratio	$b/d_{tot}$	3.86	
Reference Area (m <sup>2</sup> )	$A_{ref}$	177.48	m <sup>2</sup>
Wind Load Factor	$C_f$	1.5	
Wind Force on element (kN)	$F_w$	318.8	kN
Wind Distributed Load (kN/m)	$p$	4.1	kN/m

**c. Temperature**

The force due to temperature variation was determined from the data due to climate and a value of 28 °C was applied as the maximum positive temperature, with a minimum temperature of 18 °C. The positive and negative gradients  $\Delta t$  of +/-15 °C were also applied to the bridge according to section 2.3.2.2.c. Using these values, some temperature parameters were computed and reported on Table 3.10.

**Table 3.10.** Temperature load parameters

Coefficient of Thermal Expansion	$a_c$	0.000012	/°C
Concrete Cross Sectional Area	$A_c$	7.02	m <sup>2</sup>
Total Length of Bridge	L	78.5	m
Uniform Thermal Variation			
Uniform Change in Temperature	$\Delta T$	15	°C
Strain	$\epsilon$	0.00022	
Bridge Elongation	$\Delta L$	0.017	m

**d. Shrinkage effect**

From Figure 3.10, it is seen that at  $t = \infty$ , the creep coefficient of concrete is  $\rho = 1.9612$ .

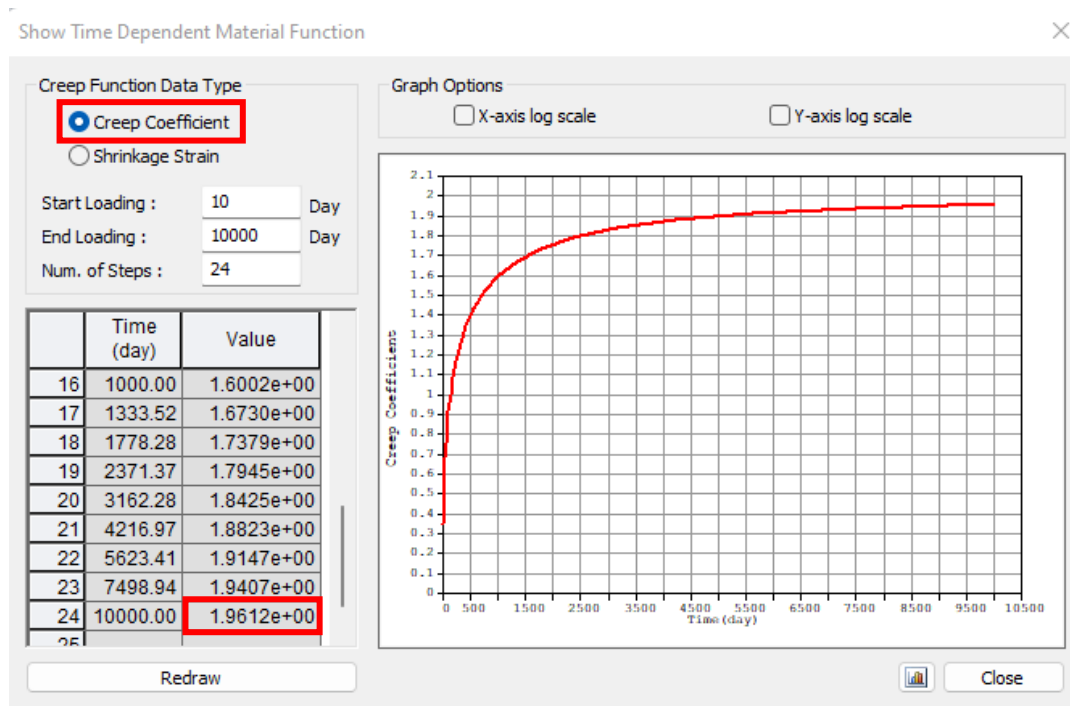


**Figure 3.10.** Graph of creep coefficient of concrete with time

Moreover, looking at graph on Figure 3.11, the long-term shrinkage strain value of the concrete deck is  $\varepsilon_{cs}(\infty) = -2.8829 \times 10^{-4}$

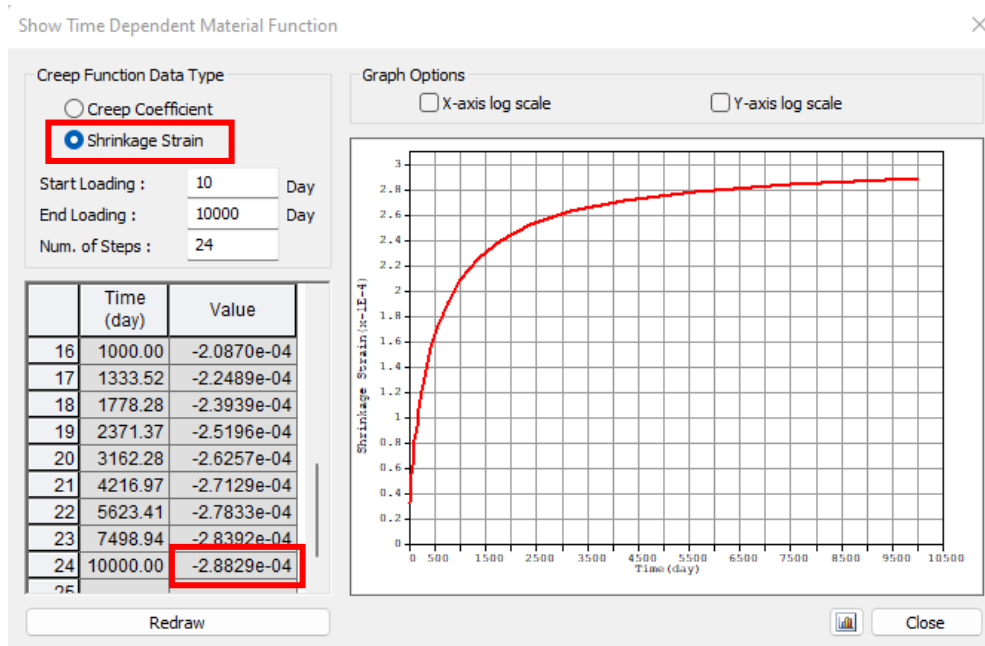


Figure 3.11. Graph of the evolution of shrinkage strain with time

So, using the formulations in section 2.3.2.2d, the values of different coefficients and axial force value due to shrinkage were obtained and presented in Table 3.11.

Table 3.11. Computation of the shrinkage force

Designation	Symbol	Values	Units
Concrete-steel homogeneity coefficient for short-term loading	$n_0$	6.16	/
Concrete-steel homogeneity coefficient for long-term loading	$n_L$	13.65	/
Effective elastic modulus of concrete	$E_{c,eff}$	11262	$N/mm^2$
Total shrinkage force	$N_{c,r\infty}$	22792	$kN$
Shrinkage force per effective section	$N_{beam}$	11396	$kN$

### 3.3.2. Load combinations

In reference to the Eurocode 0 guidelines for combining actions on a structure as illustrated in section 2.3.3, the load combinations at ULS and SLS were obtained and presented on Table 3.13 and Table 3.14 respectively. It should be noted that the combinations presented

are sufficient for the design and verification of the arch bridge but yet not exhaustive. Table 3.12 shows the different symbols used to represent the loads in the combinations.

**Table 3.12. Load description symbols**

Load	Description
$G_{1a}$	Self-weight of structural elements
$G_{1,c}$	Self-weight of concrete slab
$G_2$	Self-weight of non-structural elements
$M$	Moving Load (traffic)
$S$	Shrinkage
$T(+or-)$	Thermal actions (temperature rise or fall)
$W$	Wind action

**Table 3.13. ULS load combinations**

ULS Load Comb	Description	Load Factors ( $\psi$ factors included)							
		$G_{1a}$	$G_{1,c}$	$G_2$	$M$	$W$	$T_+$	$T_-$	$S$
ULS 1	1.35G+1.45M[1]+1.125W[1]+1.2S	1.35	1.35	1.35	1.45	1.125			1.2
ULS 2	1.35G+1.45M[1]-1.125W[1]+1.2S	1.35	1.35	1.35	1.45	-1.125			1.2
ULS 3	1.35G+1.45M[2]+1.125W[1]+1.2S	1.35	1.35	1.35	1.45	1.125			1.2
ULS 4	1.35G+1.45M[2]-1.125W[1]+1.2S	1.35	1.35	1.35	1.45	-1.125			1.2
ULS 5	1.35G+1.45M[1]+1.125W[1]+0.9T[+]+1.2S	1.35	1.35	1.35	1.45	1.125	0.9		1.2
ULS 6	1.35G+1.45M[1]+1.125W[1]+0.9T[-]+1.2S	1.35	1.35	1.35	1.45	1.125		0.9	1.2
ULS 7	1.35G+1.45M[1]-1.125W[1]+0.9T[+]+1.2S	1.35	1.35	1.35	1.45	-1.125	0.9		1.2
ULS 8	1.35G+1.45M[1]-1.125W[1]+0.9T[-]+1.2S	1.35	1.35	1.35	1.45	-1.125		0.9	1.2
ULS 9	1.35G+1.45M[2]+1.125W[1]+0.9T[+]+1.2S	1.35	1.35	1.35	1.45	1.125	0.9		1.2
ULS 10	1.35G+1.45M[2]+1.125W[1]+0.9T[-]+1.2S	1.35	1.35	1.35	1.45	1.125		0.9	1.2
ULS 11	1.35G+1.45M[2]-1.125W[1]+0.9T[+]+1.2S	1.35	1.35	1.35	1.45	-1.125	0.9		1.2
ULS 12	1.35G+1.45M[2]-1.125W[1]+0.9T[-]+1.2S	1.35	1.35	1.35	1.45	-1.125		0.9	1.2
ULS 13	1.35G+1.16M[1]+1.5W[1]+1.2S	1.35	1.35	1.35	1.16	1.5			1.2
ULS 14	1.35G+1.16M[2]-1.5W[1]+1.2S	1.35	1.35	1.35	1.16	-1.5			1.2
ULS 15	1.35G+1.5T[1]+1.2S	1.35	1.35	1.35			1.5		1.2
ULS 16	1.35G+1.5T[2]+1.2S	1.35	1.35	1.35				1.5	1.2

**Table 3.14.** SLS load combinations

SLS Load Comb	Description	Load Factors ( $\psi$ factors included)							
		$G_{1a}$	$G_{1,c}$	$G_2$	$M$	$W$	$T +$	$T -$	$S$
SLS 1	Ch: 1.0G+1.0M[1]+0.6W[1]+1.0S	1	1	1	1	0.6			1
SLS 2	Ch: 1.0G+1.0M[1]-0.6W[1]+1.0S	1	1	1	1	-0.6			1
SLS 3	Ch: 1.0G+1.0M[2]+0.6W[1]+1.0S	1	1	1	1	0.6			1
SLS 4	Ch: 1.0G+1.0M[2]-0.6W[1]+1.0S	1	1	1	1	-0.6			1
SLS 5	Ch: 1.0G+0.8M[1]+0.6T[+]+1.0S	1	1	1	0.8		0.6		1
SLS 6	Ch: 1.0G+0.8M[1]+0.6T[-]+1.0S	1	1	1	0.8			0.6	1
SLS 7	Ch: 1.0G+1.0W[1]+1.0S	1	1	1		1			1
SLS 8	Ch: 1.0G-1.0W[1]+1.0S	1	1	1		-1			1
SLS 9	Ch: 1.0G+1.0T[+]+1.0S	1	1	1			1		1
SLS 10	Ch: 1.0G+1.0T[-]+1.0S	1	1	1				1	1
SLS 11	Fr: 1.0G+0.2W[1]+1.0S	1	1	1		0.2			1
SLS 12	Fr: 1.0G-0.2W[1]+1.0S	1	1	1		-0.2			1
SLS 13	Fr: 1.0G+0.6T[+]+1.0S	1	1	1			0.6		1
SLS 14	Fr: 1.0G+0.6T[-]+1.0S	1	1	1				0.6	1
SLS 15	QP: 1.0G+0.5T[+]+1.0S	1	1	1			0.5		1
SLS 16	QP: 1.0G+0.5T[-]+1.0S	1	1	1				0.5	1
SLS 17	QP: 1.0G+1.0S	1	1	1					1

Where:

Ch: Characteristic combination

Fr: Frequent combination

QP: Quasi-permanent combination

It is necessary to highlight that the design and verification of the bridge was done using the envelope of the load combinations, which provides the worst possible loading scenarios for each element both at ULS and SLS.

### 3.4. Design and verifications

In this section, the results of the structural analysis and the design of the bridge are presented. Firstly, the model obtained in the FEM software followed by the results of the verifications of the main structural elements.

#### 3.4.1. Numerical modelling

The numerical modelling of the bridge was done in MIDAS/Civil 2022 following the global procedure in section 2.4.1 and the result presented in Figure 3.12. It is necessary to precise that although the bridge is a two-span arch bridge. However, for this work, only one arch was modelled since the two arches are identical and structurally independent one from the other due to the presence of a joint of separation.

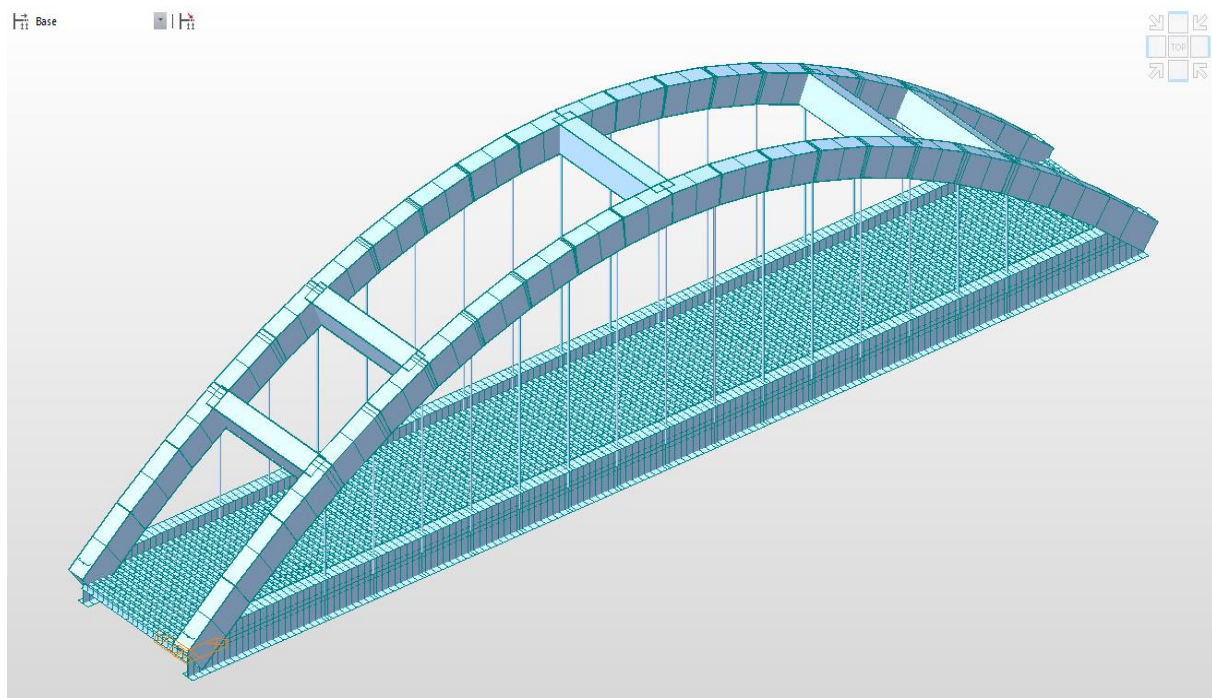


**Figure 3.12.** Numerical model for the arch bridge in MIDAS/Civil software

#### 3.4.2. Steel section presentation and classification

Classes of different structural sections of the main girder, cross beams and arch ribs are presented in this section. It concerns web and flange classifications for the I cross sections (main girder, cross beam) and the arch rib rectangular section.

3.4.2.1. Main girder

The section properties of the main girder are reported on Table 3.15.

Table 3.15. Main girder section properties

Main girder properties		
Section Properties		Unit
$f_{yk}$	420	N/mm <sup>2</sup>
$E$	210000	N/mm <sup>2</sup>
$A$	1.89E+05	mm <sup>2</sup>
$h$	2800	mm
$h_w$	2720	mm
$d$	2720	mm
$t_w$	40	mm
$b$	1000	mm
$r$	0	mm
$t_{f1}$	40	mm
$t_{f2}$	40	mm
$A_v$	108800	mm <sup>2</sup>
$W_{pl}$	999999780	mm <sup>3</sup>

The parameters for the classification of the main girder cross section are reported on Table 3.16.

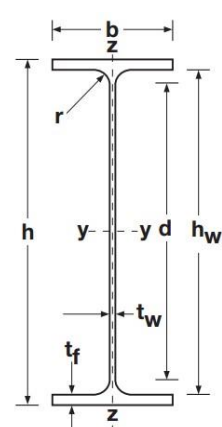
Table 3.16. Main girder section classification

Main girder classification	
<b>Web classification</b>	
d (mm)	2720
$t_w$ (mm)	40
d/t	68
$\epsilon$	0,74
124 $\epsilon$	91,76
→Class 3	
<b>Flange classification</b>	
c (mm)	480
$t_f$ (mm)	40
c/t	12
$\epsilon$	0.74
42 $\epsilon$	31.08
→Class 3	

3.4.2.2. Cross beam

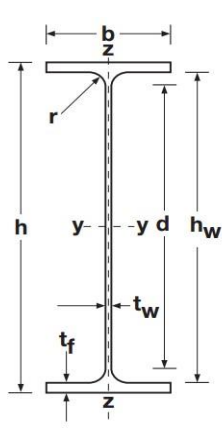
The section properties of the cross beams (HEB 600) are reported on Table 3.17.

Table 3.17. Cross beam section properties

		Cross beam properties	
		Section Properties	Unit
$f_{yk}$	420	N/mm <sup>2</sup>	
$E$	210000	N/mm <sup>2</sup>	
$A$	2.70E+04	mm <sup>2</sup>	
$h$	600	mm	
$h_w$	520	mm	
$d$	486	mm	
$t_w$	15.5	mm	
$b$	300	mm	
$r$	27	mm	
$t_{f1}$	30	mm	
$t_{f2}$	30	mm	
$A_v$	108800	mm <sup>2</sup>	
$W_{pl}$	5700000.0	mm <sup>3</sup>	

The parameters for the classification of the cross beam are reported on Table 3.18.

Table 3.18. Cross beam section classification

		Cross beam classification	
		Web classification	
$d$ (mm)	486		
$t_w$ (mm)	15.5		
$d/t$	31.35		
$\epsilon$	0,74		
$72\epsilon$	53.28		
<b>→Class 1</b>			
Flange classification			
$c$ (mm)	115.25		
$t_f$ (mm)	30		
$c/t$	3.84		
$\epsilon$	0.74		
$9\epsilon$	6.66		
<b>→Class 1</b>			

### 3.4.2.3. Arch rib

The section properties of the arch rib are reported on Table 3.19.

**Table 3.19.** Arch rib section properties

Arch rib properties			
Section properties			Unit
Height of section	<b>H</b>	2000	mm
Width of Section	<b>B</b>	1500	mm
Thickness of web	<b>t<sub>w</sub></b>	30	mm
Thickness of upper flange	<b>t<sub>f1</sub></b>	35	mm
Thickness of lower flange	<b>t<sub>f2</sub></b>	35	mm
Spacing between two webs	<b>C</b>	1370	mm
Cross sectional area	<b>A<sub>s</sub></b>	220800	mm <sup>2</sup>
Height of centroid	<b>y<sub>G</sub></b>	1000	mm
Resistance Modulus of steel	<b>W</b>	999999779.7	mm <sup>3</sup>

The parameters for the classification of the arch rib section are reported on Table 3.20.

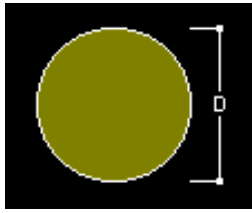
**Table 3.20.** Arch rib section classification

Arch rib classification	
<b>Web classification</b>	
c (mm)	1930
t <sub>w</sub> (mm)	30
d/t	64.33
ε	0,74
124ε	91.76
→Class 3	
<b>Flange classification</b>	
c (mm)	1370
t <sub>f</sub> (mm)	35
c/t	39.14
ε	0.74
42ε	31.08
→Class 3	

### 3.4.2.4. Hangers

The arch is connected to the main girder by means of 15 hangers with a 4 m pitch consisting of round bars in special S 460 NL steel with nominal diameter Φ 130 mm. The cross-section characteristics of hangers are shown on Table 3.21.

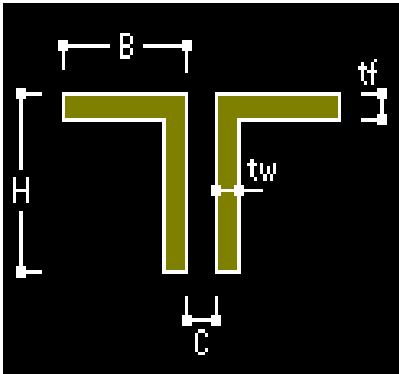
**Table 3.21.** Hanger section properties

	Hanger section			
	Section properties			Unit
	Diameter	<b>D</b>	130	mm
	Cross sectional area	<b>A<sub>s</sub></b>	13273.23	mm <sup>2</sup>

**3.4.2.5. Bracing elements**

The slab bracings are transverse elements which provide stability and resists lateral loads. Bracing system serves to stabilize the main girders during construction, to contribute to the distribution of load effects and to provide lateral buckling stability to the deck. The bracing elements distributed as shown on the slab view of the deck in Figure B.2 of the Annex B. Their section properties are outlined on Table 3.22.

**Table 3.22.** Bracing element properties

	Bracing element			
	Section properties			Unit
	Height of section	<b>H</b>	100	mm
	Width of Section	<b>B</b>	100	mm
	Thickness of web	<b>t<sub>w</sub></b>	10	mm
	Thickness of flange	<b>t<sub>f</sub></b>	10	mm
	Spacing between two webs	<b>C</b>	10	mm
	Cross sectional area	<b>A<sub>s</sub></b>	3800	mm <sup>2</sup>
	Height of centroid	<b>y<sub>G</sub></b>	71.32	mm
Resistance Modulus of steel	<b>W</b>	49200	mm <sup>3</sup>	

**3.4.3. Section verifications**

In order to verify the different structural sections which are present in the arch bridge, it is necessary to determine the internal actions in each element. Following a linear static analysis conducted in the FEM software, the different envelopes of the actions were extracted and eventually used for verifications. This section presents the different envelope diagrams of actions on major structural elements followed by verifications.

### 3.4.3.1. Diagrams of internal actions

Following the load combinations presented in section 3.3.2, a large number of diagrams of internal actions were drawn. Without being exhaustive, some of the diagrams showing the maximum internal actions in the main structural elements of the bridge are presented in Figure 3.13, Figure 3.14 and Figure 3.15.

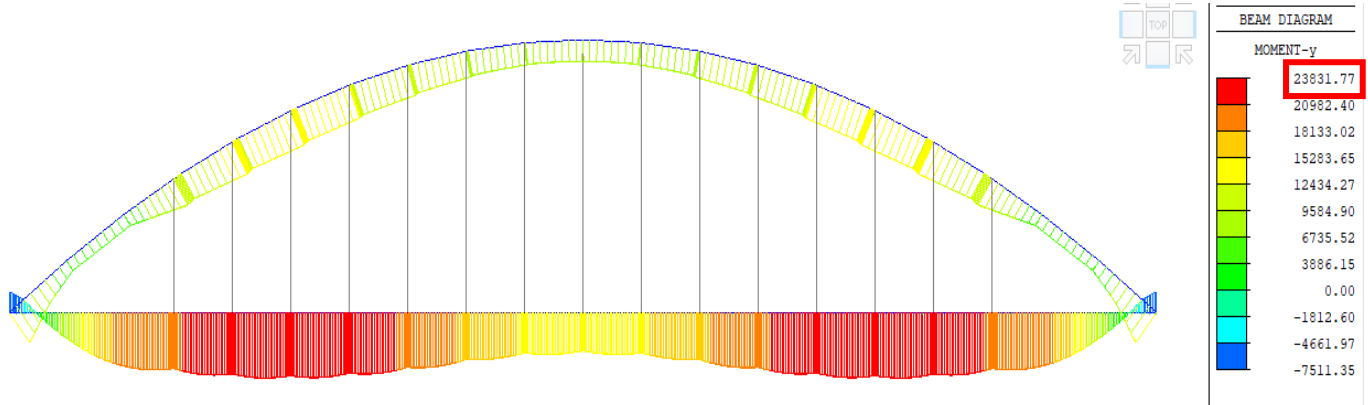


Figure 3.13. Diagram for maximum positive bending moment (kNm) in the main girder

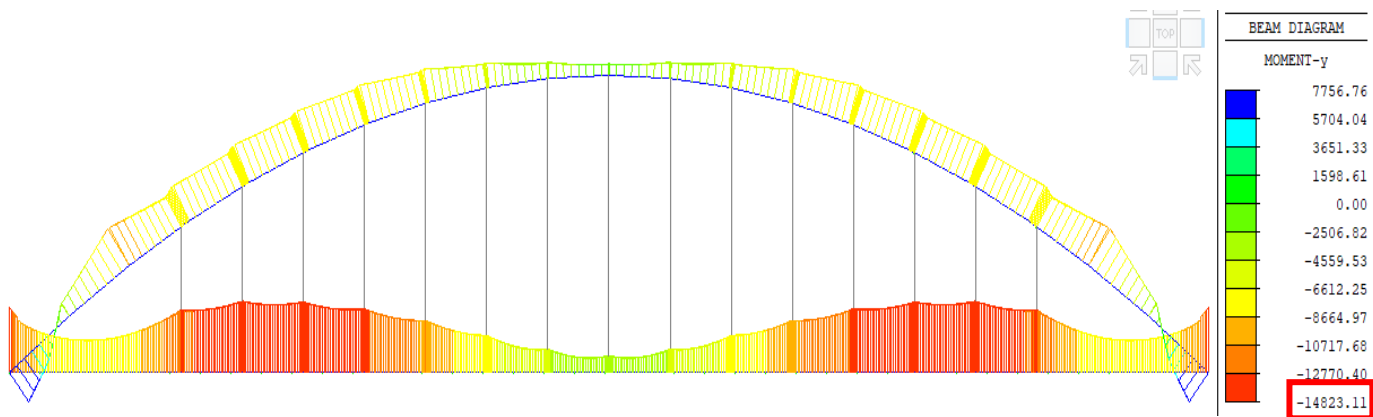


Figure 3.14. Diagram for maximum negative bending moment (kNm) in the main girder

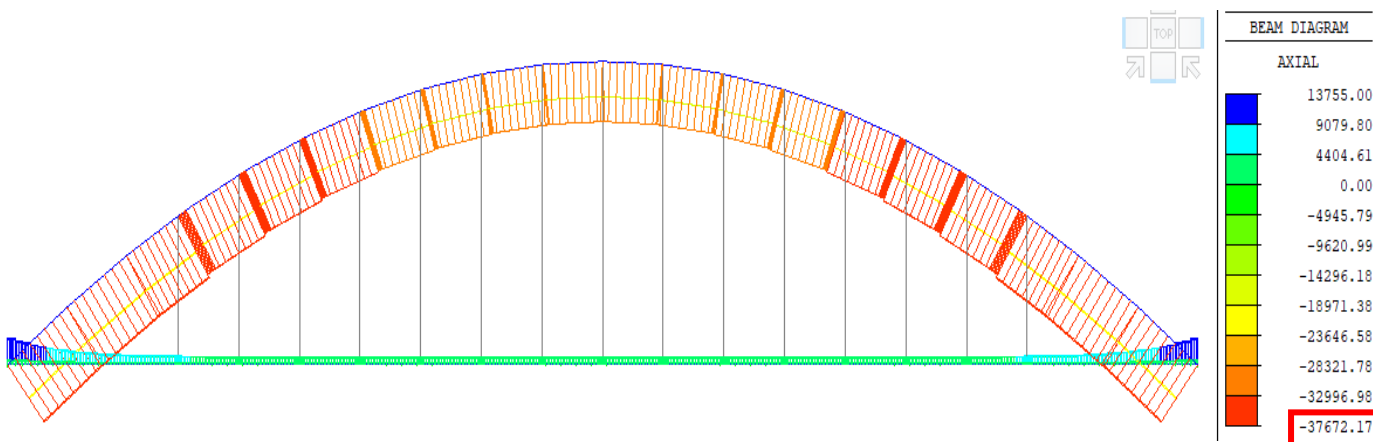


Figure 3.15. Maximum axial compression (kN) in the arch rib

With regards to the large number of load combinations considered, envelope diagrams which show the most unfavourable case for each element in all the combinations, were plotted. Thus, the diagrams on Figure 3.16 to Figure 3.22 show the envelopes of the main internal action in the structural elements. The values of moments are in kNm, shear force, axial force in kN and stresses in MPa.

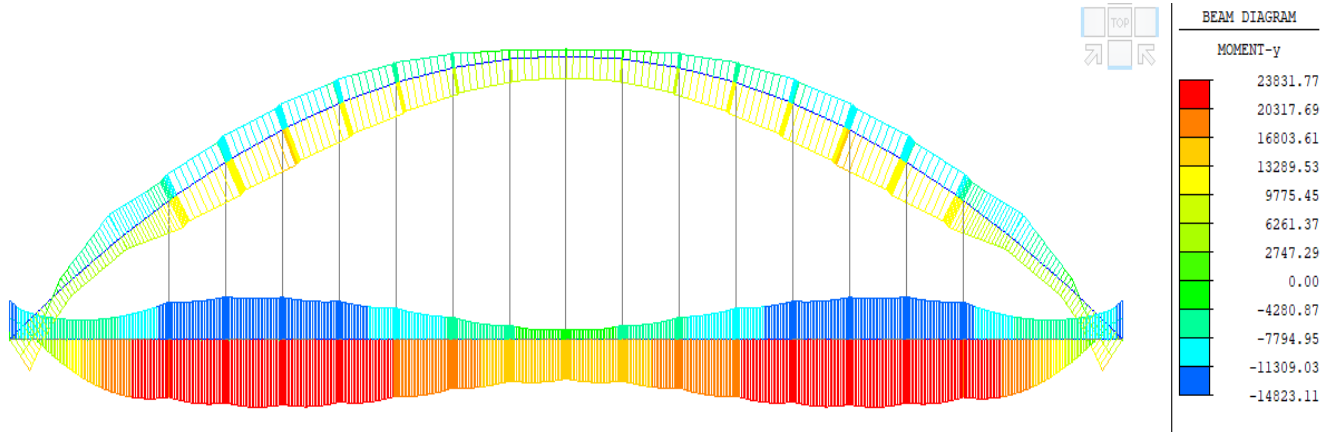


Figure 3.16. Envelope of bending moment for the arch ribs and main girders

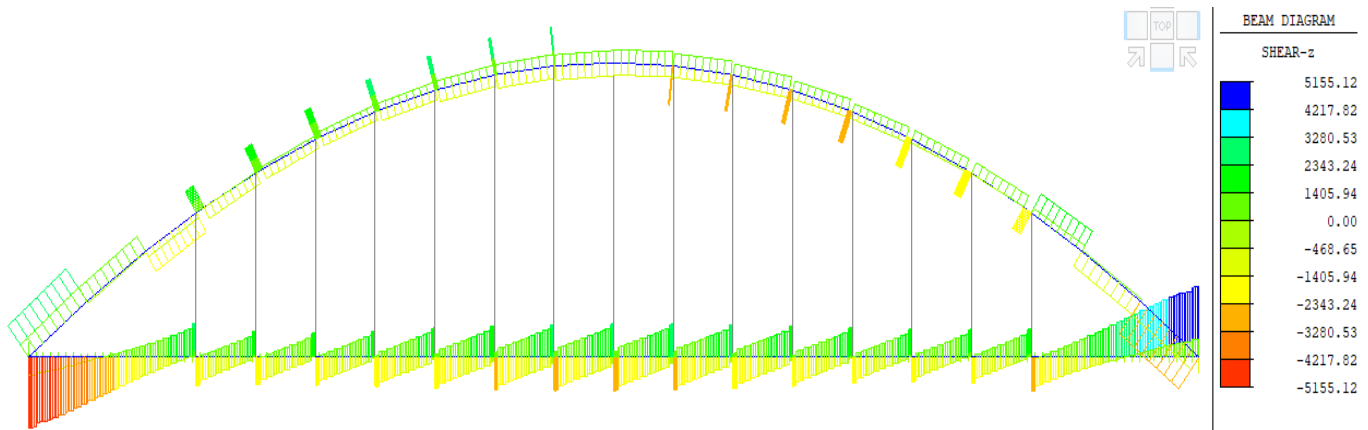


Figure 3.17. Envelope shear force for the arch ribs and main girders

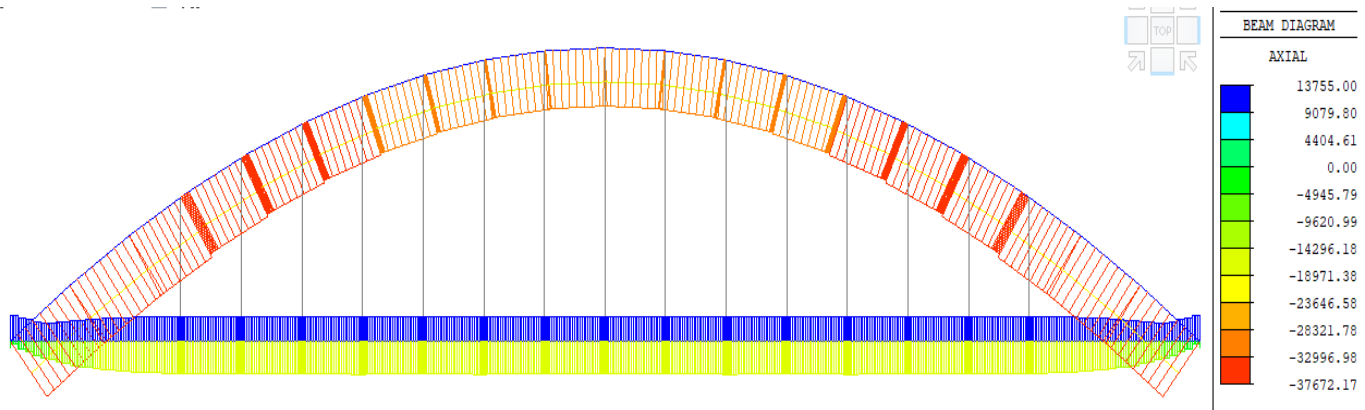


Figure 3.18. Envelope of axial force for the arch ribs and main girders

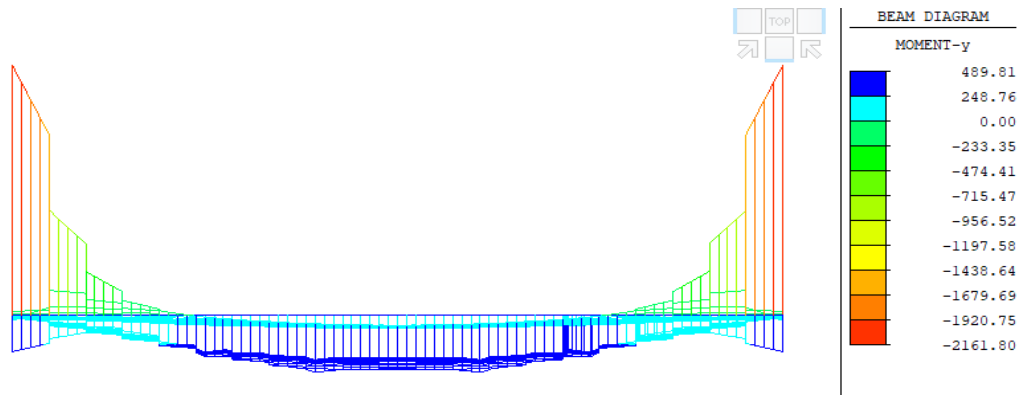


Figure 3.19. Envelope of bending moment for cross beams

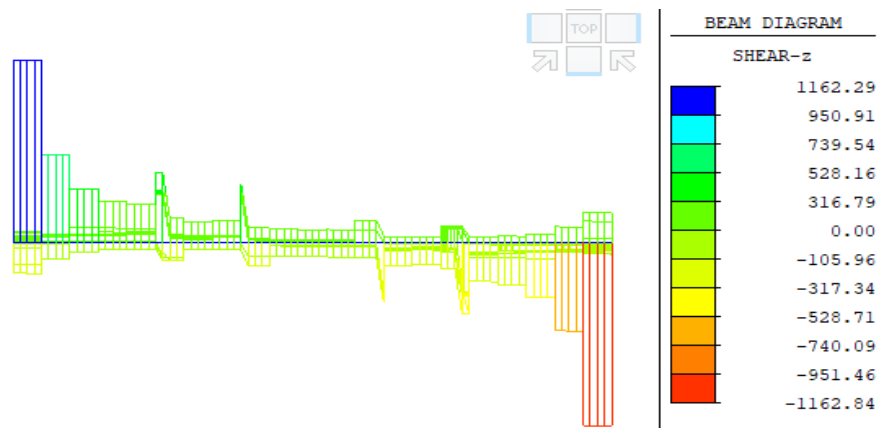


Figure 3.20. Envelope of shear force for cross beams

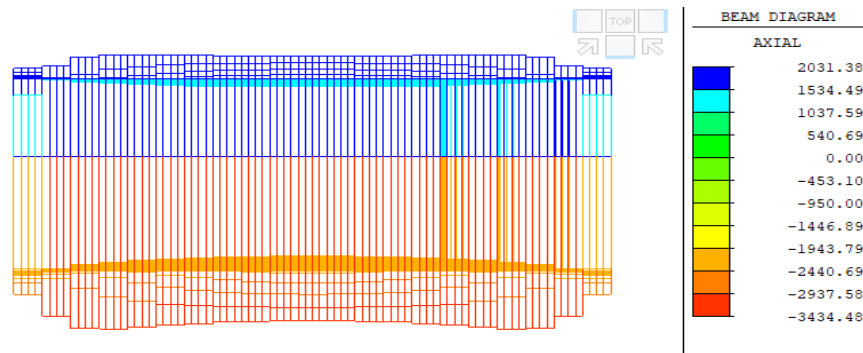


Figure 3.21. Envelope of axial force for cross beams

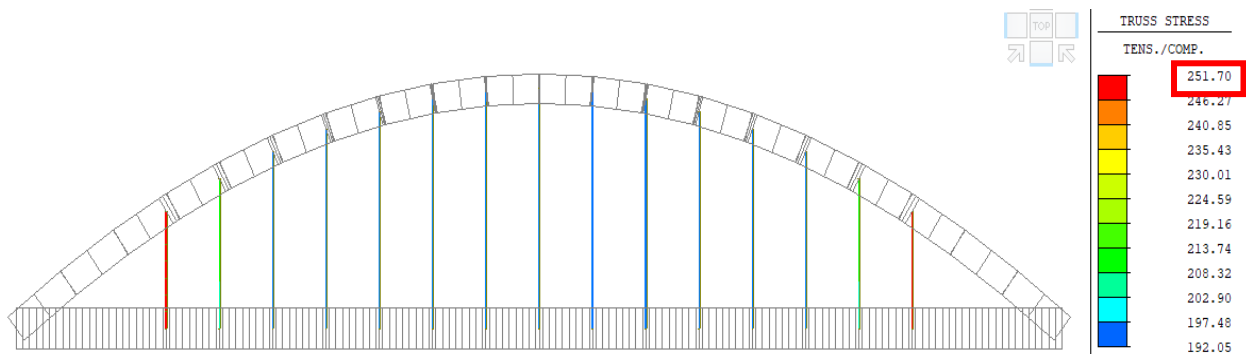


Figure 3.22. Tensile stresses in the hangers

Table 3.23 shows the tensile stress value in each of hanger 1 to 8 only, given that the values are just the same for hangers 9 to 15 as the structure is symmetric.

**Table 3.23.** Tensile stress in each hanger of the arch bridge

Hanger position	1 & 15	2 & 14	3 & 13	4 & 12	5 & 11	6 & 10	7 & 9	8
Stress (MPa)	251.7	209.2	195.1	193.0	195.1	196.2	196.5	196.2

### 3.4.3.2. Verifications of sections

#### a. Main girder

The main actions on the girders were verified according as shown on Table 3.24.

**Table 3.24.** Main girder section verifications

Design values of actions (A)	$M_{y, Ed}$ (kNm)	$M_{z, Ed}$ (kNm)	$V_{y, Ed}$ (kN)	$V_{z, Ed}$ (kN)	$N_{Ed}$ (kN)
	23 831.77	47.81	5 155.12	-1 816.50	13 755.00
Design section resistance (R)	$M_{y, Rd}$ (kNm)	$M_{z, Rd}$ (kNm)	$V_{y, Rd}$ (kN)	$V_{z, Rd}$ (kN)	$N_{Rd}$ (kN)
	62 581.70	5 593.12	19 399.00	23 302.90	79 296.00
Verification (A < R)	<b>OK</b>	<b>OK</b>	<b>OK</b>	<b>OK</b>	<b>OK</b>

#### b. Arch rib

The main actions on the arch rib were verified according as shown on Table 3.25.

**Table 3.25.** Arch rib section verifications

Design values of actions (A)	$M_{Ed}$ (kNm)	$V_{Ed}$ (kN)	$N_{Ed}$ (kN)
	13 951.00	3 010.00	-37 672.17
Design section resistance (R)	$M_{Rd}$ (kNm)	$V_{Rd}$ (kN)	$N_{Rd}$ (kNm)
	41 999.91	28 080.00	92 700.00
Verification (A < R)	<b>OK</b>	<b>OK</b>	<b>OK</b>

Also, the arch rib buckling parameters are computed as prescribed in section 2.4.3.1 and the element is verified for buckling. The computations are reported on Table 3.26. The values of  $C_1$  and  $C_2$  are obtained by interpolation on Table 2.11.

**Table 3.26.** Arch rib buckling verification

Parameter designation	Symbol	Value
Rise to span ratio	$\frac{h(m)}{L(m)}$	$\frac{18}{80} = 0.225$
Critical Load parameter for axial force	$C_1$	26.7
Critical Load parameter for distributed load	$C_2$	47.65
Elastic modulus of the steel	$E$	210 000 MPa
Moment of Inertia of the section	$I$	$1.373 \times 10^{11} \text{ mm}^4$
Uniform buckling force	$H$	$120\,287.8 \text{ kN} > N_{Ed}$ <b>OK</b>
Uniform buckling distributed load	$q$	2683.4 kN/m

### c. Cross beam

The main actions on the cross beams were verified according as shown on Table 3.27.

**Table 3.27.** Cross beam section verifications

<b>Design values of actions (A)</b>	<b><math>M_{y, Ed}</math> (kNm)</b>	<b><math>M_{z, Ed}</math> (kNm)</b>	<b><math>V_{y, Ed}</math> (kN)</b>	<b><math>V_{z, Ed}</math> (kN)</b>	<b><math>N_{Ed}</math> (kN)</b>
	-2 160.50	-65.95	-8.70	1 162.00	-3 434.00
<b>Section resistance (R)</b>	<b><math>M_{y, Rd}</math> (kNm)</b>	<b><math>M_{z, Rd}</math> (kNm)</b>	<b><math>V_{y, Rd}</math> (kN)</b>	<b><math>V_{z, Rd}</math> (kN)</b>	<b><math>N_{Rd}</math> (kN)</b>
	2 698.92	580.62	4 517.53	2 687.97	11 340.00
<b>Verification (A &lt; R)</b>	<b>OK</b>	<b>OK</b>	<b>OK</b>	<b>OK</b>	<b>OK</b>

#### d. Hangers and slab bracing elements

Since the hangers and slab bracings are truss elements (tension only members), the verification of the maximum stresses  $\sigma_{s,max}$ , shown on Table 3.28, are sufficient for these elements.

**Table 3.28.** Hanger and slab bracing element stress verification

Element	Maximum stress in element $\sigma_s$ in MPa	Design maximum admissible stress $\sigma_{max}$ in MPa	Verification
Hangers S 460	251.70	460/1.15 = 400	<b>OK</b>
Slab bracing (2 L100x10) S 420	63.39	420/1.05 = 400	<b>OK</b>

It is necessary to point out the fact the safety coefficient for hangers is greater than that of structural steel since the hangers are constantly subject to high tensile stresses and so are more exposed to yielding.

#### 3.4.4. Serviceability limit state verifications

##### 3.4.4.1. Stress limitation

The SLS stress limitations for the steel types was verified as presented on Table 3.29.

**Table 3.29.** Serviceability state stress limitation verification

Structural steel class	Maximum element stress at SLS $\sigma_{s,sls}$ in MPa	$0.8f_{yk}$ in MPa	Verification
S 460	150.13	368	<b>OK</b>
S 420	245.64	336	<b>OK</b>

Also, the stress in the hangers verify the condition fatigue criteria as presented below.

$$\sigma_{s,sls} < 0.45f_u = 0.45 \cdot 540 = 243 \text{ MPa}$$

### 3.4.4.2. Deflection control

Also, with regards to the deflection, it is more useful to consider the global deflection of the bridge. However, as shown on Figure 3.23, the maximum deflection of the bridge girder at SLS is equal to 71.7 mm.

As prescribed by the Eurocode, this deflection was assessed in reference to the limit.

$$\frac{L}{500} = \frac{80\,000}{500} = 160\text{ mm} > 71.7\text{ mm}$$

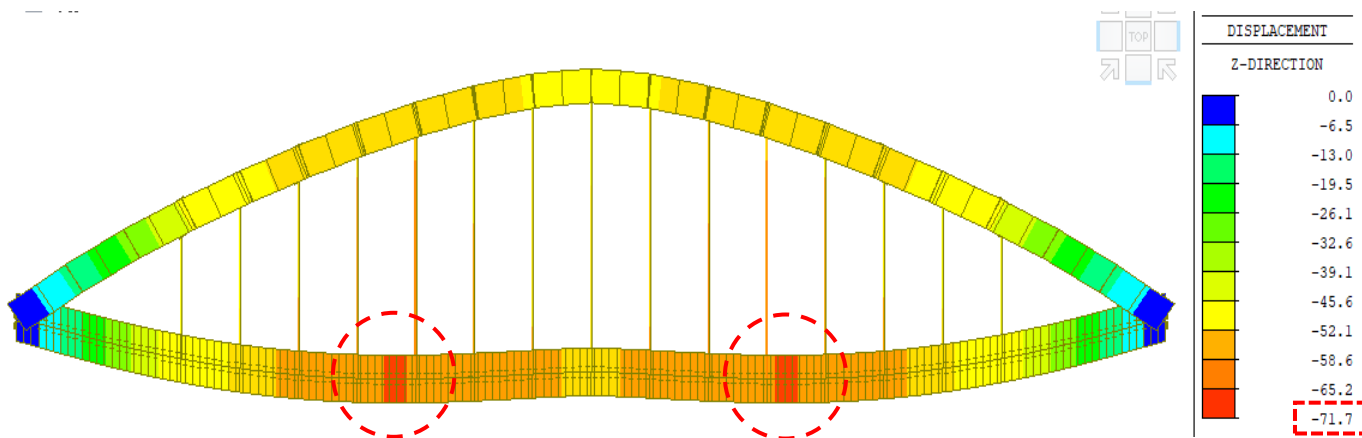


Figure 3.23. Deflection of the arch bridge

## 3.5. Redundancy analysis results

For the purpose of this work, the redundancy analysis was focused essentially on the hangers. It is necessary to point out the fact that they are one of the most important elements of the arch bridge because they ensure the transfer of loads from the bridge deck to the arch. Also, the concept of redundancy is more feasible when talking about the hangers since in tied arch bridges, there are generally a large number of them. In this section, the result of the behaviour of the bridge following different configurations of hanger failures will be illustrated.

### 3.5.1. Hanger failure cases

For a better presentation and analysis of the redundancy, a notation was adopted to identify each hanger. Given that the arch bridge has 15 hangers on each side, they were numbered from 1 to 15 R or L (representing Right and Left side respectively). The hanger failures were considered in symmetric and asymmetric configurations with respect to the midspan of the bridge as presented in Table 3.30.

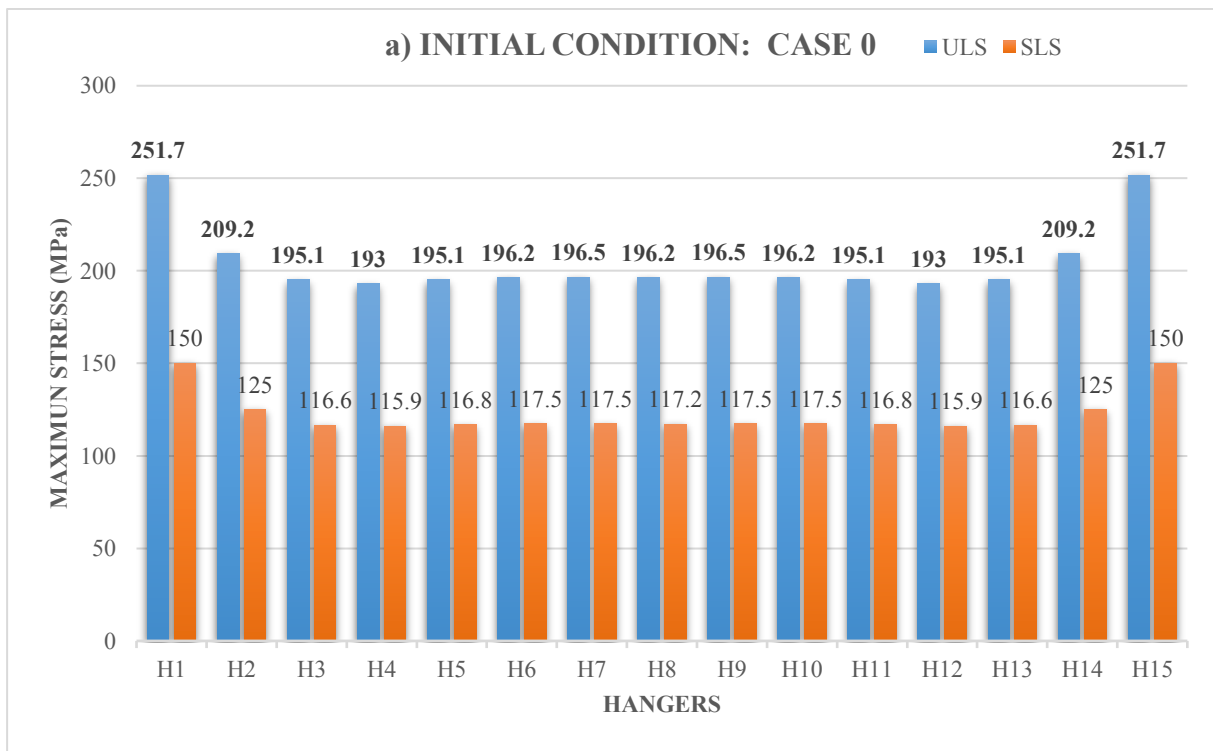
**Table 3.30.** Hanger failure configurations

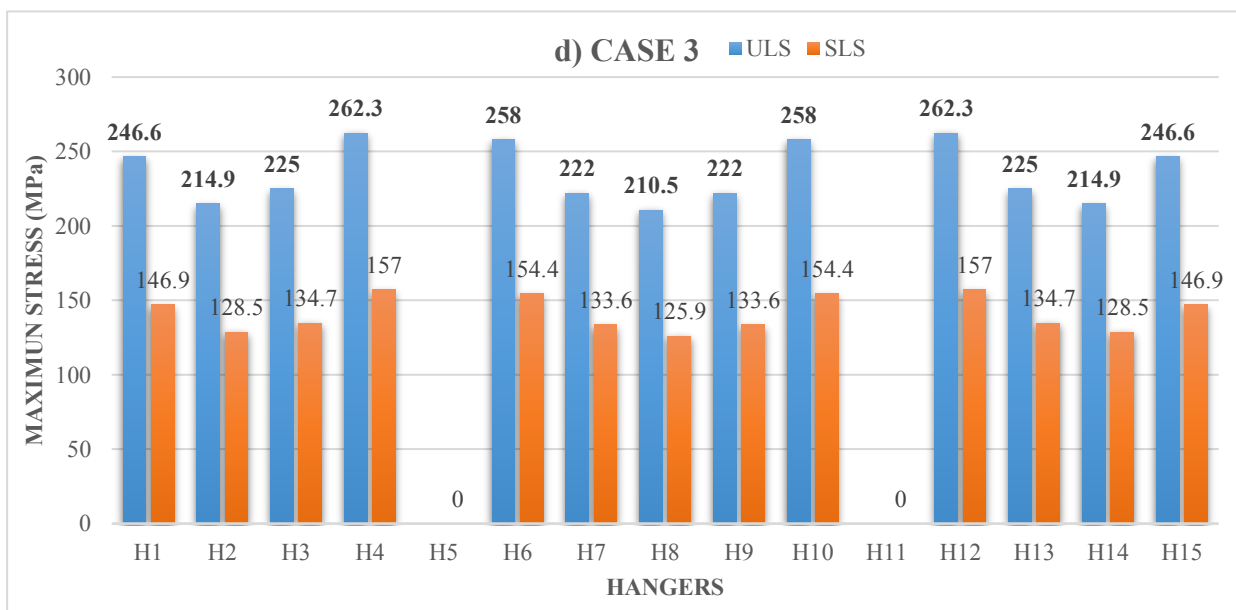
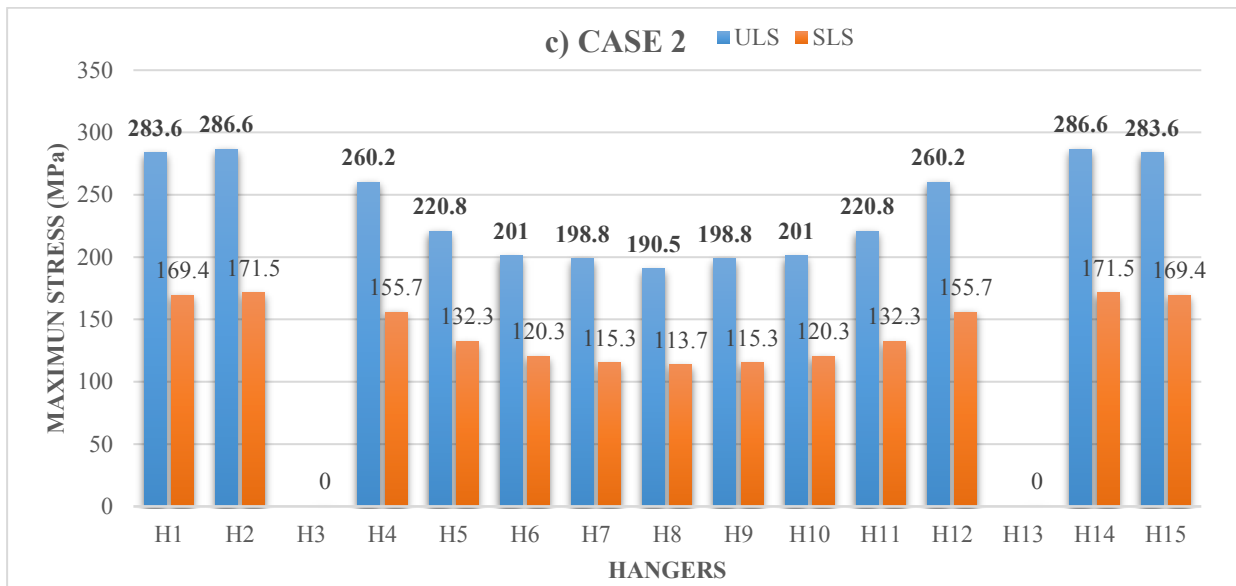
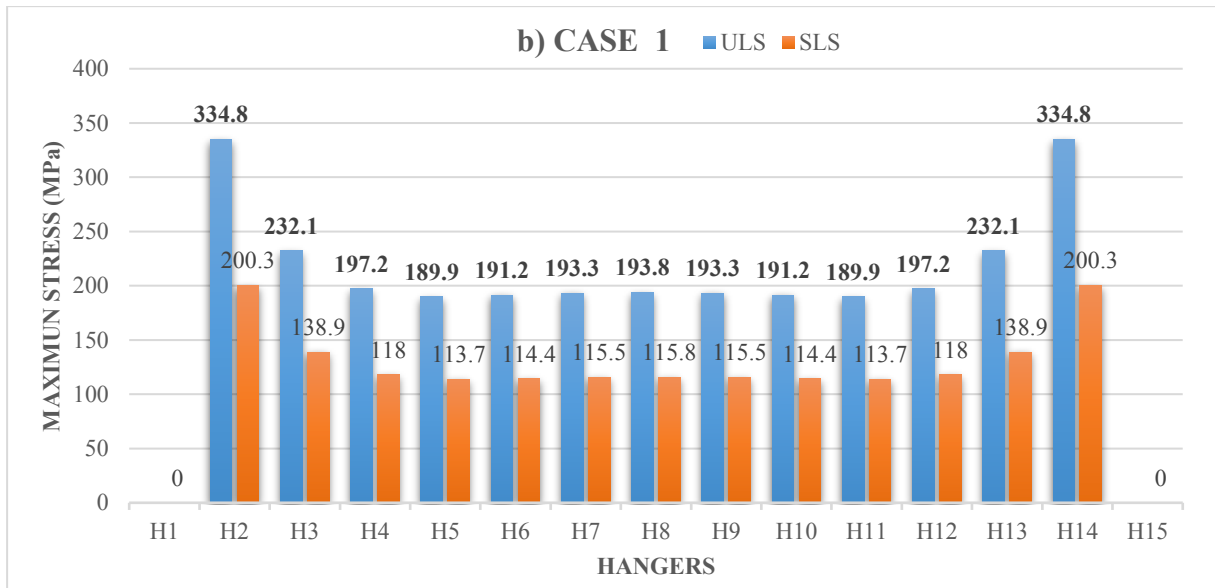
Symmetric configurations	Asymmetric configurations
<b>Case 1:</b> 1 and 15 R&L	<b>Case 8:</b> 1 and 3 R&L
<b>Case 2:</b> 3 and 13 R&L	<b>Case 9:</b> 1, 4 and 7 R&L
<b>Case 3:</b> 5 and 11 R&L	<b>Case 10:</b> 2, 5 and 8 R&L
<b>Case 4:</b> 7 and 9 R&L	
<b>Case 5:</b> 1, 2, 14, 15 R&L	
<b>Case 6:</b> 2, 4, 12, 14 R&L	
<b>Case 7:</b> 2, 5, 8, 11, 13 R&L	

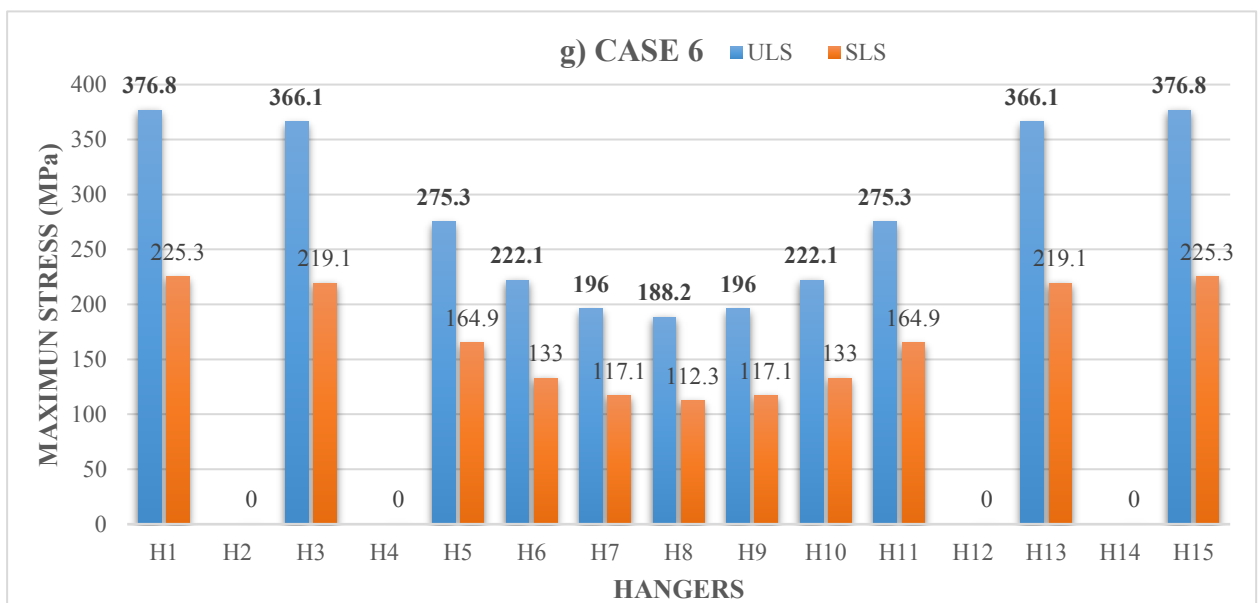
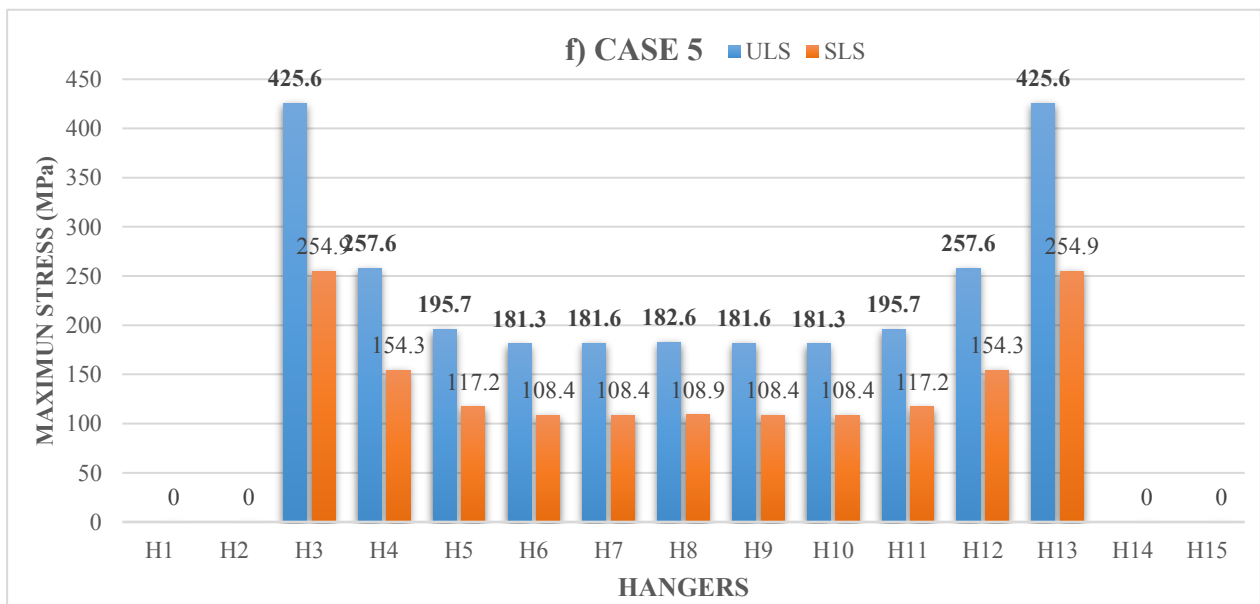
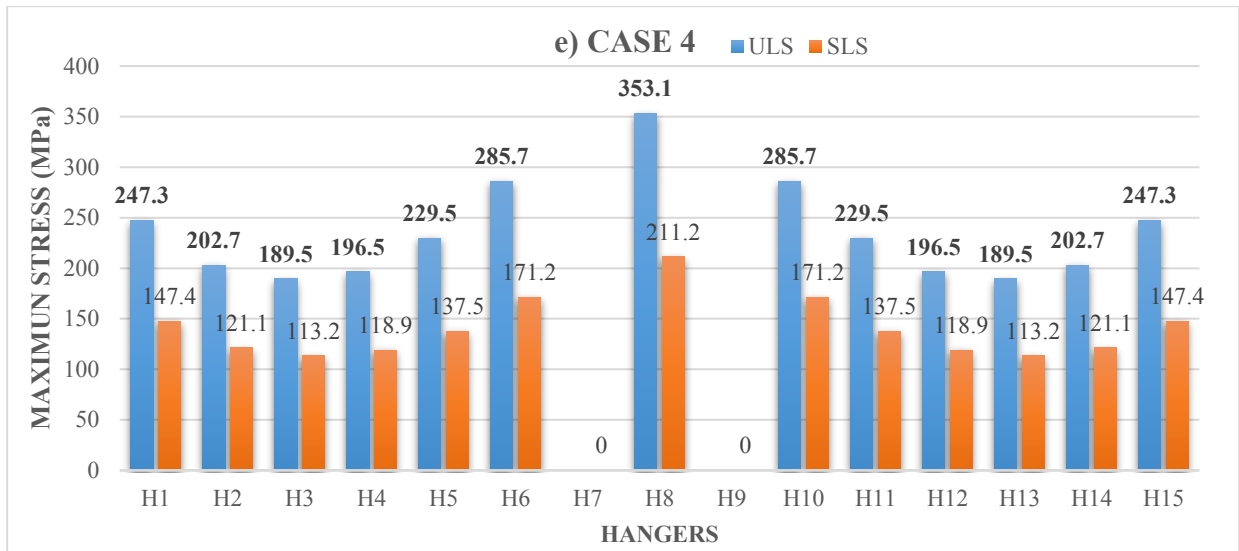
**3.5.2. Symmetric configuration**

**3.5.2.1. Stresses distribution for hangers following hanger failure**

This section aims at presenting the results of the analysis of the arch bridge under the various symmetric hanger failure cases assumed in Table 3.30 (see Figure 3.24 *a* to *h*). It should be noted that the initial condition represents the configuration of the hangers before failure.







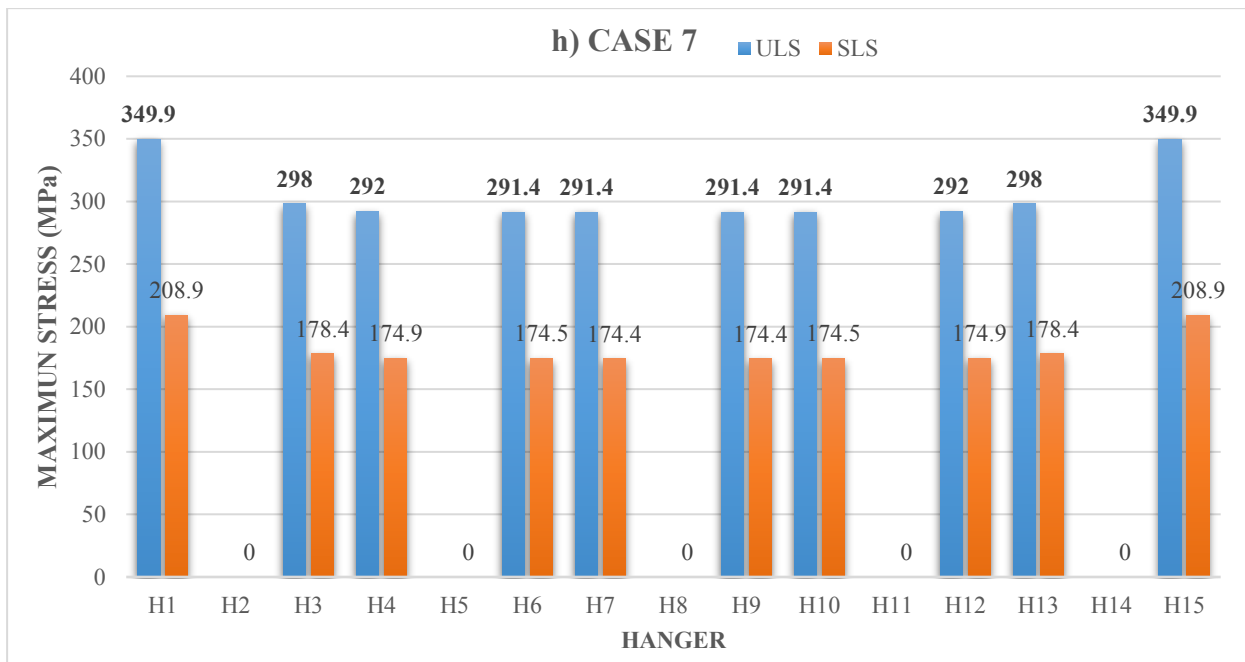


**Figure 3.24.** Stress distribution in hangers following symmetric failure mechanism

From the figures above, the behaviour of the stresses in the hangers are illustrated for the different hanger failure scenarios assumed. Firstly, it can be observed that the stress distribution in the hangers is symmetric about the middle hanger (H8) since the symmetric failure configuration is considered. So, the stresses are redistributed in the same way on both sides of the arch. Also, it is observed that for the majority of cases, the hanger stress is maximum for the hangers at the both edges. This can be due to the fact that, the spacing between these hangers and the support are greater than the spacing between the following successive hangers making the end hangers to have a greater influence area than the others. Also, this is due to the mechanism of the arch bridge since globally, the bridge members (girder, arch rib) closer to the supports are more stressed.

With regards to the stress redistribution following hanger failure (alternate load path), it can be observed that failure of the end hangers causes a great increase in stress in the next ones but this increase reduces significantly while moving towards the midspan of the bridge. In case 1, the failure of H1 and H15 cause an increase in stress in H2 and H14 from 209.2 MPa to 334.8 MPa, thus a percentage increase of 60%. However, the increase is not sufficient to cause failure. So, redundancy requirement is satisfied in this case. The percentage drops from 60% in H2 to 19% in H3 and then to 2% in the next. The trend is similar for case 5. From this, it can

be concluded that for the failure of the end hangers, there is a local redistribution of stress to the adjacent hangers why the ones further away are quite unaffected.

On the other hand, the failure of the intermediate hangers causes a global distribution of stresses as seen in cases 2, 3 and 7. In these cases, it is observed that the stresses increase in a quite similar way in all the hangers and there's in no more a great difference between the maximum and minimum distributions.

Lastly, the hangers are all verified at ULS, SLS and for fatigue in the different cases except case 5 where there the stress in H3 and H13 (425 MPa) is above the design limit so the failure of these hangers occur. Moreover, the bridge will have a progressive collapse since the failure of H3 and H13 will induce excessively high stress in their neighbours (H4 and H12) which will fail in their turn and the process will continue till the bridge collapses totally.

### 3.5.2.2. Maximum stress in the arch rib and main girder

The variation of the maximum stresses in the arch rib and the main girder for the different failure cases is presented in Figure 3.25 and Figure 3.26.



Figure 3.25. Variation of the maximum stress in the arch for the different cases

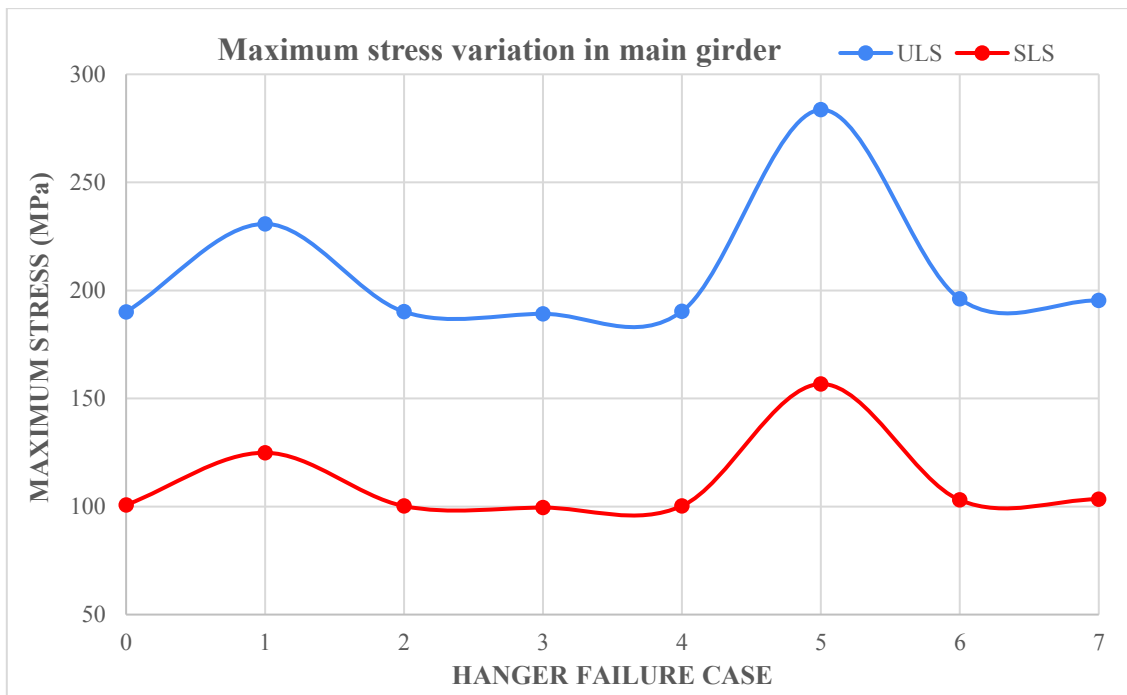


**Figure 3.26.** Variation of the maximum stress in the main girder for the different cases

A maximum value is observed at case 5 since it is the most critical case. However, the stresses in the arch and girder are not enough to cause failure. Thus, it can be concluded that the failure of the bridge is essentially due to the progressive collapse of the hangers.

### 3.5.2.3. Variation of the global bridge deflection

The global deflection of the bridge for the various cases are shown on in Figure 3.27.

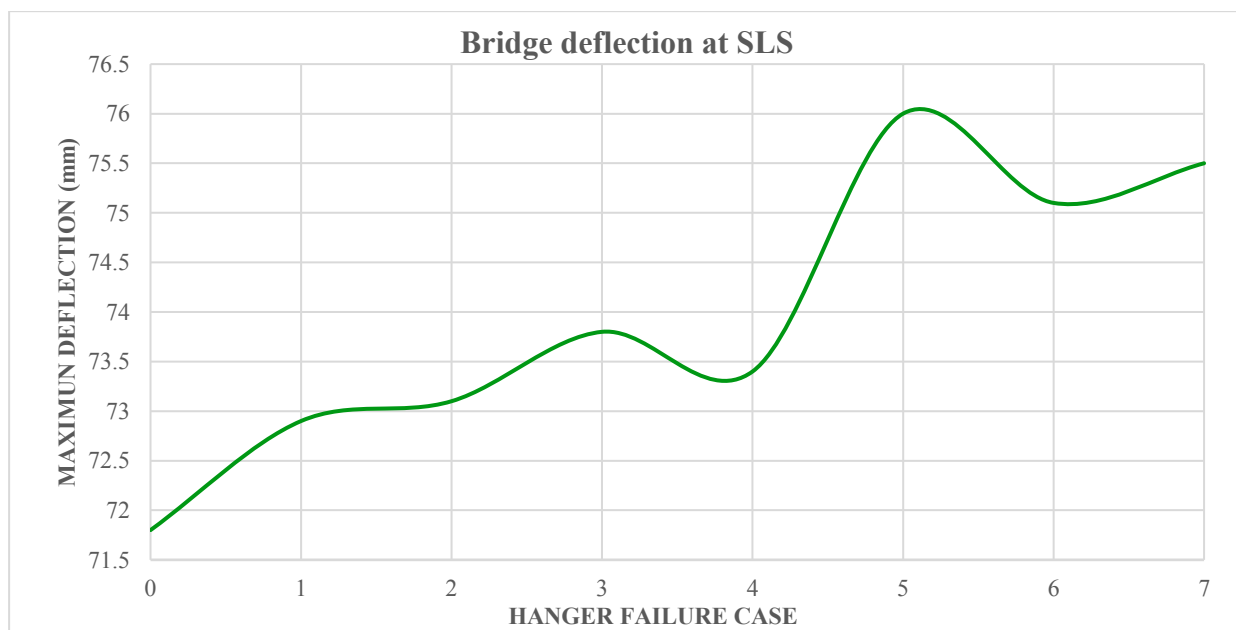


**Figure 3.27.** Variation of global bridge deflection

The global deflection of the bridge varies in a similar way to that of the stresses in the arch and main girder. A peak is also observed in case 5 which is the worst case. Nevertheless, the peak value is less than the limit of the SLS and so the bridge maintains an acceptable level of service before the eventual progressive collapse.

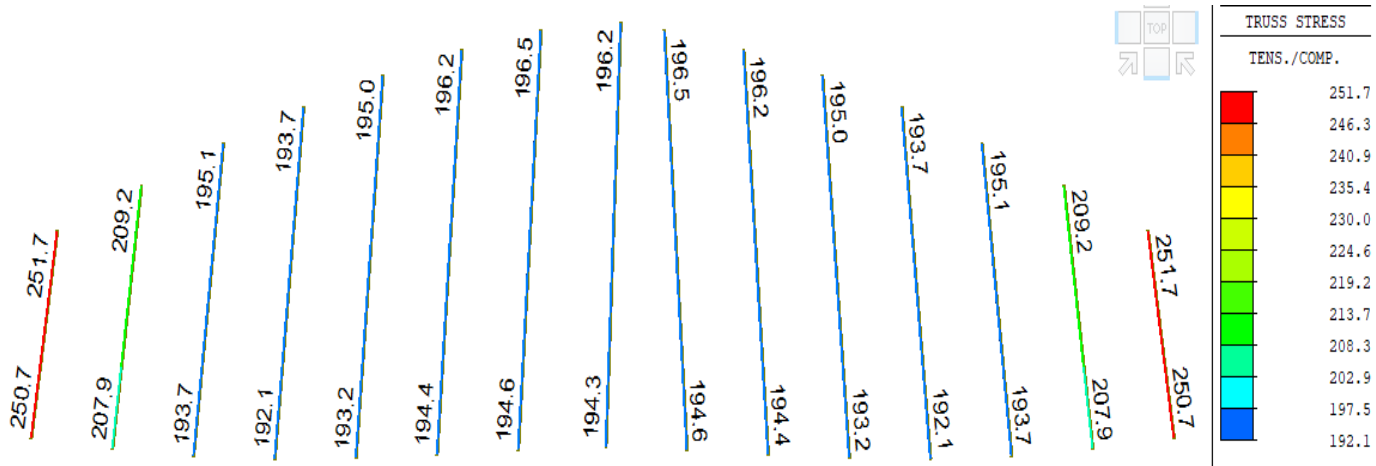
### 3.5.3. Asymmetric configuration

Here, the results of the analysis of the arch bridge under the various asymmetric hanger failure cases assumed in Table 3.30 are presented.

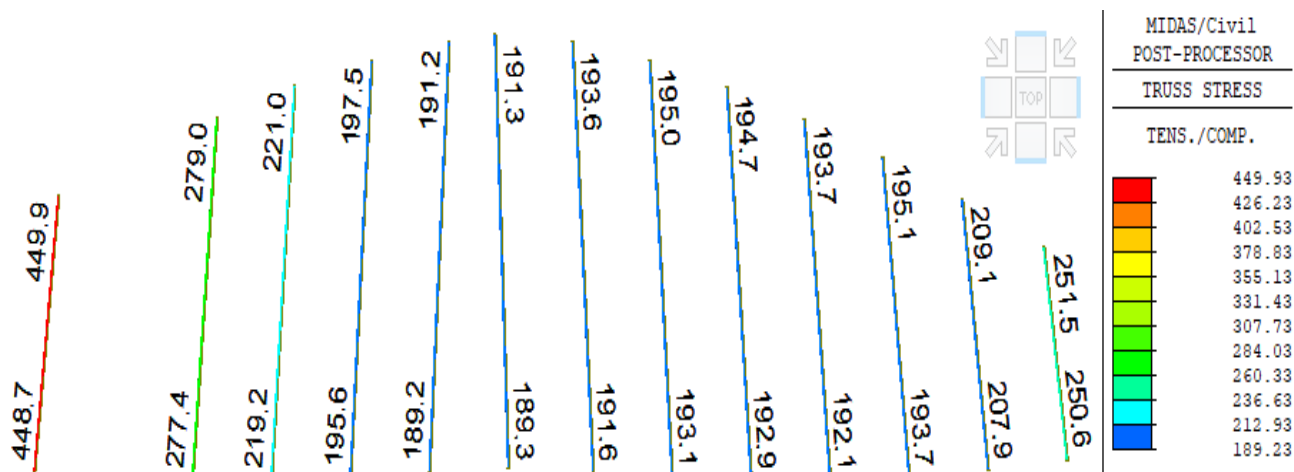
#### 3.5.3.1. Maximum hanger stress

The hanger stresses (in MPa) at the ULS for the bridge in the asymmetric configuration are presented in Figure 3.28b, c and d (Figure 3.28a presents the stress in initial configuration).

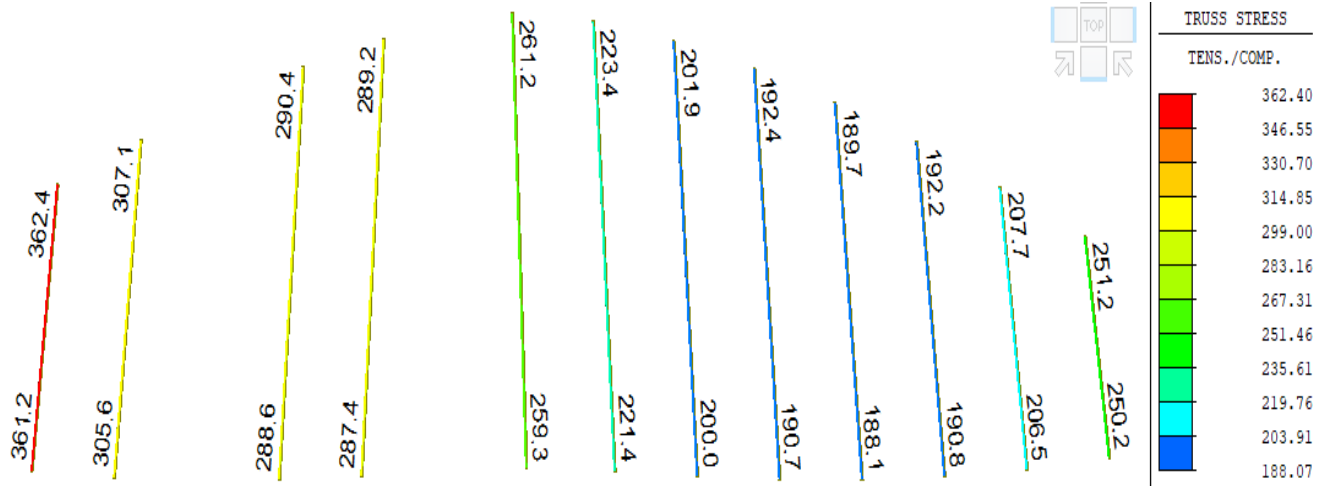
a) Case 0



a) Case 8



b) Case 9



c) Case 10

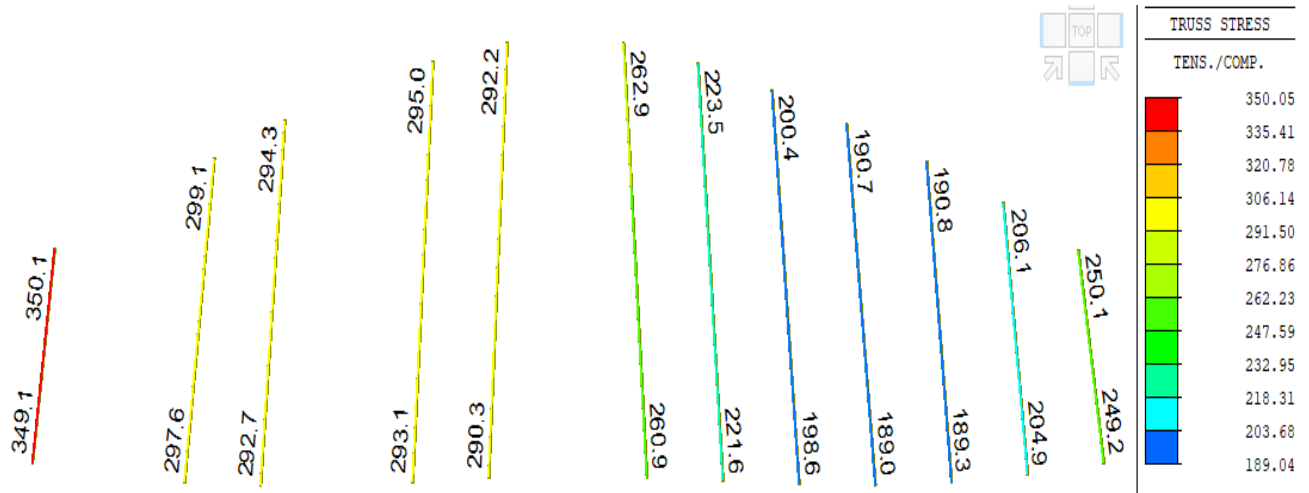


**Figure 3.28.** Hanger stress distribution for asymmetric configuration

From the data illustrated, it is observed that the hangers on the right end of the bridge are not affected by the removal of hangers on the left end, since the value of the stress is approximately the same as in the initial configuration (Case 0), that is 251.7 MPa. Adding to that, the stress increment on the hangers on the right side is small compared to those closer to the failed hangers. Noting that this increase reduces rapidly until reaching the right end, it can be deduced that in the asymmetric configuration, the stress redistribution is more local. Also, in case 8, there is the collapse of H2 because when H1 and H3 are removed, the stress in H2 is 449.9 MPa which is greater than the stress limit. It can be added that the collapse of these H2 will create a situation of progressive collapse because the stress in the neighbouring H4 will exceed the limit and the situation will just propagate to the rest of the bridge.

### 3.5.3.2. Maximum stress in elements and deflection

For the 3 asymmetric cases considered, the stress in the girder varies from 236.6 MPa through 228 MPa to 195.7 MPa for cases 8, 9 and 10 respectively. Also, for the arch, the stress values are 324, 314,93 and 280 MPa for the 3 cases. It is clearly seen that case 8 is the most unfavourable for the bridge in the asymmetric configuration considered.

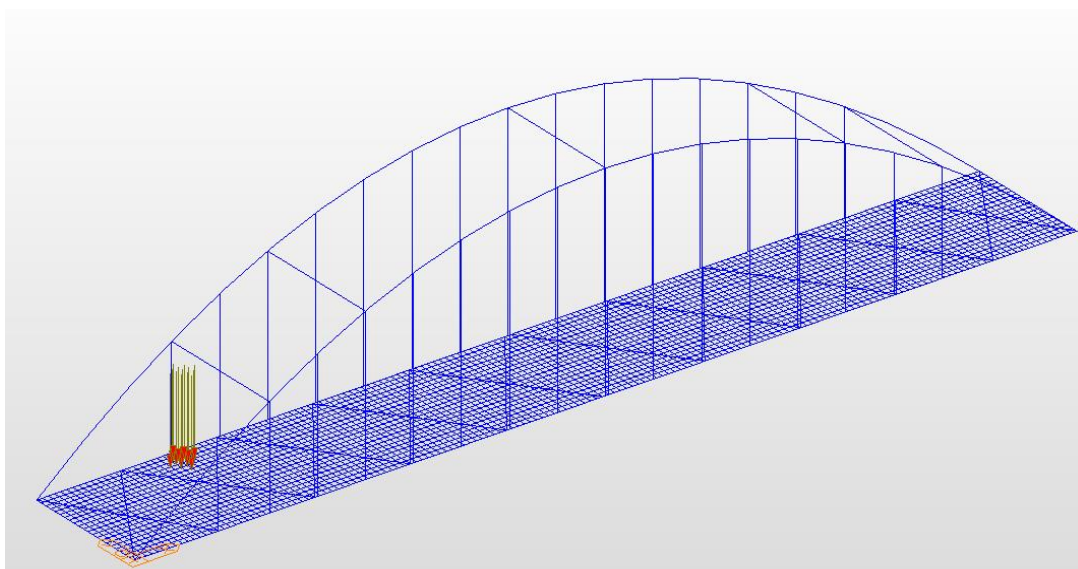
On the other hand, the deflection of the bridge is 73.5, 75.0 and 74.6 mm for the three cases. Here, it is observed that the case 8 has a minimum deflection even though it is the worst case for the bridge in asymmetric configuration. This can be explained by the fact that the hanger failure in case 8 are close to the supports compared to the other cases so the effect is less pronounced than if it was at the midspan where the bridge is more vulnerable to bending and deflection.

## 3.6. Resilience analysis results

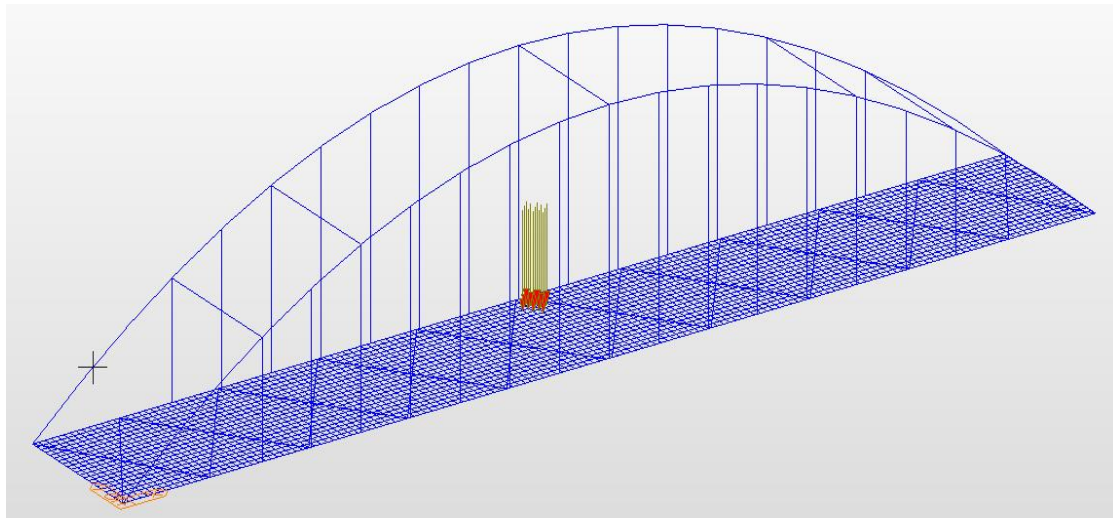
This section aims at presenting the results obtained following the resilience analysis. Firstly, the blast loading considerations and computations will be presented followed by the results of the different analysis conducted.

### 3.6.1. Blast loading positions

As considered in section 2.6.1, the two positions for the blast loading are presented on Figure 3.29a and b.



a) At the level of the first hanger ( $x = 10$  m)



b) At the middle of the bridge ( $x = 40\text{ m}$ )

**Figure 3.29.** Blast loading positions along the bridge

### 3.6.2. Blast load computation

The results of the main parameters of the blast wave computed using the software RCblast are presented on Figure 3.30. Further data processing was done by exporting this data to Microsoft Excel in order to obtain the time history behaviour of the blast wave to be applied in the FEM software.

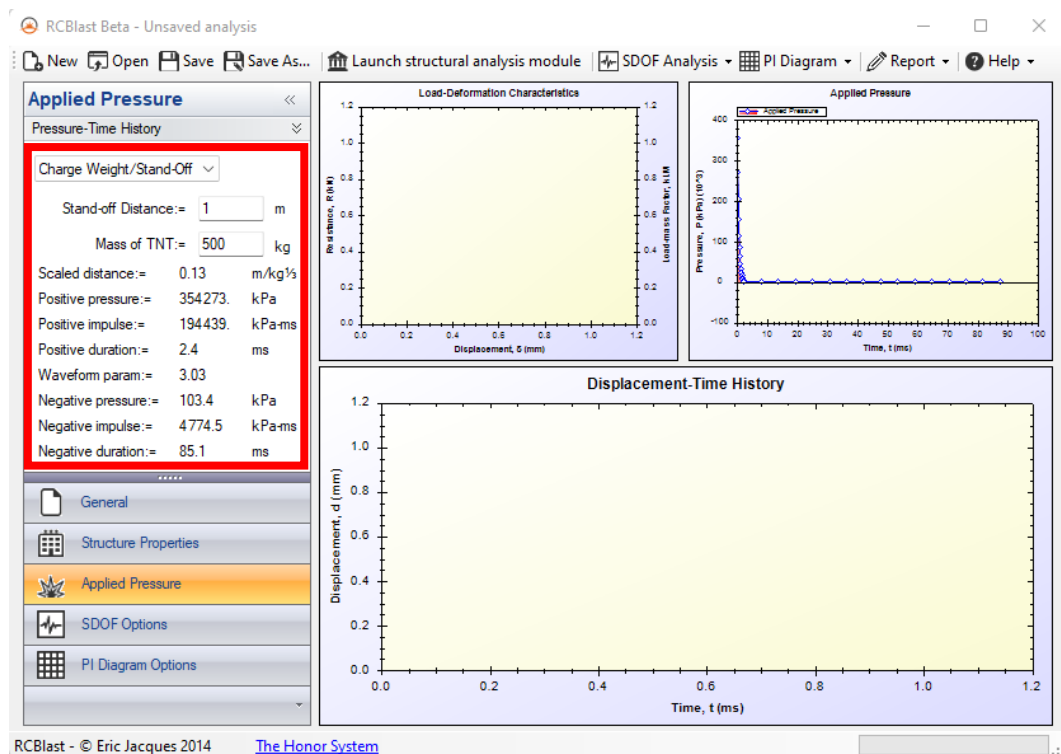


**Figure 3.30.** Blast loading parameters computation

### 3.6.3. Eigen value analysis result

Having defined the mass of the structure from the characteristics of elements and conversion of self-weights to masses, a modal analysis was performed in the software MIDAS/Civil. This analysis is done in order to obtain the fundamental information about the dynamic characteristics of the bridge structure. In the Table 3.31 and Table 3.32 it is possible to find the periods and effective mass ratios of the first 10 modes. These values are important for the dynamic time-history analysis of the bridge.

**Table 3.31.** Frequency and periods of the first 10 modes

<b>EIGEN VALUE ANALYSIS</b>				
<b>Mode</b>	<b>Frequency</b>		<b>Period</b>	<b>Tolerance</b>
<b>No</b>	<b>(rad/sec)</b>	<b>(cycle/sec)</b>	<b>(sec)</b>	
<b>1</b>	1.37	0.22	4.59	0
<b>2</b>	9.61	1.53	0.65	0
<b>3</b>	10.31	1.64	0.61	0
<b>4</b>	16.01	2.55	0.39	3.8209E-94
<b>5</b>	16.37	2.61	0.38	1.3416E-92
<b>6</b>	16.65	2.65	0.38	2.7337E-92
<b>7</b>	22.72	3.62	0.28	3.6806E-76
<b>8</b>	23.46	3.73	0.27	6.6901E-74
<b>9</b>	23.93	3.81	0.26	8.3693E-74
<b>10</b>	32.79	5.22	0.19	6.578E-60

**Table 3.32.** Modal participation ratios for the first 10 modes

<b>MODAL PARTICIPATION MASSES PRINTOUT</b>												
<b>Mode</b>	<b>TRAN-X</b>		<b>TRAN-Y</b>		<b>TRAN-Z</b>		<b>ROTN-X</b>		<b>ROTN-Y</b>		<b>ROTN-Z</b>	
<b>No</b>	<b>MASS (%)</b>	<b>SUM (%)</b>										
<b>1</b>	<b>100.00</b>	100.00	0.00	0.00	0.00	0.00	0.00	0.00	0.00	0.00	0.00	0.00
<b>2</b>	0.00	100.00	<b>56.00</b>		0.00	0.00	26.89		0.00	0.00	0.00	0.00
				56.00				26.89				
<b>3</b>	0.00	100.00	0.00		0.00	0.00	0.00		<b>52.22</b>		0.00	0.00
				56.00				26.89	52.23			

4	0.00	100.00	21.48	77.47	0.00	0.00	6.90	33.79	0.00	52.23	0.00	0.00
5	0.00	100.00	0.00	77.47	0.00	0.00	0.00	33.79	0.00	52.23	15.62	15.62
6	0.00	100.00	0.00	77.47	58.04	58.04	0.00	33.79	0.00	52.23	0.00	15.62
7	0.00	100.00	9.53	87.00	0.00	58.04	38.53	72.32	0.00	52.23	0.00	15.62
8	0.00	100.00	0.00	87.00	0.00	58.04	0.00	72.32	0.00	52.23	13.88	29.50
9	0.00	100.00	0.00	87.00	30.84	88.88	0.00	72.32	0.00	52.23	0.00	29.50
10	0.00	100.00	0.24	87.24	0.00	88.88	17.04	89.36	0.00	52.23	0.00	29.50

### 3.6.4. Effect of blast on the bridge

This section aims at presenting the result of the blast load of the bridge. The different actions and responses of the main elements of the bridge will be presented for the two blast loading scenarios considered.

#### 3.6.4.1. Blast case 1

The results for the blast at the level of hanger 1 ( $x = 10$  m) are portrayed in this section.

##### a. Stress of in slab

The effect of the blast on the slab at  $x = 10$  m is portrayed on Figure 3.31.

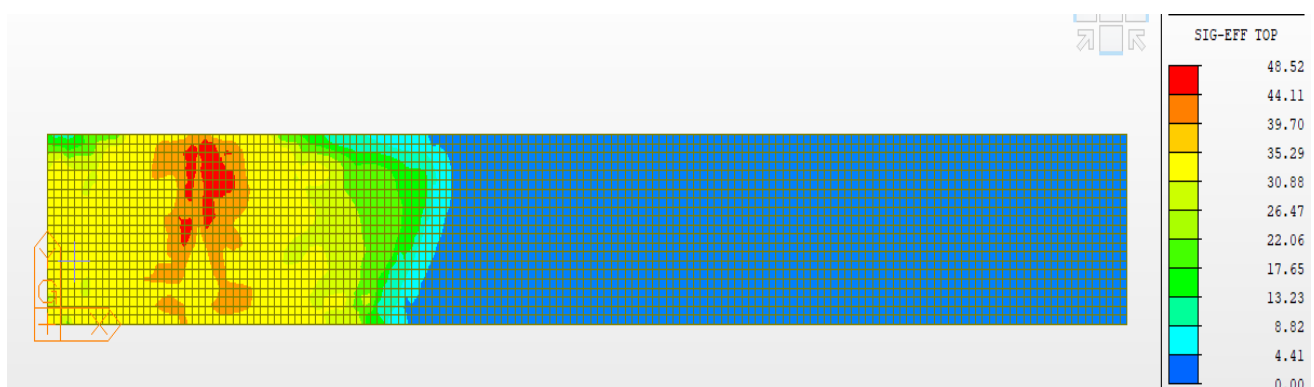


**Figure 3.31.** Stress distribution in the slab for blast case 1.

It can be observed that the increase in stress inside the slab (48.52 MPa) is greater than the maximum value for slab concrete of class C32/40. So, there's a local failure of the slab.

**b. Stress in the hangers**

The final incremental stress due to the dynamic blast loading on the bridge at x=10m is portrayed on Figure 3.32.

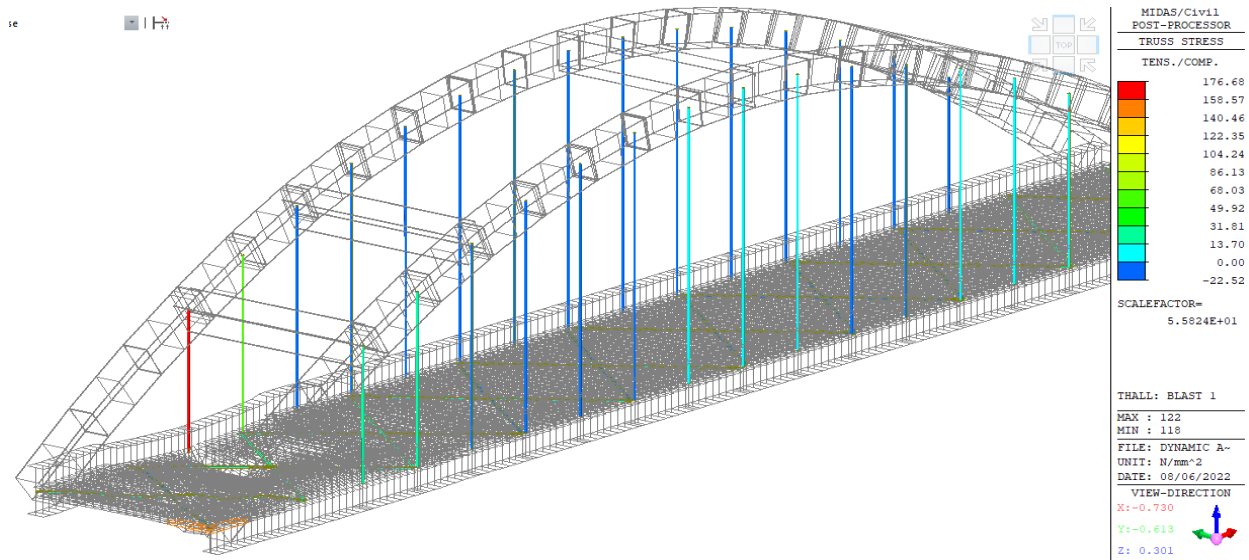


**Figure 3.32.** Stress distribution in the hangers for blast case 1.

It is observed that an increase in stress of 176.68 MPa is experienced in hanger 1. This causes the failure of this hanger since the maximum stress is exceeded (addition of 251.1 MPa and 176.68 MPa gives 428.38 MPa). However, the increase in stress in the other hangers (less than 60 MPa) are not sufficient to cause their failure.

**c. Stress in the arch and girder**

The blast induces stress values in the main girders and arch rib shown in Figure 3.33

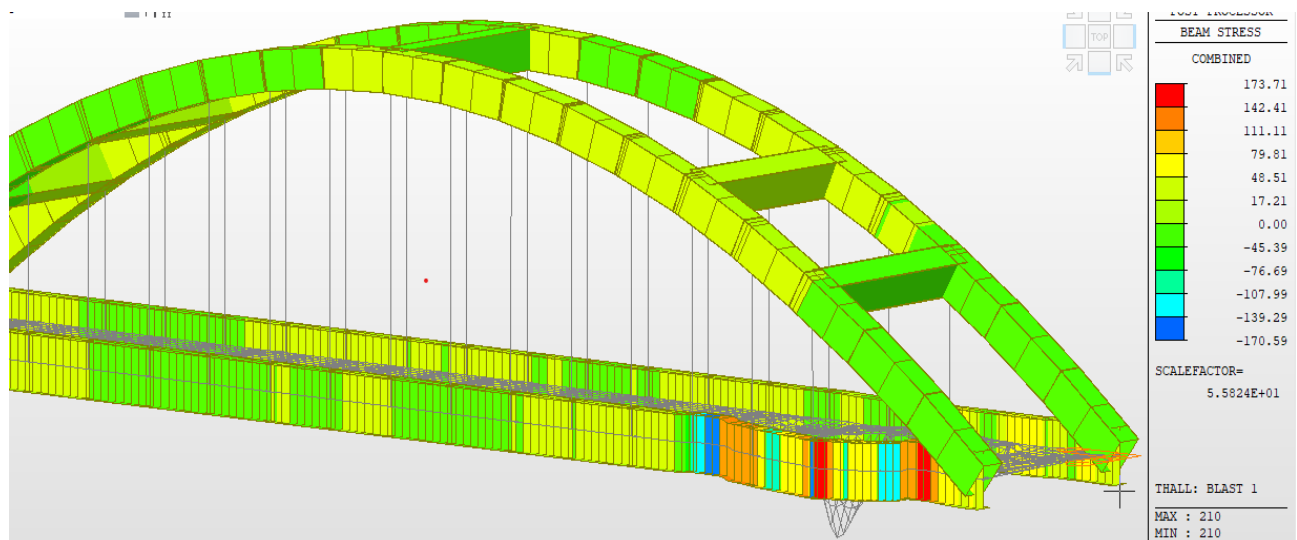


**Figure 3.33.** Stress distribution in the arch and girder for blast case 1.

With regards to the arch rib, the stress increment is not significant to cause failure for blast case 1. However, the girder is destroyed by the blast loading at this section since a stress increment of up to 173 MPa is observed.

### 3.6.4.2. Blast case 2

The results for the blast at the level of hanger 8 ( $x = 40$  m) are portrayed in this section.

#### a. Stress of in slab

The effect of the blast on the slab at  $x = 40$  m is portrayed on Figure 3.34.

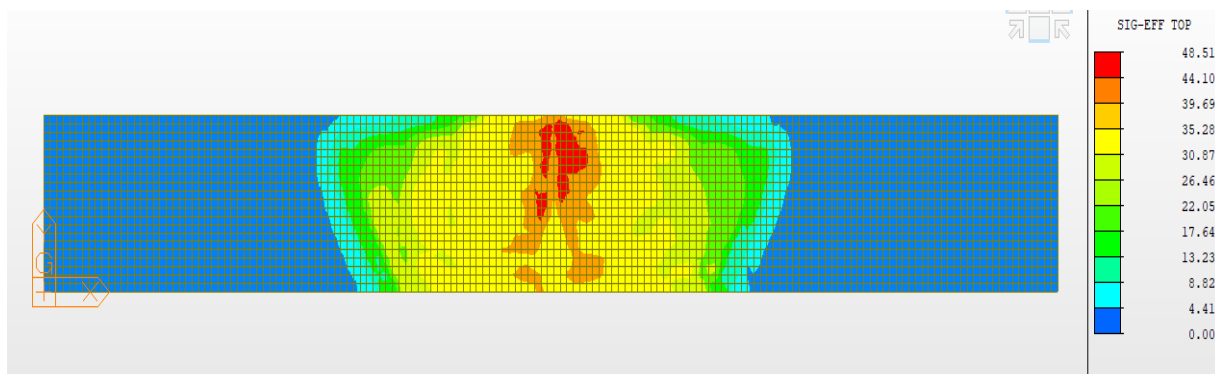


**Figure 3.34.** Stress distribution in the slab for blast case 2.

As for blast case 1, it can be observed that the increase in stress inside the slab (48.52 MPa) is greater than the maximum value for slab concrete of class C32/40. So, there's a local failure of the slab. Also, the stress increment due to the blast at the middle of the bridge is more spread out compared to case 1.

#### b. Stress in the hangers

The final incremental stress due to the dynamic blast loading on the bridge at  $x = 40$  m is portrayed on Figure 3.35.

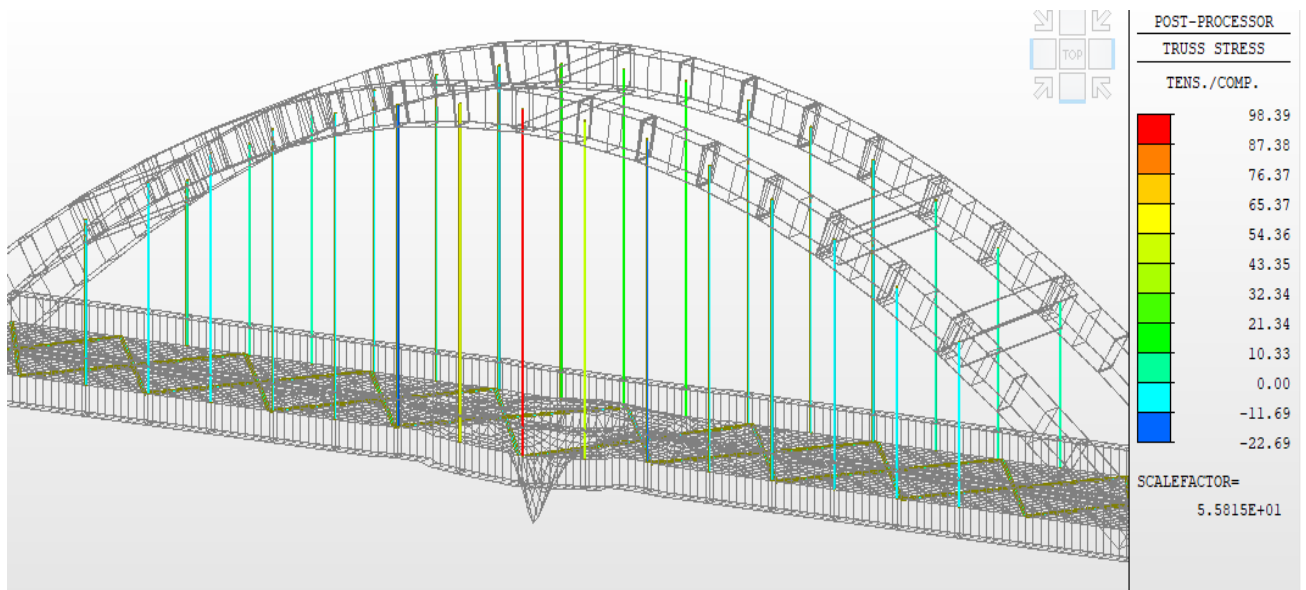


**Figure 3.35.** Stress distribution in the hangers for blast case 2.

It is observed that an increase in stress of 98.39 MPa is experienced in hanger 8. This does not cause the failure of the hanger since the total stress is below the limit ( $196.6 + 98.38$  MPa = 295 MPa). So, a blast load at the middle section is more uniformly redistributed to the hanger.

**c. Stress in the arch and girder**

The blast induces stress values in the main girders and arch rib shown in Figure 3.36.

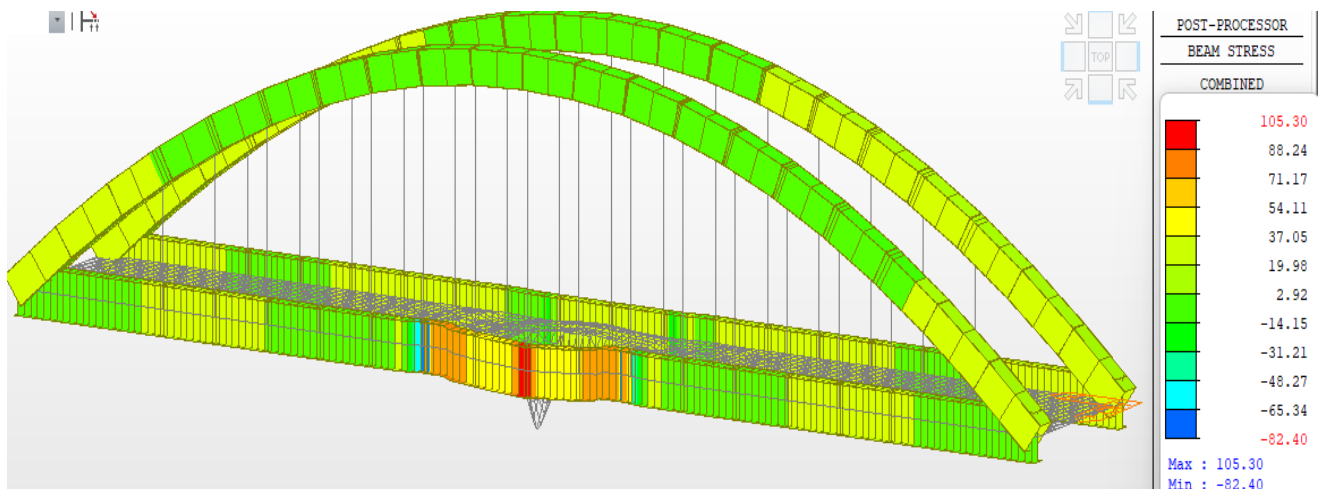


**Figure 3.36.** Stress distribution in the arch and girder for blast case 1.

The behaviour of the arch rib and the main girder is similar to that of the case 1. But here, the increase in stress in the girder is just 40% less than the for case 1. Also, there is no failure of the girder in this configuration.

### 3.6.5. Time history results

Here, some results of the time-history dynamic analysis are presented. Following that analysis, many time-history results could be extracted concerning, the deformation, stress, evolution of actions (moment, shear and axial forces), acceleration and so on. But in order to be more precise, only the time history results of related to stress and displacement were judged necessary to discuss the resilience of the structure.

#### 3.6.5.1. Blast case 1

The variation of the stress and vertical displacement in the hangers with time in the hangers 1 and 2 close to the point of detonation are shown on Figure 3.37 and Figure 3.38.

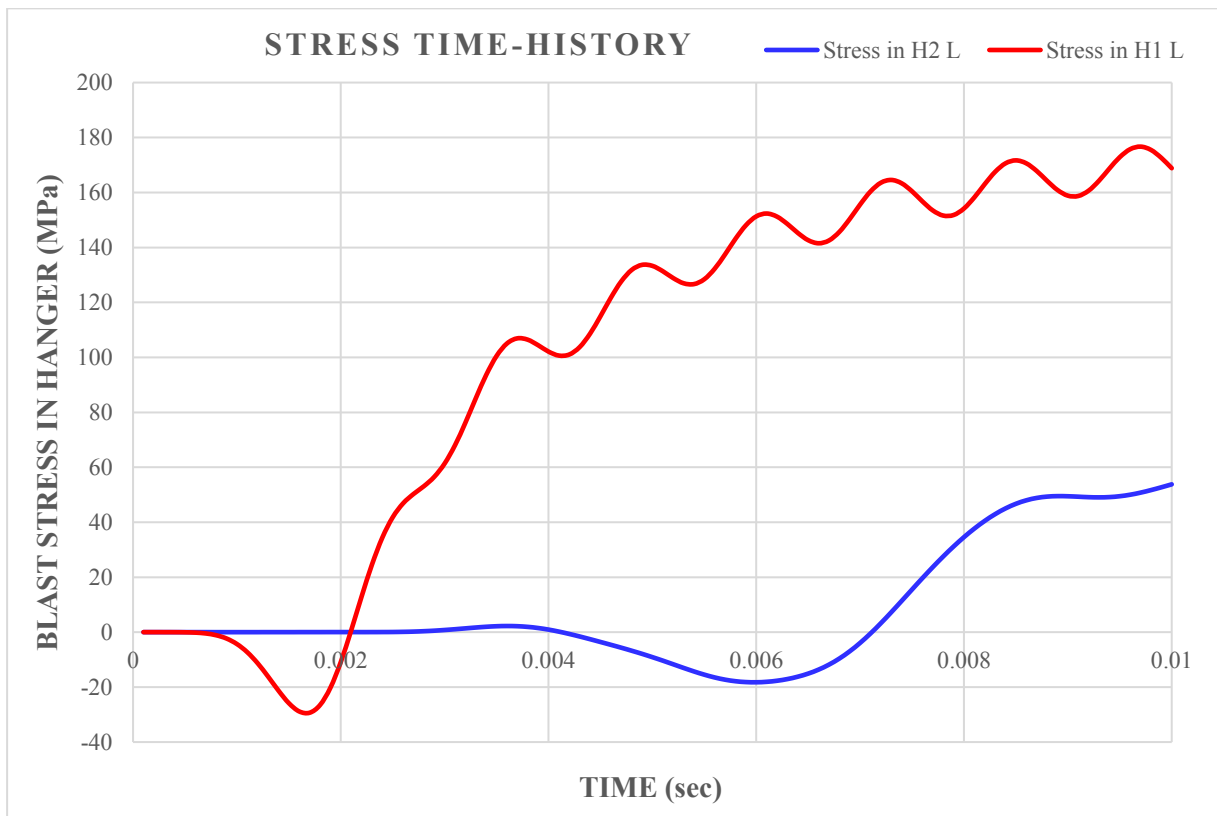


**Figure 3.37.** Evolution of stresses in Hanger 1 and 2 after blast loading case 1.

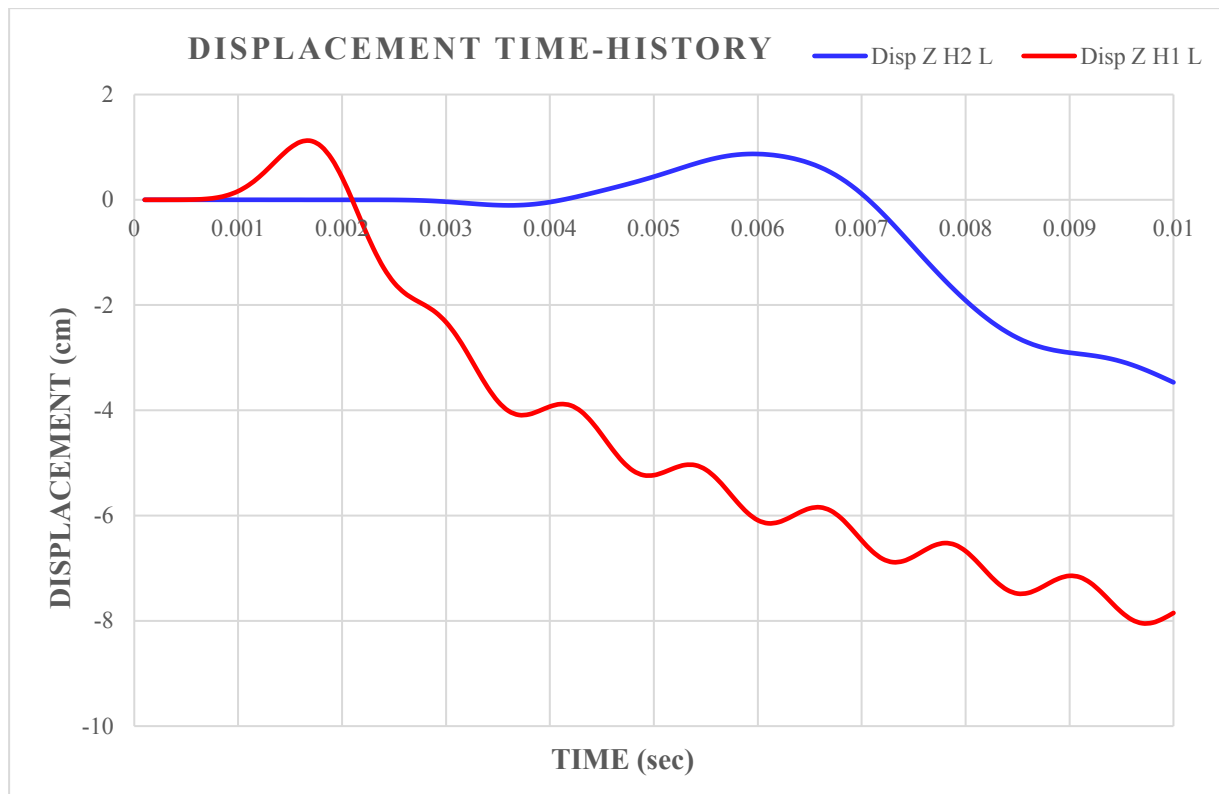


**Figure 3.38.** Evolution of node elongation 1 and 2 after blast loading case 1.

From these two graphs, it can be observed that the stress and node displacement variations in the hanger 1 and 2 have different time variations but the overall trend is similar. The time lapse is due to the arrival time of the blast wave which is different for the two hangers due to their different distances from the point of impact (1 m for hanger 1 and more than 4 m for hanger 2). Also, the effect of the blast loading is less pronounced in hanger 2 because of the rapid drop in blast pressure with time. The negative stress generated at the beginning of the wave is due to the effect of the deformation of the slab. Since the slab receives the wave before the hangers, it deforms accordingly causing a slight rotation of the slab and inducing a sort of compressive stress in the adjacent hangers. This compressive stress creates the positive vertical displacement of the hanger between  $t = 0.001$  s and  $t = 0.002$  s. The variation of stress after  $t = 0.002$  s is monotonic and quite sinusoidal due to the dynamic nature of the blast load which creates vibrations in the structure. The hanger 1 fails but hanger 2 does not.

### 3.6.5.2. Blast case 2

The variation of the stress and vertical displacement in the hangers with time in the hangers 8 and 7 close to the point of blast loading re shown on Figure 3.39 and Figure 3.40.

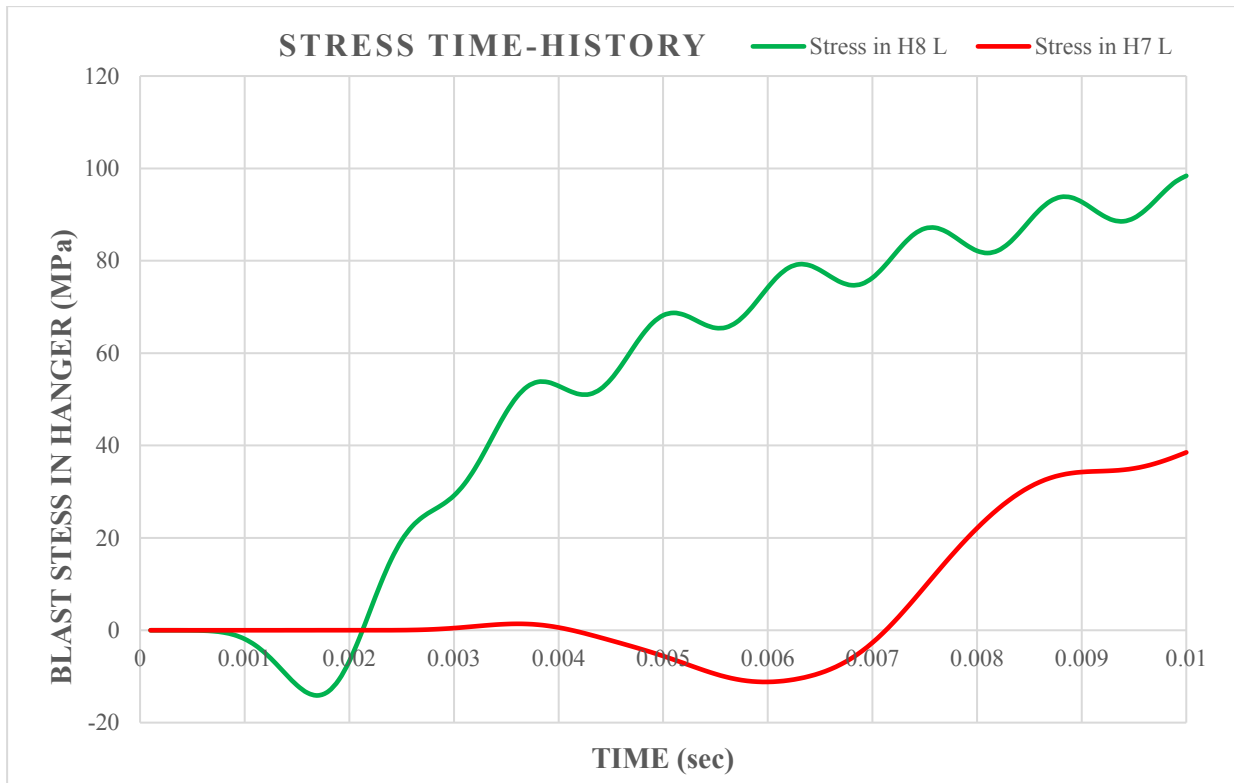


**Figure 3.39.** Evolution of stresses in Hanger 8 and 7 after blast loading case 2.

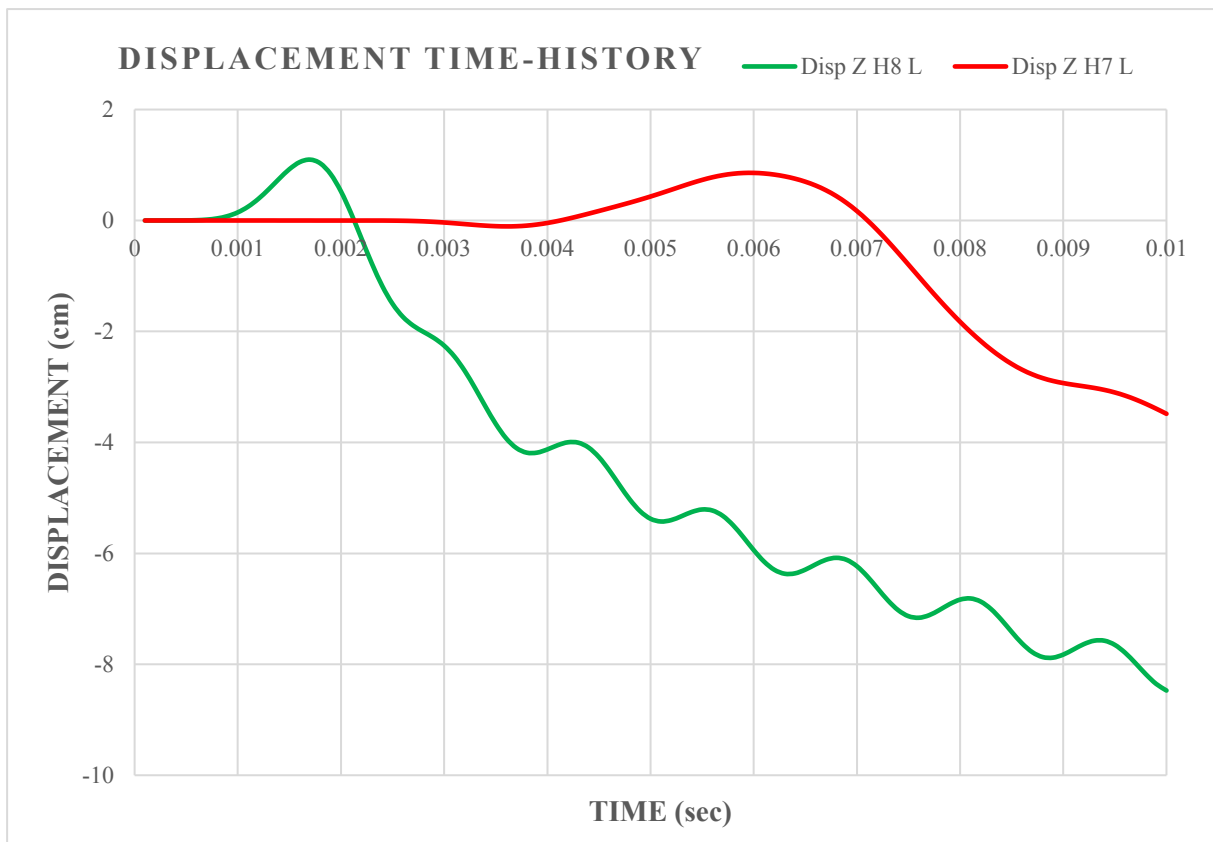


**Figure 3.40.** Evolution of node elongation 8 and 7 after blast loading case 2.

The result obtained for the blast case 2 follows the same trend as for case 1. However, it is important to point out the fact that the displacement is a little more pronounced in this case. This is due to the position of the blast load which is at the midspan, a section where the bridge is generally more vulnerable to deflection. Furthermore, it can be said that the bridge is more resilient in this case because of the ease with which it can absorb the stress due to the blast loading without failure of some major elements compared to case 1.

### 3.6.5.3. Effect of the blast loading on slab displacement

The effect of the blast load on different sections of the slab was also investigated and the results portrayed on Figure 3.41.

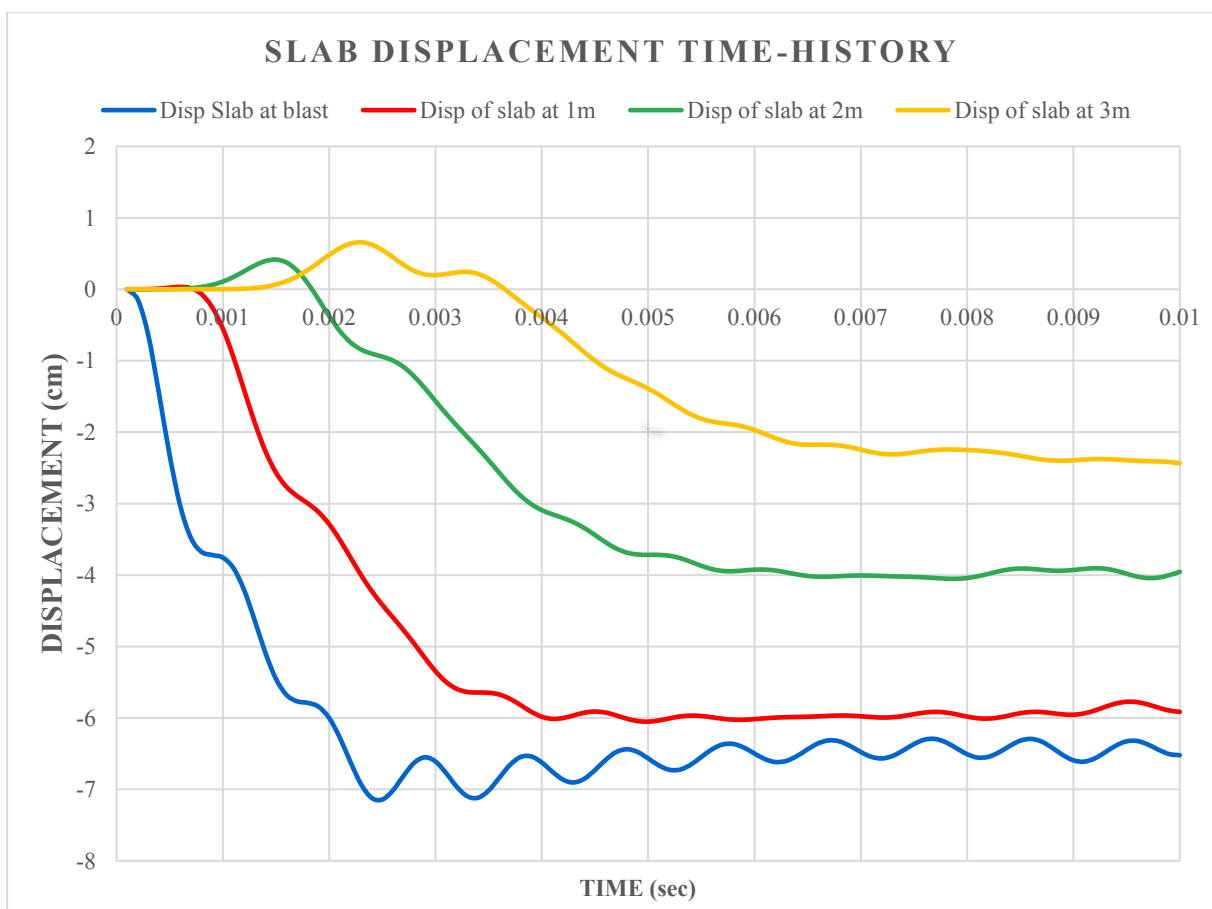


**Figure 3.41.** Variation of the displacement of the slab with time at different positions from the blast load.

It is observed from the displacement time graph that the points far away from the blast point are the least affected by the load. Also, the reduction is quite similar as the distance from the blast point increases.

### **3.6.6. Comments on the robustness of arch bridge**

From the observations made regarding the collapse analysis, comments can be drawn for the robustness of the investigated arch bridge. In general, robustness can be defined as insensitivity to local failure. Robustness is therefore always related to the size of the initial failure and to the accepted amount of damage to the remaining structure. If the design aim is that no or only small plasticisations are allowed, the investigated bridge does not act robustly. Here, alternate paths can develop. Loads are transferred through the bridge girder to adjacent hangers. Local plasticisations develops in the bridge girder and in hangers that already undergo blast load. If only total collapse should be avoided, the bridge can be termed robust regarding the loss of 4 to 5 hangers on each arch depending on the configuration. The failure of more hangers is not possible without serious damages. The bridge's robustness is therefore limited to the failure of a certain number of hangers depending on the predefined design criteria.

## **Conclusion**

The main objective of this chapter was to present the results of the redundancy analysis, that was conducted considering different configurations of hanger loss in the arch bridge and dynamic time history resilience analysis of blast load effect on the bridge. Firstly, a general presentation of the site based on its geographical location, its geology, its climate, its hydrology and socio-economic activities was conducted in order to contextualise the study. Then, a linear static structural analysis was performed on the different elements of the arch bridge and verifications made in compliance with Eurocode 3 guidelines. Equally actions and actions combinations were chosen and defined ideally. Furthermore, the analysis of redundancy was made considering 10 hanger failure cases in symmetric and asymmetric configurations. The position of the hanger failure on the longitudinal profile of the bridge was also found to be a determining factor in the bridge redundancy, since edge hanger failure caused more stress increase in the adjacent ones due to local stress redistribution. Also, the asymmetric hanger loss was found to generate higher local stress increase in remaining neighbouring hangers and greater probability of collapse. With regards to resilience, the bridge was found to be more vulnerable to blast load located at the beginning of the bridge longitudinal section. All these results were made possible due to ease of a dynamic modelling of the structure on MIDAS/Civil software. Also, Microsoft Excel enabled the easy assessment of different results and the elaboration of different curves explaining the variation of stresses and displacements.

## **GENERAL CONCLUSION**

---

Haven come to the end of this thesis work, it is necessary to recall that the main objective of this work was to explore the concept of arch bridges with focus on the redundancy of the hangers and the resilient behaviour of the bridge when subjected to accidental extreme loading. In order to achieve this objective, the work was partitioned in three main chapters, the first of which was a state of art on arch bridges, their main features, types, mechanism and generalities on their design. Besides, a review of available works on redundancy and resilience of bridge systems when subjected to extreme events such as blast loadings was made in order to have deeper insights of the subjects to be dealt with. The second chapter was the methodology where the data collection and modelling procedure of a tied-arch bridge were firstly depicted. Later on, a linear static analysis of the bridge was conducted following proper determination of load and load combinations. Afterwards, a redundancy and resilience analysis were conducted accordingly. In the former, various hanger failure configurations were considered and the load path redistribution assessed while in the latter, the behaviour of the bridge under accidental blast loading was assessed through a non-linear dynamic analysis using the MIDAS/Civil software and the RCblast software for the determination of the blast load pressure-time function. In the last chapter, the results of the various analysis were presented.

The results obtained from the redundancy analysis revealed that, the stress distribution is the same on both side of the arch in case of symmetric hanger failure pointing out the fact that the extreme hangers were the most stressed in the majority of cases. Also, it was observed that a hanger failure close to the supports has the worst effect on the neighbouring one, a 60% stress increment was observed in the second hanger when the first one close to the support failed. On the other hand, failure of hangers close to the midspan induces a redistribution of stresses quite equally to next ones. As such it can be deduced that, for edge hanger failure, there is a local load path redistribution while for hanger failure around the centre, there is a global load path redistribution. Furthermore, in the asymmetric configurations, the load redistribution was just on one side such that the hangers on the other edge of the arch bridge experienced little or no change. Also, depending on the number and position of hanger failure, a situation of progressive collapse of the bridge hangers could arise, in which the collapse of some hangers induces excessively high stresses in the others which in turn collapse and the process propagates itself until a part or the whole bridge collapses.

With regards to the resilience analysis, it was found that the effect of the blast load on the bridge was greatly dependent on the position with respect to the bridge. Elements that were closest to the detonation experienced the most extreme damages and stress variations but these damages greatly reduced with increasing distance from the blast point. In line with the results obtained from the redundancy analysis, it was observed that the consequence of the blast load was more severe for the structural elements when the blast load was close to the beginning of the bridge longitudinal section. The resilience of the bridge is then function of the degree of the severity of the effect.

The subject dealt with is very vast and it was necessary to limit the field of research for this work. However, having in mind the complexity related to the topic discussed and in order to improve this work, the following suggestions can be made for future studies:

- Elaboration of suitable guidelines for the quantification of the structural redundancy and resilience of bridge structures;
- Evaluation of the resilience of a bridge when exposed to prolonged extreme events;
- Effect of the geometry and configuration of an arch bridge on its redundancy and resilience.

## BIBLIOGRAPHY

---

- AASHTO. (2002). “*Standard Specifications for Highway Bridges American Association of State Highway and Transportation Officials*”, ABD.
- Alipour, A. (2017). Enhancing resilience of bridges to extreme events by rapid damage assessment and response strategies. *Transportation Research Record*, 2604(1), 54–62. <https://doi.org/10.3141/2604-07>
- Alipour, A., & Shafei, B. (2016). Seismic Resilience of Transportation Networks with Deteriorating Components. *Journal of Structural Engineering*, 142(8), 1–12. [https://doi.org/10.1061/\(asce\)st.1943-541x.0001399](https://doi.org/10.1061/(asce)st.1943-541x.0001399)
- ASCE/SEI 7-10. (2010). ASCE STANDARD Loads for Buildings. In *Minimum Design Loads for Buildings and Other Structures*.
- Bernabei, M., Macchioni, N., Pizzo, B., Sozzi, L., Lazzeri, S., Fiorentino, L., Pecoraro, E., Quarta, G., & Calcagnile, L. (2019). The wooden foundations of Rialto Bridge (Ponte di Rialto) in Venice: Technological characterisation and dating. *Journal of Cultural Heritage*, 36, 85–93. <https://doi.org/10.1016/j.culher.2018.07.015>
- Beyer, L. (2012). Arched Bridges. *Scientific American*, 1(23), 2–2. <https://doi.org/10.1038/scientificamerican02191846-2b>
- Bier, V. M., Haimes, Y. Y., Lambert, J. H., Matalas, N. C., & Zimmerman, R. (1999). A Survey of Approaches for Assessing and Managing the Risk of Extremes. *Risk Analysis*, 19(1), 83–94. <https://doi.org/10.1111/j.1539-6924.1999.tb00391.x>
- Bruneau, M., Chang, S. E., Eguchi, R. T., Lee, G. C., O’Rourke, T. D., Reinhorn, A. M., Shinozuka, M., Tierney, K., Wallace, W. A., & Von Winterfeldt, D. (2003). A Framework to Quantitatively Assess and Enhance the Seismic Resilience of Communities. *Earthquake Spectra*, 19(4), 733–752. <https://doi.org/10.1193/1.1623497>
- Caltrans. (2004). *Memo to Designers 12-2: Guidelines for Identification of Steel Bridge Members*. [http://www.dot.ca.gov/hq/esc/techpubs/manual/bridgemanuals/bridge-memo-to-designer/page/Section 12/12-2m.pdf](http://www.dot.ca.gov/hq/esc/techpubs/manual/bridgemanuals/bridge-memo-to-designer/page/Section%2012/12-2m.pdf)

- Chen, W. F., & Duan, L. (2014). Bridge engineering handbook: Fundamentals. In *Bridge Engineering Handbook: Fundamentals, Second Edition*. <https://doi.org/10.1201/b15616>
- EN 1990. (2002). *EN 1990:2002E - Basis of structural design - EC0*.
- EN 1990 Annex A2. (2005). ANNEX A2: Application for bridges. *Eurocode 0, EN 1990:2005 – Annex A2*.
- EN 1991-1-4. (2005). *Eurocode 1 : Actions on structures - Part 1-4: General actions - Wind actions, Committee for Standardization (Vol. 3)*.
- EN 1991-1-4. (2011). *EN 1991-1-4 (Vol. 1, Issue 2005)*.
- EN 1991-1-5. (2003). *Eurocode 1 : Part 1-5: General actions - Thermal actions (Vol. 3, Issue 1)*.
- EN 1991-2. (2003). Part 2: Traffic loads on bridges. In *Eurocode 1: Actions on structures (Vol. 3, Issue EN 1991-2:2003)*.
- EN 1992-1-1. (2004). Eurocode 2 : Part 1-1: General rules and rules for buildings. In *Eurocode 2: Vol. BS En 1992*. <http://www.python.org/doc/>
- EN 1993-1-1. (2005). *Eurocode 3: Part 1-1: General rules and rules for buildings (Vol. 3, Issue 1)*. <http://doi.wiley.com/10.1002/9783433601099>
- Faccini, F., Giardino, M., Paliaga, G., Perotti, L., & Brandolini, P. (2021). Urban geomorphology of Genoa old city (Italy). *Journal of Maps, 17(4)*, 51–64. <https://doi.org/10.1080/17445647.2020.1777214>
- Fang, Z. X., & Fan, H. T. (2011). Redundancy of structural systems in the context of structural safety. *Procedia Engineering, 14*, 2172–2178. <https://doi.org/10.1016/j.proeng.2011.07.273>
- FEMA 310. (1998). Handbook for the Seismic Evaluation of Buildings: A Prestandard. In *Fema 310*.
- FHWA Bridge Design Handbook Vol. 9. (2012). *Steel Bridge Design Handbook: Redundancy (Vol. 12, Issue November)*.

- Finke, J. E. (2016). *Static and dynamic characterization of tied arch bridges*.
- Frangopol, D., & Curley, J. (1987). EFFECTS OF DAMAGE AND REDUNDANCY ON STRUCTURAL RELIABILITY 3 By Dan M, Frangopol, 1 M. ASCE, and James P. Curley 2. *Journal of Structural Engineering*, 113(7), 1533–1549.
- Fu, C. C., & Wang, S. (2014). Computational analysis and design of bridge structures. In *Computational Analysis and Design of Bridge Structures*. <https://doi.org/10.1201/b17878>
- Ghosn, M., & Moses, F. (1998). *NCHRP Report 406: Redundancy in Highway Bridge Superstructures*.
- Ghosn, M., Moses, F., & Wang, J. (2003). NCHRP Report 489. Design of Highway Bridges for Extreme Events. In *Transportation Research Board*.
- Ghosn, M., Yang, J., Beal, D., & Sivakumar, B. (2014). NCHRP REPORT 776 : Bridge System Safety and Redundancy. In *Bridge System Safety and Redundancy*. <https://doi.org/10.17226/22365>
- Karlos, V., & Solomos, G. (2013). Calculation of blast loads for application to structural components, JRC Technical report, EUR 26456 EN. In *Luxembourg: Publications Office of the European Union*. <https://doi.org/10.2788/61866>
- Karlos, V., Solomos, G., & Larcher, M. (2016). *Analysis of blast parameters in the near-field for spherical free-air explosions*.
- Khuyen, H. T. (2016). *Redundancy and Progressive Collapse Analysis Methods for Steel Truss Bridges* (Issue December). Nagaoka University of Technology.
- Maiorana, E., Zorzan, M., & Genova, L. (n.d.). *Il montaggio e il varo del ponte ferroviario sul Polcevera a Genova The assembly and launch Genoa*. 32–40.
- Mbakop, W. (2020). *Blast effect of the vertical structural elements in reinforced concrete buildings blast effect of the vertical structural elements in reinforced concrete*. National Advanced School of Public Works Yaounde.
- McCullah, J., & Gray, D. (2005). *NCHRP Report 458: Redundancy in Highway Bridge Substructures* (Vol. 10).

- Owen, J. B. B. (2017). Arch bridges. *Masonry Bridges, Viaducts and Aqueducts*, 275–292. <https://doi.org/10.4324/9781315249513-16>
- Paliaga, G., Luino, F., Turconi, L., & Faccini, F. (2019). Inventory of geo-hydrological phenomena in Genova municipality (NW Italy). *Journal of Maps*, 15(2), 28–37. <https://doi.org/10.1080/17445647.2018.1535454>
- Pipinato, A. (2016). The history, aesthetics, and design of bridges. In *Innovative Bridge Design Handbook: Construction, Rehabilitation and Maintenance*. Elsevier Inc. <https://doi.org/10.1016/B978-0-12-800058-8.00001-3>
- Pipinato, A. (2021). Innovative Bridge Design Handbook: Construction, Rehabilitation and Maintenance. In *Innovative Bridge Design Handbook: Construction, Rehabilitation and Maintenance* (Issue October). <https://doi.org/10.1016/B978-0-12-823550-8.09986-8>
- Sonda, D. (2019). *Course of Structural Engineering - NASPW Yaounde*.
- Starossek, U. (2007). Disproportionate collapse: A pragmatic approach. *Proceedings of the Institution of Civil Engineers: Structures and Buildings*, 160(6), 317–325. <https://doi.org/10.1680/stbu.2007.160.6.317>
- Trahair, N. S. (1989). Guide to stability design criteria for metal structures (4th edition). In *Engineering Structures* (Vol. 11, Issue 3). [https://doi.org/10.1016/0141-0296\(89\)90009-6](https://doi.org/10.1016/0141-0296(89)90009-6)
- UTCPC. (2014). Enhancing Disaster Resilience of Highway Bridges to Multiple Hazards. *UTC Spotlight, April*. <https://doi.org/10.1002/eqe.2392.Zhou>

## WEBOGRAPHY

---

Accelerated Bridge Construction – University Transportation Center. (2021). *Risk and Resilience of Bridges: Toward Development of Hazard-Based Assessment Framework, Research Needs, and Benefits of Accelerated Construction*. [Consulted on: 2<sup>nd</sup> August 2022]. <https://abc-utc.fiu.edu/research-projects/isu-research-projects/risk-and-resilience-of-bridges-toward-development-of-hazard-based-assessment-framework-research-needs-and-benefits-of-accelerated-construction/>

American Society of Civil Engineers Library. (2022). *Redundancy and Robustness in the Design and Evaluation of Bridges: European and North American Perspectives*. [Consulted on: 2<sup>nd</sup> August 2022]. <https://ascelibrary.org/doi/10.1061/%28ASCE%29BE.1943-5592.0000545>

Britannica. (2021). *Bridge engineering*. [Consulted on: 4<sup>th</sup> March 2022]. <https://www.britannica.com/technology/bridge-engineering/>

Britannica. (2021). *Old London Bridge*. [Consulted on: 7<sup>th</sup> March 2022]. <https://www.britannica.com/topic/Old-London-Bridge>

Climate-Data. (2021). *Climate Genoa (Italy)*. [Consulted on: 3<sup>rd</sup> August 2022]. <https://en.climate-data.org/europe/italy/liguria/genoa-1133/#climate-graph>

ConstroFacilitator. (2021). *What are the different components and types of arch bridges?* [Consulted on: 20<sup>th</sup> March 2022]. <https://www.constrofacilitator.com/what-are-different-components-and-types-of-arch-bridge/>

History of Bridges. (2022). *Arch Bridge – Facts about bridges*. [Consulted on: 27<sup>th</sup> February 2022]. <http://www.historyofbridges.com/facts-about-bridges/arch-bridges/>

Midas Bridge. (2021). *Arch bridge – Solution*. [Consulted on: 25<sup>th</sup> February 2022]. <https://www.midasbridge.com/en/solutions/arch-bridges#none>

RoughGuides. (2021). *Iterative Italy map*. [Consulted on: 31<sup>st</sup> July 2022].

<https://www.roughguides.com/maps/europe/italy/>

ShanghaiMetal. (2022). *The History of the Arch Bridge*. [Consulted on: 27<sup>th</sup> February 2022].

<https://www.shanghaimetal.com/7697-7697.htm>

The Institution of Structural Engineers. (2022). *Resilience*. [Consulted on: 27<sup>th</sup> July 2022].

<https://www.istructe.org/resources/resilience/>

TripAdvisor. (2022). *Telford Bridge*. [Consulted on: 7<sup>th</sup> March 2022].

[https://www.tripadvisor.com/Attraction\\_Review-g1015398-d8806290-Reviews-Telford\\_Bridge-Craigellachie\\_Moray\\_Scotland.html](https://www.tripadvisor.com/Attraction_Review-g1015398-d8806290-Reviews-Telford_Bridge-Craigellachie_Moray_Scotland.html)

Waku. (2022). *Visiting one of the three great bridges in Japan – the Kintaikyo Bridge in Yamaguchi*. [Consulted on: 10<sup>th</sup> March 2022]. <https://wakuwaku.today/story/visiting-one-of-the-three-great-bridges-in-japan-the-kintaikyo-bridge-in-yamaguchi-b7O2OCLE>

Wikimedia Commons. (2019). *Alcántara Bridge*. [Consulted on: 10<sup>th</sup> March 2022].

[https://commons.wikimedia.org/wiki/Alc%C3%A1ntara\\_Bridge](https://commons.wikimedia.org/wiki/Alc%C3%A1ntara_Bridge)

Wikipedia. (2022). *Arch Bridge*. [Consulted on: 25<sup>th</sup> February 2022].

[https://en.wikipedia.org/wiki/Arch\\_bridge](https://en.wikipedia.org/wiki/Arch_bridge)

Wikipedia. (2022). *Genoa*. [Consulted on: 3<sup>rd</sup> August 2022].

<https://en.wikipedia.org/wiki/Genoa>

Midas manual. (2022). *Eigenvalue Analysis Control*. [Consulted on: 30<sup>th</sup> July 2022].

[http://manual.midasuser.com/EN\\_Common/Civil/895/Start/06\\_Analysis/Eigenvalue\\_Analysis\\_Control.htm](http://manual.midasuser.com/EN_Common/Civil/895/Start/06_Analysis/Eigenvalue_Analysis_Control.htm)

Your Article Library. (2021). *Arch Bridges: Types, Components and Shape*. [Consulted on: 28<sup>th</sup> February 2022]. <https://www.yourarticlelibrary.com/bridge-construction/arch-bridges-types-components-and-shape/94039>

# ANNEXES

## ANNEX A: Table and figures used in methodology

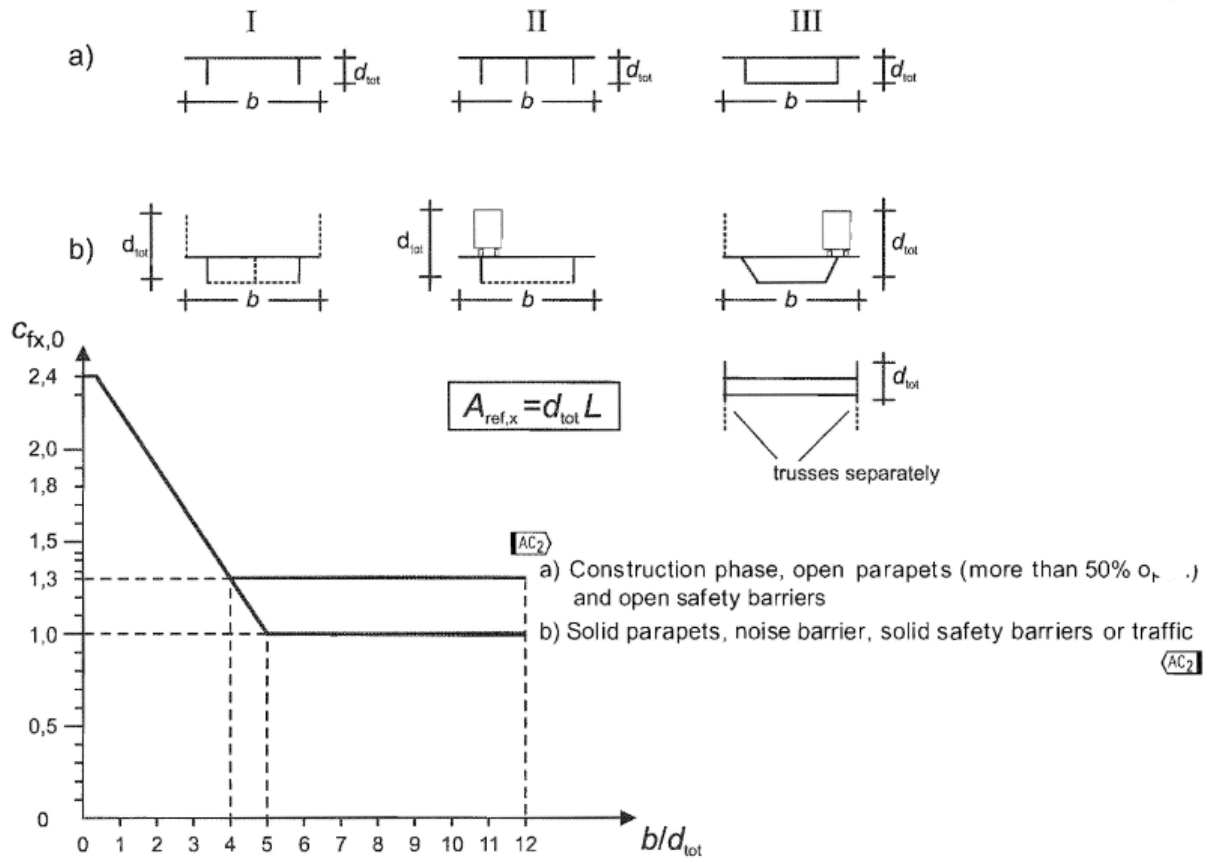


Figure A.1. Force coefficient for bridges,  $C_{fx,0}$  (EN 1991-1-4, 2011)

Road restraint system	on one side	on both sides
Open parapet or open safety barrier	$d + 0,3 \text{ m}$	$d + 0,6 \text{ m}$
Solid parapet or solid safety barrier	$d + d_1$	$d + 2d_1$
Open parapet and open safety barrier	$d + 0,6 \text{ m}$	$d + 1,2 \text{ m}$

Table A.1. Depth  $d_{tot}$  to be used for  $A_{ref,x}$

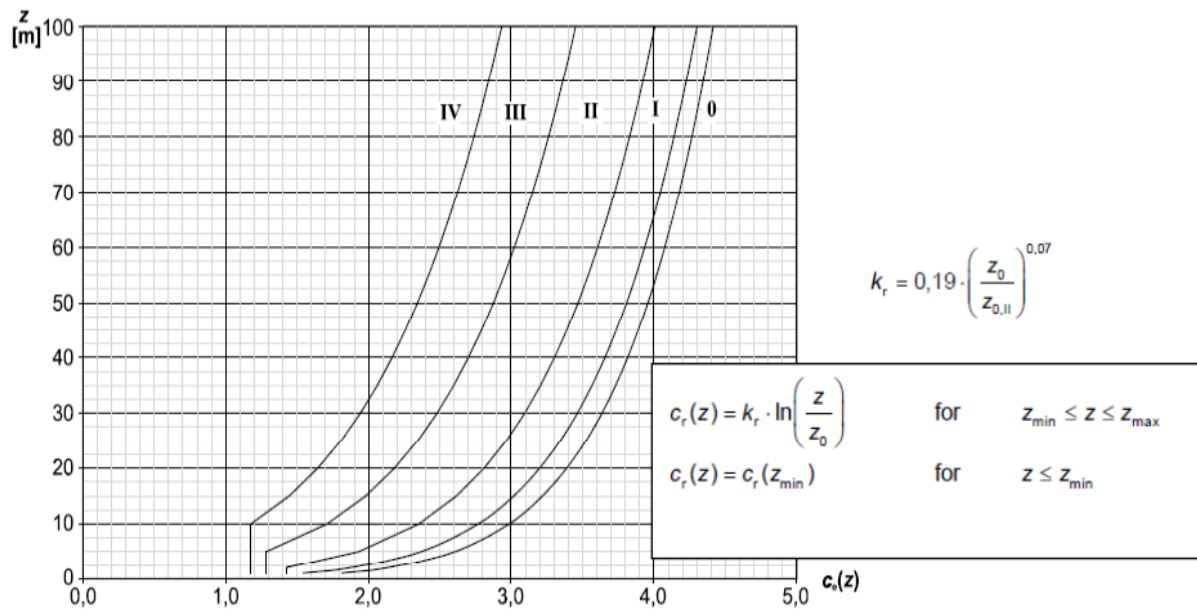


Figure 4.2 — Illustrations of the exposure factor  $c_e(z)$  for  $c_0=1,0$ ,  $k_r=1,0$

**Figure A.2.** Illustration of the exposure factor  $c_e(z)$  (EN 1991-1-4, 2011)

## ANNEX B: Structural detailing of the arch bridge

### CHARACTERISTIC DATA

**Weight:**

2,600 t

**Period of activity on site:**

2009-2011

**Length:**

78.5 + 78.5 + 24 (n ° 3

spans) **Length:**

1,080 m

**Height:**

18.70 m

**Tender executive project (for RFI):** dr.

ing. P. Pistoletti, Seteco Ingegneria srl

(Genoa)

**General project for the contractor:**

dr. ing. A. Forlani, Studio SGAI

(Morciano di R.)

**Contractor:**

Coopsette Soc. Coop.

**Construction of metal structures:** OMBA

Impianti & Engineering SpA, Torri di

Quartesolo

**Design, construction and assembly of**

**launching equipment:** OMBA Impianti &

Engineering SpA, Torri di Quartesolo

**Table B.1.** Polcevera railway arch bridge project characteristics (Maiorana et al., n.d.)

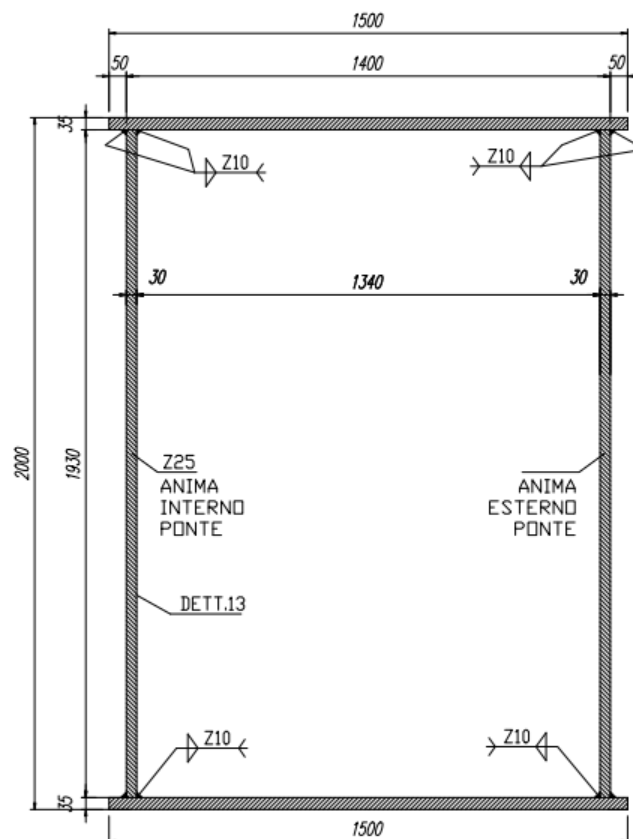


**Figure B.1.** Arch rib structural steel section

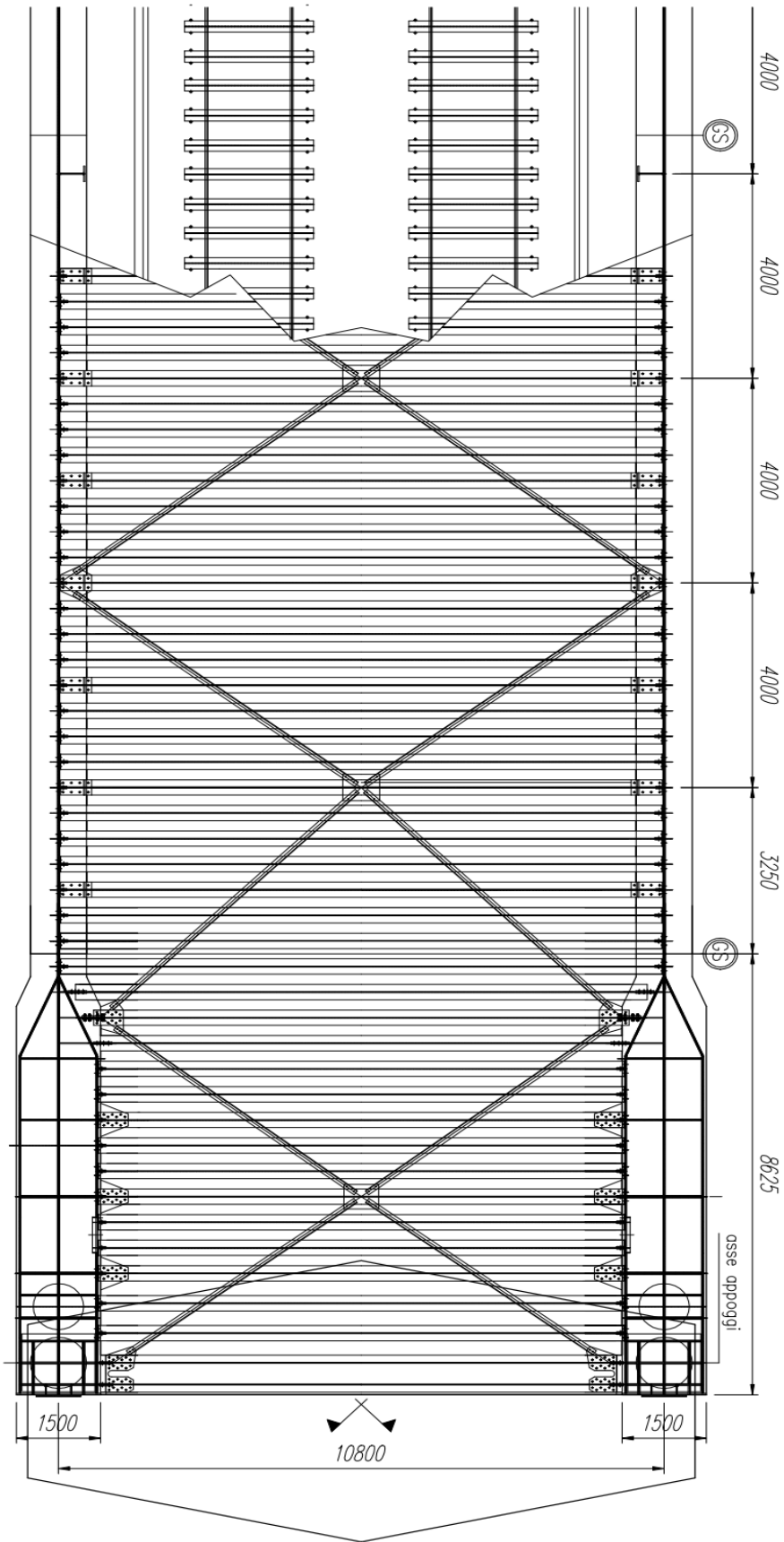


Figure B.2. Structural plan of arch bridge deck